MEASUREMENT AND MODELING OF WHEELCHAIR PROPULSION ABILITY FOR PEOPLE WITH SPINAL CORD INJURY

A thesis submitted in partial fulfilment of the

requirements for the Degree

of Master of Mechanical Engineering

in the University of Canterbury

by FEI YAO

University of Canterbury

2007

ABSTRACT

Wheelchair propulsion is an important part of daily living for many people with spinal cord injuries (SCI's). The aim of this project was to establish the validity of using a new approach for measuring wheelchair propulsion ability. The variation in methods observed by subject's hands in contacting and propelling their wheelchair, namely, using the push rims only; wedging the hands between push rims and tyre and grasping both push rims and tyres, highlighted that earlier studies using instrumented push rims (including the SMART^{Wheel}) for people with tetraplegia would not provide a true indication of propulsion ability for the participants in this study. As a result, a new inertia dynamometer was built and calibrated for measuring wheelchair propulsion ability. Kinetic and kinematic models were developed to calculate wheelchair propulsion parameters such as power output, wheelchair velocity and arm motion patterns. After testing 22 subjects with different SCI levels, the results indicated that arm function was a more important factor in wheelchair propulsion, in terms of power output, than trunk stability and strength. More importantly, people with C5/C6 tetraplegia had a significantly reduced capability in terms of wheelchair propulsion compared with other subjects with a lower lesion (T1-T8, T9-T12 and L1-S5). A further study for quantifying the contribution of triceps function on improving wheelchair propulsion for people with tetraplegia was performed by comparing kinetic and kinematics parameters in C5/C6 tetraplegia subjects. Depending on the control of elbow extension, the subjects were divided into groups with: no active elbow extension, deltoid to triceps transfer surgery (TROIDS) to provide elbow extension, and incomplete C5/C6 tetraplegia with retained active triceps function providing elbow extension. The results demonstrated that the restoration of triceps following TROIDS surgery not only allows active elbow extension, but also increased

the amplitude and strength as well as the speed of arm movement. Finally, the results also point to TROIDS allowing a more pronounced and natural push phase and an improved arm movement pattern during both propulsion and recovery phase under normal and extreme conditions.

Chapters 2, 3 and 4 of this thesis are based on the following manuscripts and titles prepared for submission as listed below:

- Paper 1: A Procedure for Measuring Manual Wheelchair Propulsion Ability for People with Spinal Cord Injuries
- Paper 2: Quantifying Manual Wheelchair Propulsion Ability vs. Injury Level for People with Spinal Cord Injuries
- Paper 3: Evaluation of posterior deltoid to triceps transfer surgery in C5/C6 tetraplegia on manual wheelchair propulsion

ACKNOWLEDGEMENTS

I would like to thank Dr. Shayne Gooch from the Mechanical Engineering Department at the University of Canterbury for his guidance throughout the project. Huge thanks also go to Dr. Tim Woodfield whose biomechanical engineering expertise has been a vital part of any progress made in my research. The help of Professor Alastair Rothwell and Jennifer Dunn from the Burwood hospital is greatly appreciated. I would also like to thank the help of the technical staff, in particular, Ken Brown, Paul Wells and Julian Murphy from the Mechanical Engineering Department at the University of Canterbury for the dynamometer setup and development. Finally, I would like to thank all the people from the Burwood Hospital Spinal Injury Unit, Christchurch, New Zealand.

TABLE OF CONTENTS

LIST OF FIGURES

LIST OF TABLES

CHAPTER 1

GENERAL INTRODUCTION

Nomenclature

Algebraic symbols	
C	Cervical spinal segments
T	Thoracic spinal segments
L & S	Lumbar and Sacral spinal segments
RF & RR	The vertical reaction forces at the front and rear wheels respectively (N) (assumes equal load sharing at each end)
m	Mass of wheelchair and occupant (kg)
g	Gravity (9.81m/s^2)
$l_1 \& l_2$	Length in horizontal direction from the rear and front wheel centres to the system centre of gravity (m)
$\hat{l}_1 \& \hat{l}_2$	Length in ‘x’ direction from the rear and front wheel centres to the system centre of gravity (m)
I	Polar mass moment of inertia (kgm^2)
F_N	Normal wheel force at ground (N)
x	Linear wheelchair displacement (m)
$\dot{x}$	Linear wheelchair velocity (m/s)
$\ddot{x}$	Linear wheelchair acceleration (m/s^2)
θ	Angular wheelchair displacement (rad)
$\dot{\theta}$	Angular wheelchair velocity (rad/s)
$\ddot{\theta}$	Angular wheelchair acceleration (rad/s^2)
r	Wheel radius (m)
e	The distance from the wheel centre line (normal to ground) to the applied normal ground forceF_N (m)
F_t	Tractive force (N)
F_D	Aerodynamic force (N)
A	Frontal wheelchair area including occupant (m^2)
F_{EP}	Effective push rim force (N)
rp	Radius at which effective push rim force is applied (m)
TLF	Tractive force losses due to bearing friction and windage (N)
W	Work (J)
P	Power (w)
rr	Radius of roller (m)
Greek symbols	
$\hat{\theta}$	Gradient (rad)
ρ	Air density (1.23 kg/m^3)
Suffixes	
FW	Front Wheel
RW	Rear Wheel
RR	Right side roller
LR	Left side roller
R	Roller

1.1 Motivation

An important aspect of daily life in the majority of persons with spinal cord injury (SCI) is their dependence on a wheelchair. They prefer to use a hand rim wheelchair in everyday life, with rims of a relatively large diameter [1]. This type of wheelchair offers many advantages with respect to ease of transportation and flexibility of use in general. Wheelchair use is to achieve independent mobility. To function independently, manual wheelchair users must possess a variety of wheelchair skills, enabling them to deal with the physical barriers they will inevitably encounter in various environments. Mastering wheelchair skills can make the difference between dependence and independence in daily life. From the literature [2-14], physical capacity, functional status, lesion level, motor completeness of the lesion and age are directly related to wheelchair propulsion ability. As a result, understanding manual wheelchair propulsion for people with different SCI levels is important for a number of reasons [15-21] such as prevention of repetitive strain injuries and improvement of quality of life in general. In the evaluation of surgical interventions in SCI, most studies [22-32] have focused on the improvements in many daily life activities, such as arm raising, driving, swimming, writing, interview and questionnaires, which are not specific to subjects. However, until recently, few investigations [33] have been done on a systematic functional quantification of wheelchair propulsion mechanics for people with SCI.

1.2 Research on spinal cord injury (SCI)

1.2.1 SCI classifications

In order to adequately assess wheelchair propulsion for people with SCI, it is necessary to have a basic understanding of spinal cord injury classifications. Figure 1 lists of typical effects of spinal cord injury by location (refer to the spinal cord map). An SCI is defined as a lesion within the spinal cord that results in the disruption of nerve fibre bundles that convey ascending sensory and descending motor information [34]. A complete SCI at the cervical level can cause tetraplegia resulting in variable loss of hand and upper limb motor and sensory function. Individuals with SCI rely on the use of their hands and upper limbs in order to complete basic activities of daily living such as self-feeding, dressing, bathing and toileting. Mobility needs, such as transfers from surface to surface, transitional movements such as rolling, bridging and sit-to-lying down, crutch walking and wheeled mobility are also completed by using their arms [49]. In addition to the general level of injury, i.e., tetraplegia or paraplegia, the specific neurologic level and its severity can usually be identified by performing a detailed neurologic examination [2]. The level at which the injury or lesion occurs and the completeness of the lesion (incomplete or complete) indicate the level of independence of the person [50]. In incomplete spinal cord injuries, some neural transmissions can still pass through the spinal cord but it is often fragmentary or distorted which can lead to additional neurological complications such as chronic pain or spasticity.

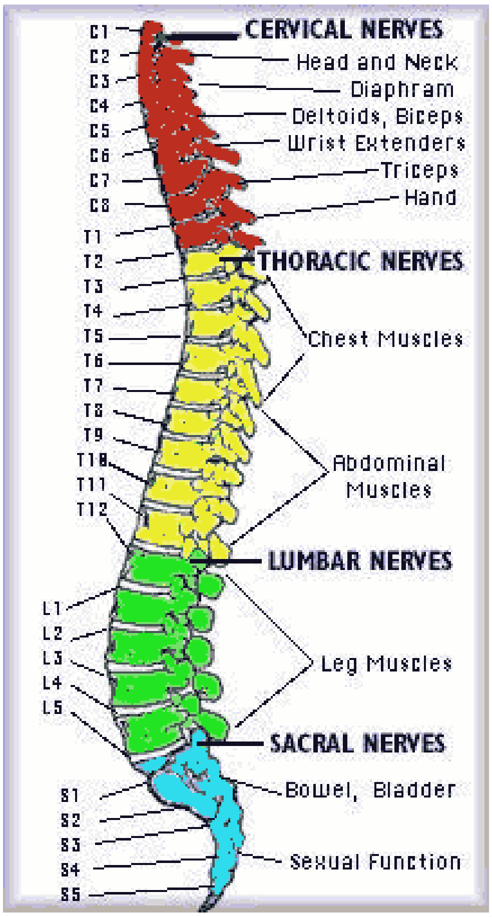

Figure 1.1 *The graphs of spinal cord map [35]*

1.2.2 Function

Subjects with an SCI below C4 (Figure 1.1) normally can use a manual wheelchair [36]. C5/C6 tetraplegia resulting from cervical spinal cord lesions typically results in the loss of triceps muscle function, and thereby loss of active elbow extension. Subjects typically have good preservation of shoulder abduction and external rotation, elbow flexion and variable wrist extension but little or no voluntary control of elbow extension and no hand function [37]. Moreover, severe weakness of trunk and lower extremities interfere with sitting balance and ability to walk. A similar functional characteristic is seen in C7 tetraplegia except added ability to straighten elbows and fingers.

In T1-T8 paraplegia, subjects have normal motor function in head, neck, shoulders, arms, hands and fingers and are totally independent when using a manual wheelchair. Subjects with T9-T12 injuries have good trunk control due to active abdominal muscle control. L1-S5 injuries have decreasing control of hip flexors and legs. The key functional limitations influencing wheelchair propulsion in people with different SCI levels are summarised in Table 1.1.

SCI Level	Function
Cervical injuries (C5-C6)	• Preservation of shoulder abduction + external rotation • Preservation of elbow flexion + variable wrist extension • Little/no voluntary control of elbow extension • No hand function
Cervical injuries (C7)	• Elbow extension • Wrist extension • Finger extension, no grasp
Thoracic injuries (T1-T8)	• Near normal upper limb function • Limited abdominal function and trunk control
Thoracic injuries (T9-T12)	• Full upper limb function • Good abdominal function and trunk control
Lumbar and Sacral injuries	• Full upper limb function • Good abdominal function and trunk control

Table 1.1 *Segmental SCI level and function adapted from Floris et al [37]*

1.2.3 Deltoid to triceps transfer surgery for C5/C6 tetraplegia

A previous study carried out by the Canadian Paraplegic Association found that the most common SCI is at the C5/C6 level as shown in Figure 1.2 [38], with paralysis to the triceps resulting in reduced upper extremity strength and stability.

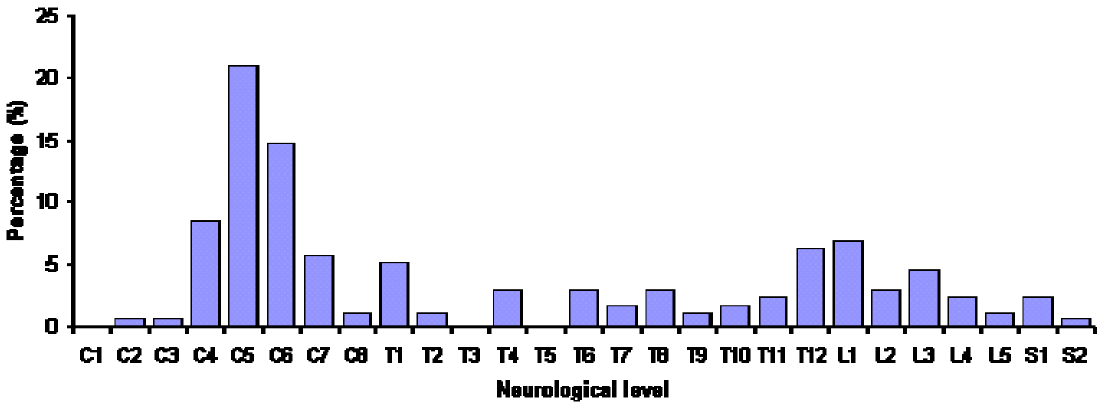

Figure 1.2 *The most common level at which spinal cord injuries occur is between the C5-C6 vertebrae*

More importantly, voluntary control of triceps was a significant determinant in the ability to perform self care tasks, such as arm raising, driving, swimming and writing [39]. Although during wheelchair propulsion, individuals can lean forward or backwards to modify their motor behaviour to best suit their physical capacities and realise further functional abilities, C5/C6 tetraplegia subjects regard improved upper limb functions as a top priority in relation of other aspects of their disability [25]. As a result, surgical restoration of active elbow extension in people with SCI at the level of C5/C6 is thought to be beneficial in increasing functional ability. The deltoid to triceps transfer (TROIDS) surgery is a term that describes the surgical transfer of a functioning posterior deltoid muscle in order to replace the action of the paralysed triceps muscle to restore elbow extension. During surgery, the posterior deltoid is detached from its insertion and re-joined to the triceps aponeurosis using either a free tendon or artificial graft [40]. This enables individuals with tetraplegia to regain some of the lost function of their arm. The posterior section of the deltoid muscle has about one third of the strength of a fully functioning triceps. Figure 1.3 gives a good indication of the relative sizes of the two muscles. Approximately one-half of this strength is available to the fully recovered patient [29, 40]. However, most of evaluations of TROIDS surgery to date have relied on interview or questionnaires

[22-23], which are not specific to subjects with tetraplegia. A systematic quantification of wheelchair propulsion mechanics for tetraplegia pre- and post-TROIDS transfer surgery has not been performed.

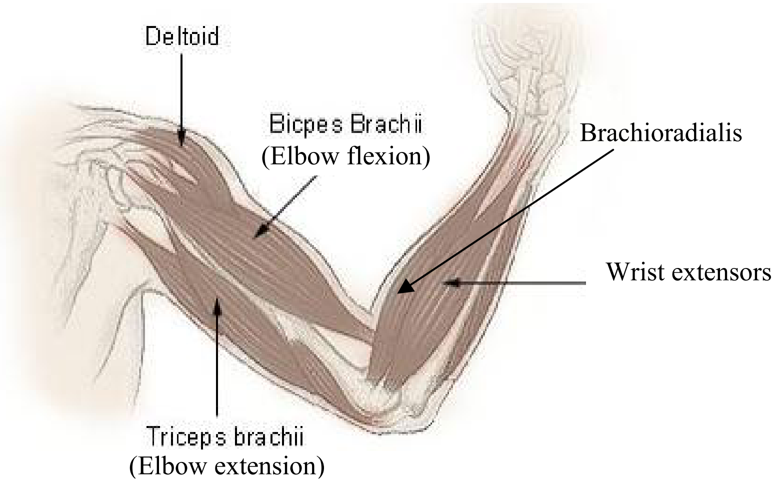

Figure 1.3 *The major muscles of upper arm*

1.3 The mechanics of wheelchair propulsion

To efficiently propel a manual wheelchair, the shoulder should be in vertical alignment with (or slightly in front of) the axle of the wheel [41] as shown in Figure 1.4. When the axle is in the correct position and the upper body is in balance, users reach as far back as possible on the rim of the wheelchair and initiate a propulsion stoke that typically has two parts (flexion and extension) rather than just one.

Figure 1.4 *Shoulders to Axle Alignment*

Wheelchair propulsion includes the actual propulsion as well as a recovery phase. The propulsion phase (PP) is a closed chain event, during which the hand is in contact with the rim and it consists of pull and push segments (Figure 1.5). The PP begins with when the hands contacting the top of the rim or at a point just behind the top and ends when the hands leave the rim, usually when the arms are extended. In this project, the PP is divided into the following five sub-phases: contact (V_c), first quarter (1/4), top dead centre (TDC), third quarter (3/4) and release (V_r) (Figure 1.5). The contact phase involves grasping the rim just behind top dead centre (TDC) then stronger muscles (e.g. biceps) can be recruited to create forward propulsion. If hand placement is far behind TDC then there is danger of damaging the joint capsule of the shoulder through the effects of the combined movement of internal rotation and shoulder extension. During the push phase, the hand centre has passed the TDC and it should be vertically aligned with the shoulder to place the hand in an optimal position for exerting forward force on the wheelchair push-rims. The recovery phase (RP) is an open chain event during which no force is exerted on the push-rim. Four segments are involved; follow through, retrieval, pre-impact and pre-load as shown in Figure 1.5. The RP begins as the hands go further down the rim to complete the stroke with maximum efficiency (follow through), and requires lifting the hands off the wheel and counter-balancing the inertia of the arms (retrieval). The RP continues with the hands swinging back past the line of the shoulders leaving them adjacent to the rim (pre-impact), and ends with the humerus at its most posterior position (pre-load).

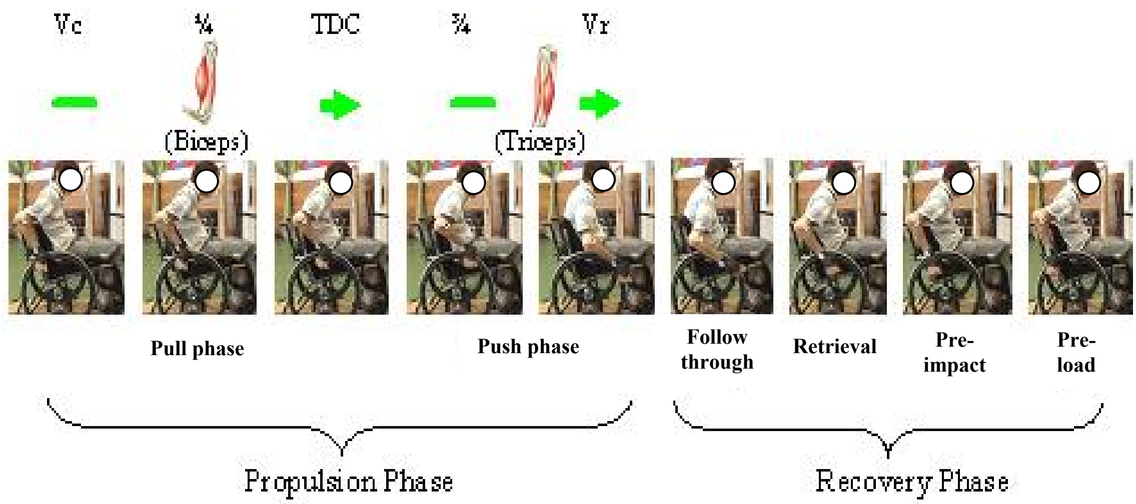

Figure 1.5 *The phases of wheelchair propulsion adapted form Cooper et al. [42]*

1.4 Existing methods for measuring wheelchair propulsion

Given the above, wheelchair propulsion is accomplished by the bilateral, simultaneous, repetitive motion of the upper extremities. Over the last decade, researchers have demonstrated that the biomechanics of wheelchair propulsion varies in relation to the subjects' levels of SCI [16, 18, 20]. The methods used in these studies for measuring wheelchair propulsion ability included the determination of biomechanical characteristics, such as upper-limb kinematics and push-rim force application. First, the test environment determined the test apparatus chosen. While measuring wheelchair propulsion in an actual outdoor environment was considered ideal (Figure 1.6A), simulation in a laboratory [1] was preferred because body movement could be better controlled and more accurately assessed. Therefore, stationary wheelchair ergometers (Figure 1.6B) and dynamometer systems (Figure 1.6C & D) were widely used to study propulsion abilities of wheelchair users.

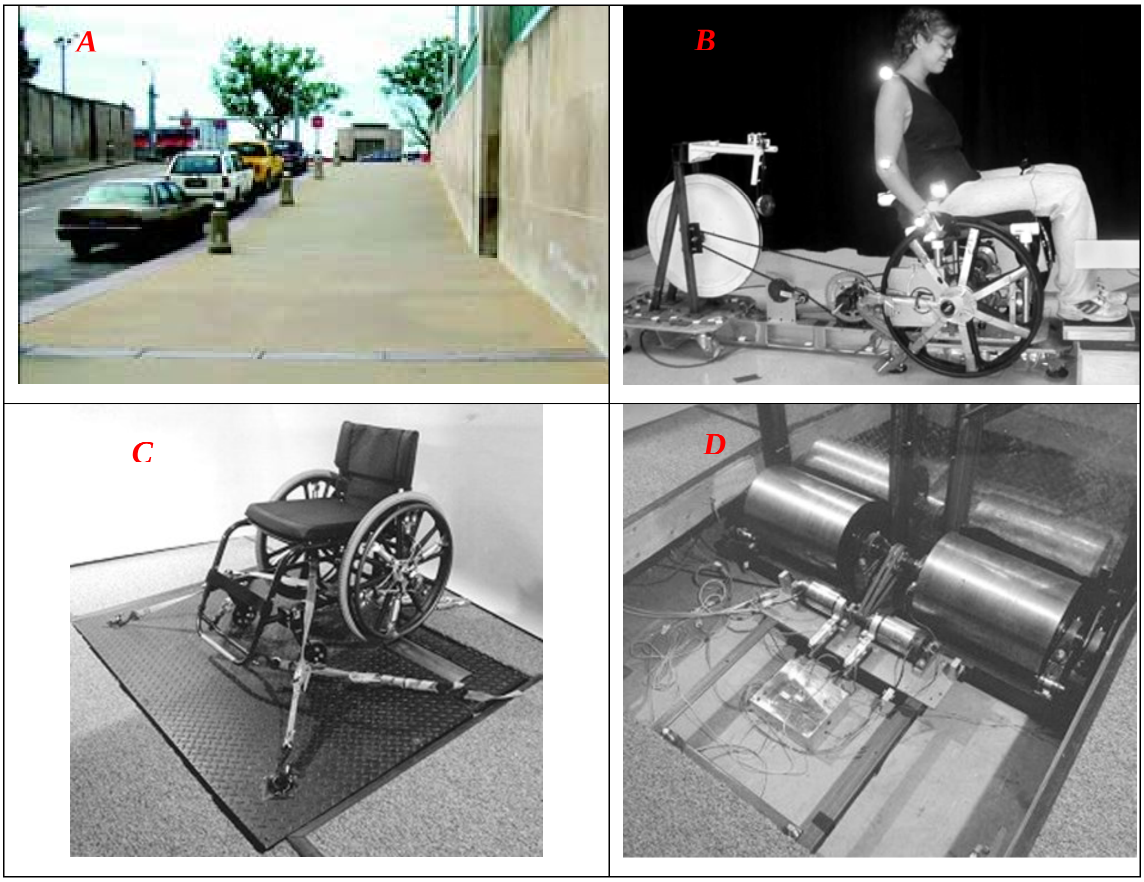

Figure 1.6 *The real outside test environment (A) [21] and the wheelchair ergometer (B) [43] and dynamometer(C & D) [44] used in early studies*

Furthermore, researchers investigated different wheel-based measurement systems, which allowed for the collection of propulsion kinetics and wheelchair kinematics. Sabick et al. [45] used a custom-developed wheelchair wheel with an instrumented push-rim, a load cell assembly, and a data logging device to collect kinetic data during wheelchair propulsion up a ramp at four different grades (level, 20:1; 12:1, and 8:1). Newsam et al. [16, 18] introduced the strain gauge force transducer for determining forces and torque applied to the push rim to identify the start and end of hand and push rim contact. Cooper et al. described the SMART^{Wheel} [15, 19, 21, 46], a commercial force- and torque- sensing push-rim wheel that has been used in several studies to examine three-dimensional (3D) propulsion forces, moments, and temporal characteristics over different surfaces and inclines. The SMART^{Wheel} contains an on-board optical encoder that determines the rotational angle of the wheel, which can determine average velocities, distances travelled per stroke as shown in Figure 1.7A. Finally, video cameras were employed for capturing the upper body motions during the test process and a 3D capturing system (Figure 1.7B) was generally used for generating better arcs.

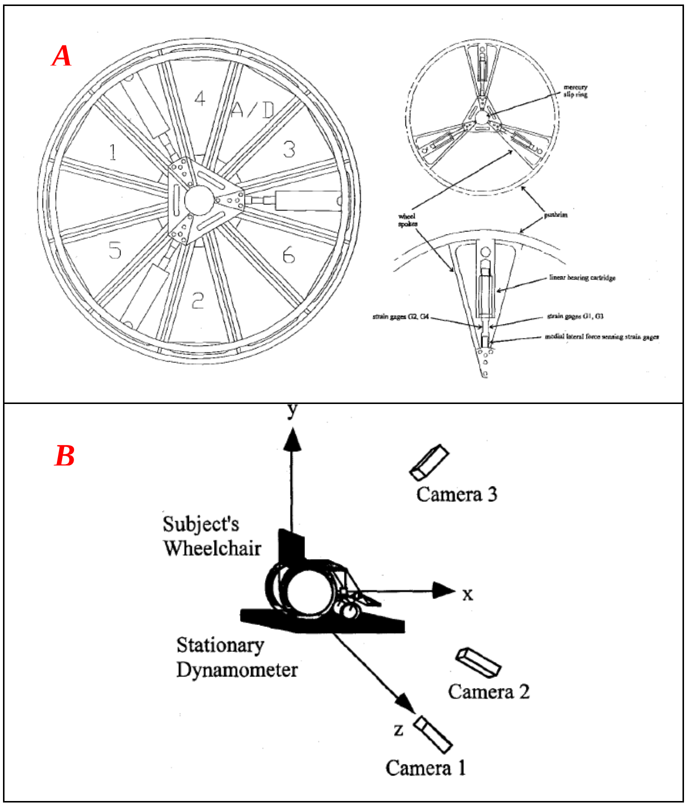

Figure 1.7 *The SMART^{Wheel} [46] and 3D kinematics measurement system [46] used in early study*

The development of biomechanical model is also essential. To clarify how the body segments, which includes shoulder, elbow, wrist and trunk, interact mechanically to execute motor tasks, mathematical models have been applied and updated initially from the sagittal plane in two dimensions (2D) to 3D kinematic analyses, as shown in Figure 1.8 (A-D).

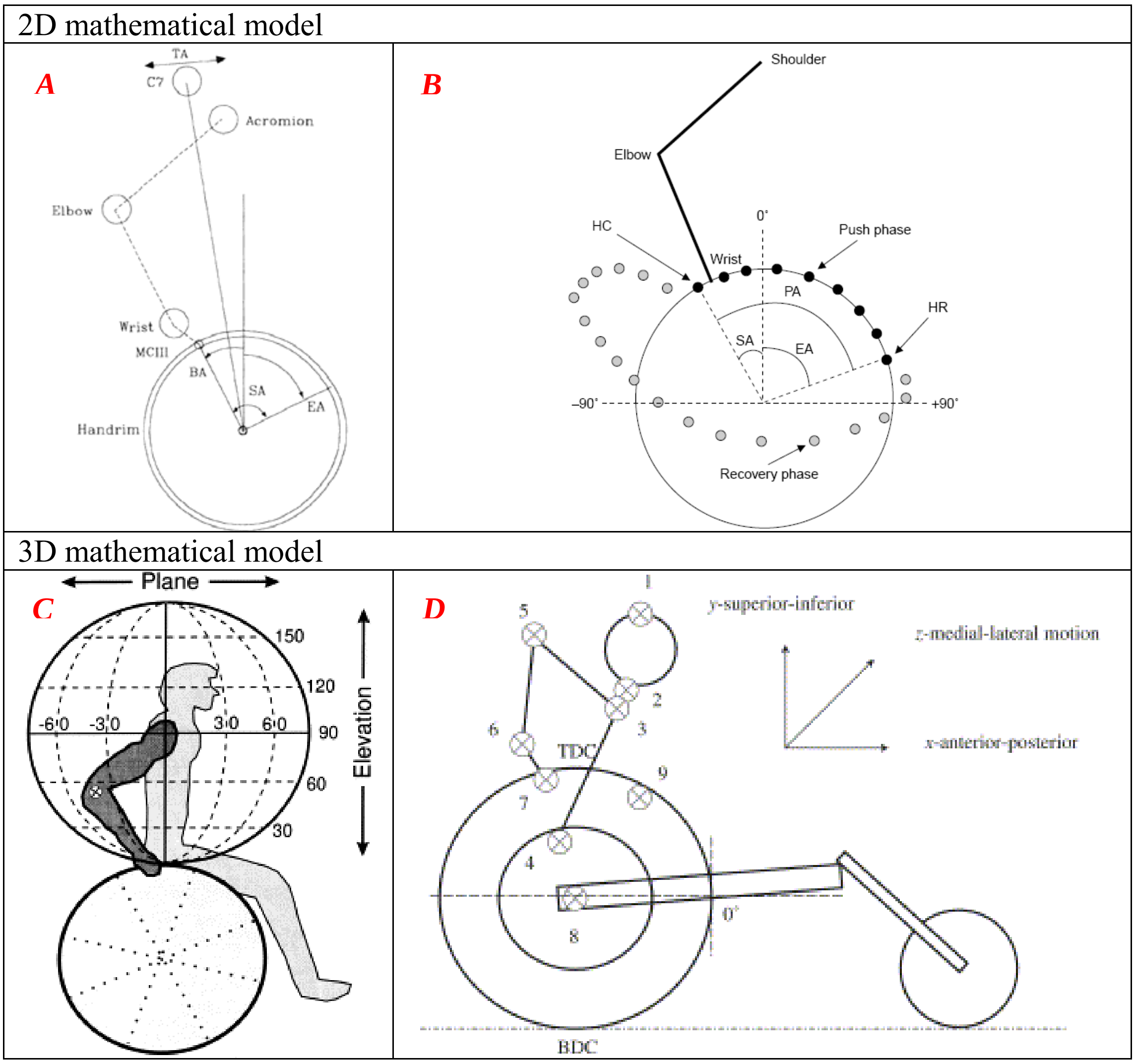

Figure 1.8 *2D (A [47] & B [1] and 3D (C [16] & D [48]) mathematical models used by early studies*

1.5 Predicting wheelchair propulsion forces

Apart from using sensors, such as strain gauge force transducers and the SMART^{Wheel} discussed above, wheelchair propulsion forces also can be predicted by the assumption of propelling a wheelchair with constant velocity on a slope. The important quantities in measuring wheelchair propulsion ability are listed below, which include wheelchair mass properties, kinematics, resistance forces, tractive force, work and power.

1.5.1 Wheelchair mass properties

Figure 1.9 shows the mass properties for the wheelchair, with the vertical ground forces written in the form:

$$RF = \frac{mgl_1}{l_1 + l_2}$$
$$RR = \frac{mgl_2}{l_1 + l_2} \qquad 1.1$$

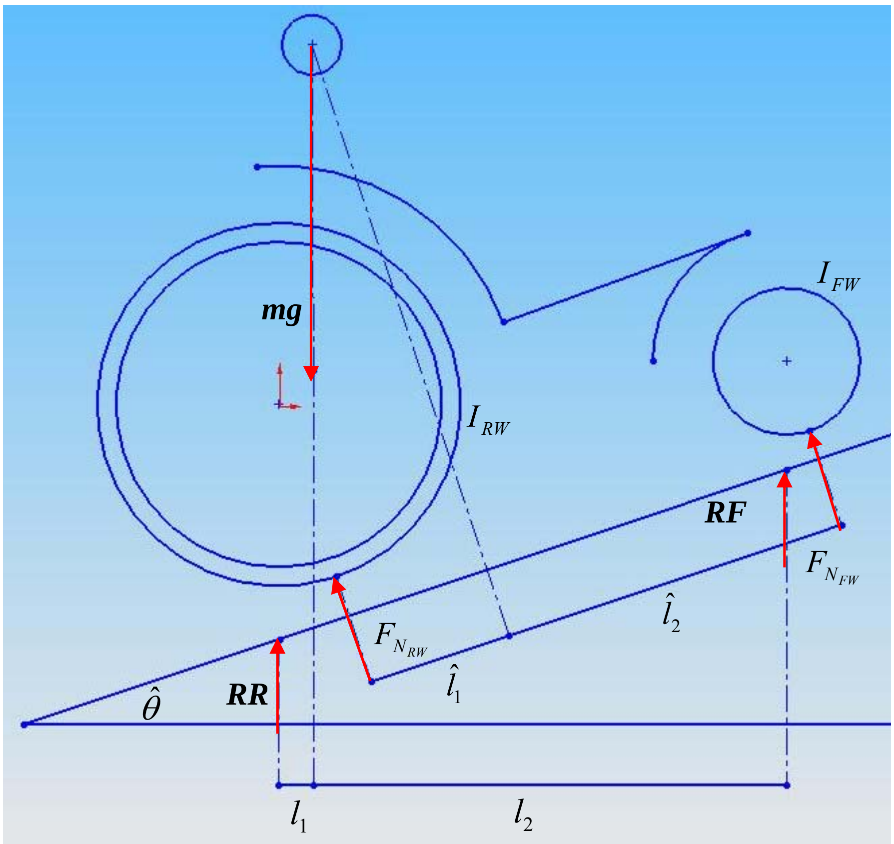

Figure 1.9 *Mass properties for the wheelchair*

I_{FW}

I_{RW}

1.5.2 Wheelchair kinematics

The linear wheelchair displacement, velocity and acceleration are defined as x, $\dot{x}$ and $\ddot{x}$ respectively. Wheelchair kinematics can also be described in terms of angular wheel displacement, velocity and acceleration as listed below:

$$x = \theta r \quad 1.2$$

$$\dot{x} = \dot{\theta} r \quad 1.3$$

$$\ddot{x} = \ddot{\theta} r \quad 1.4$$

1.5.3 Wheelchair resistance forces

In order to sustain a constant velocity, the wheelchair user must overcome resistance forces associated with tyre contact losses, aerodynamic drag and mechanical losses. Tyre contact forces are caused by surface/tyre deformation, and result in a resistive force acting in the opposite direction to the applied wheel torque. Resistance due to tyre deformation is shown schematically in Figure 1.10.

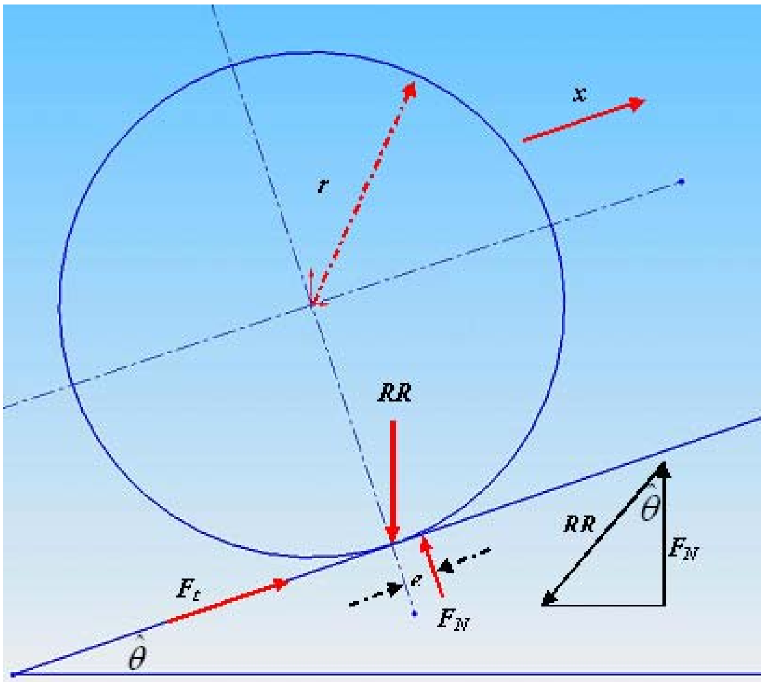

Figure 1.10 *Resistance due to tyre deformation*

The total resistance due to tyre deformation will be the sum of the resistance from all four wheels, namely:

$$F_{N_{RW}} = RR\cos\hat{\theta}\frac{e_{RW}}{r_{RW}} + RF\cos\hat{\theta}\frac{e_{RF}}{r_{RF}} \quad 1.5$$

Aerodynamic drag will be calculated as:

$$F_D = \frac{\rho A\dot{x}^2}{2} \quad 1.6$$

1.5.4 Tractive force

The tractive force is parallel with the tractive surface (x direction in Figure 1.11) at the tyre/ground interface. A tractive force is required to maintain a static position or constant velocity on a slope, maintain a constant velocity by matching the sum of the wheelchair resistance forces and accelerate the wheelchair. The tractive force, in manual wheelchair propulsion, is created by a user action, namely a force applied to the wheelchair push rim. For equilibrium, the sum of the tractive force and the resistive forces is equal to the inertia force (Newton's Second Law). The free body diagram, Figure 1.11, shows the tractive and resistive forces.

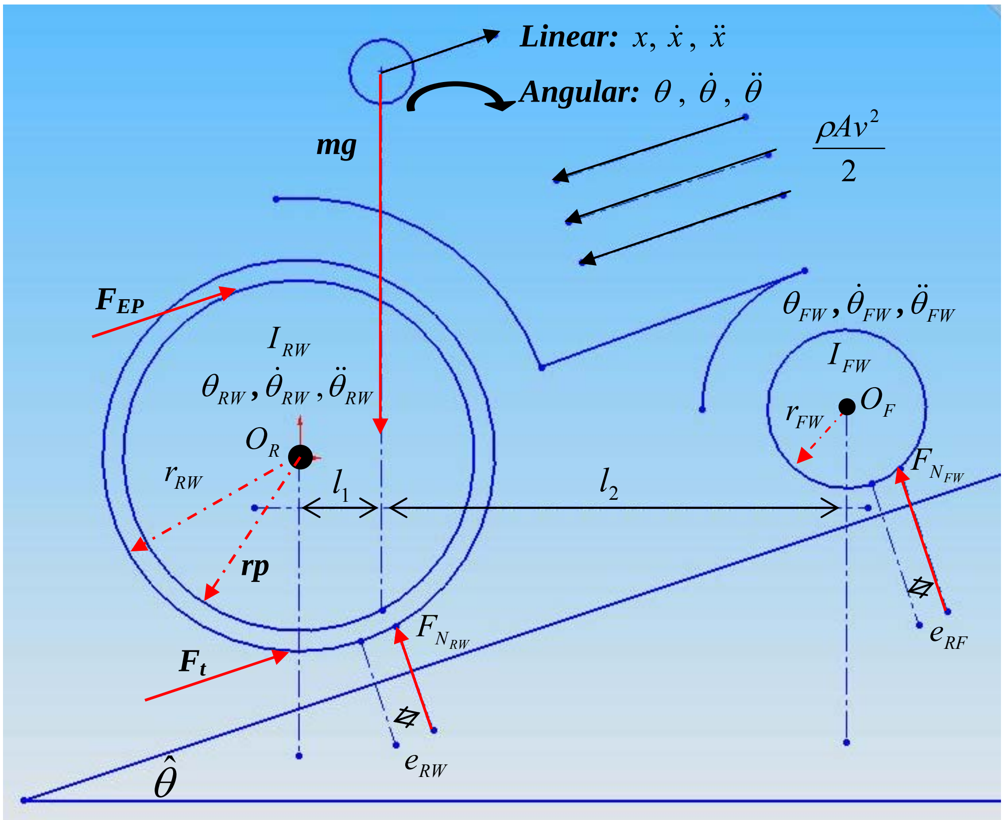

Figure 1.11 *Free body diagram of the wheelchair*

Considering Figure 1.11, applying Newton's second law, the equation of motion for the wheelchair can be written in the form

$$F_t - mg\sin\hat{\theta} - RR\cos\hat{\theta}\,\frac{\mathrm{e_{RW}}}{\mathrm{r_{RW}}} - RF\cos\hat{\theta}\,\frac{\mathrm{e_{FW}}}{\mathrm{r_{FW}}} - \frac{1}{2}\rho C_D A\dot{x}^2 - TLF_{RW} - TLF_{FW} = m\ddot{x} + 2I_{RW}\frac{\ddot{\theta}_{RW}}{r_{RW}} + 2I_{FW}\frac{\ddot{\theta}_{FW}}{r_{FW}} \qquad 1.7$$

Summing moments about the rear wheel axel 'O' and rearranging, the relationship between tractive force and push rim force is:

$$F_{EP} = \frac{F_t r_{RW}}{rp} \qquad 1.8$$

1.5.6 Work and power

The purpose of a wheelchair is to enable a person to get from one place to another, i.e. from position X_0 to position X_1. To move from position X_0 to position X_1 requires a ground force Ft to be applied over distance *X*. This ground force is created by a force F_{EP} applied at a radius *rp* over angle (θ). If a force or torque have been applied to move from position X_0 to position X_1 then work has been done. Work is therefore a useful quantity to measure because it determines whether a person has the ability to get from position X_0 to X_1. Assuming a constant push rim force, work can be defined as:

$$W = \int_{\theta_{RW_1}}^{\theta_{RW_2}} F_{EP}\, rp\, \theta_{RW} . d\theta_{RW} \qquad 1.9$$

While a certain amount of work is required to move from position X_0 to X_1, the task of moving must be completed within a reasonable time otherwise the method will be impractical. Hence, it is useful to measure of the rate at which work can be done, i.e. the power, which can be calculated using:

$$P = \frac{dW}{dt} \qquad 1.10$$

1.6 Proposed method of assessing wheelchair propulsion

In this study, to obtain insight into the basic mechanism of manual wheelchair propulsion for people with different SCI levels, a dual approach was undertaken, combining dynamic simulation and optimization procedures in mathematical modelling with experimental data collection under realistic wheelchair propulsion conditions. Both approaches were complementary because the experimental data served as input for the model and the output of the model provided insight into the mechanism of body movement, which related to the outcomes and consequences, such as performance and efficiency. After evaluating the previously adopted methods (as further discussed in Chapter 2), a dynamometer was chosen to measure values for the velocity and acceleration of the wheelchair, resulting from the force that individuals apply to the wheel of their chairs. To achieve this, data was collected directly from the dynamometer, and a computer program was employed to calculate the velocity and acceleration outputs. The kinematics system was developed for more accurate analysis of wheelchair propulsion motion. As a result, tractive effort on a dynamometer and rolling resistance coefficient was determined.

1.6.1 Tractive effort calculations using a dynamometer

The purpose of the dynamometer is to provide a resistance to propulsion that can be measured and compared with normal wheelchair propulsion. Figure 1.12 shows the free body diagram of the wheelchair on the dynamometer.

Noting that the rear wheelchair wheels are on independent rollers, applying Newton's second law, the equation of motion for the right side wheelchair wheel on the right side dynamometer drum may be written as:

$$F_{t_{RR}} - \frac{RR}{2}\frac{\mathrm{e}_{\mathrm{RW}}}{\mathrm{r}_{\mathrm{RW}}} - TLF_{RW_{RR}} - TLF_{RR} = \frac{I_R\ddot{\theta}_R}{rr} + I_{RW}\frac{\ddot{\theta}_{RW}}{r_{RW}} \qquad 1.11$$

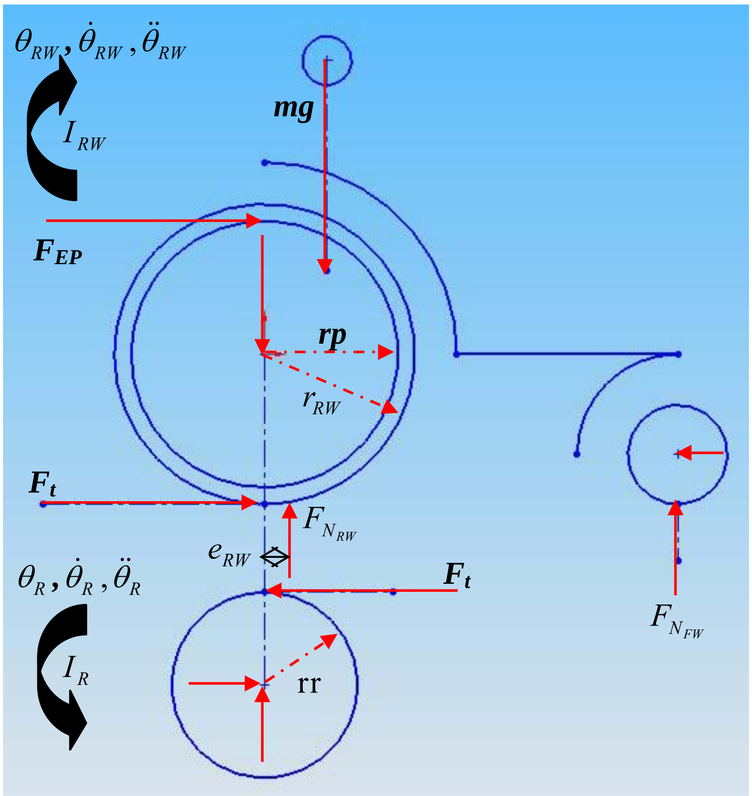

Figure 1.12 *Free body diagram for the wheelchair on the dynamometer*

1.6.2 Wheelchair loss predictions

A rolling resistance coefficient can be measured using a coast-down test. By asking participants to propel their wheelchairs at a comfortable speed in the gymnasium and then allow their wheelchair to 'coast-down' to rest, the deceleration of the wheelchair could be measured. This assumes that wheel bearing and windage losses are small compared with rolling resistance due to tyre deformation; wheel inertia forces are small compared with the total mass force; and the wheelchair is moving on a horizontal surface and the aerodynamic drag force is small. Based on the assumptions listed above, the total rolling resistance can be determined using:

$$RR\frac{\mathrm{e_{RW}}}{\mathrm{r_{RW}}} + RF\frac{\mathrm{e_{FW}}}{\mathrm{r_{FW}}} = m\ddot{x} \qquad 1.12$$

Similarly, the rolling resistance force can be determined for each roller on the dynamometer using:

$$\frac{RR}{2}\frac{\mathrm{e_{RW}}}{\mathrm{r_{RW}}} = \frac{I_R\ddot{\theta}_R}{rr} \qquad 1.13$$

1.6.3 Realistic simulation factors

Apart from the above, the approach represented in this research requires simulating wheelchair propulsion under realistic conditions. Since backward tilting [56] is prevented on most stationary dynamometers, the forces generated on the push rims will be much higher compared with the same task under flat floor conditions, especially during the start of a sprint task. Inertial forces acting on the wheelchair caused by acceleration and deceleration of the trunk and arms are neglected in stationary systems. Furthermore, the test procedure should be representative of the different components of the wheeling task, for example, starting, wheeling and sprinting. Changes in external conditions, such as slope and resistance, should be simulated aiming at performance improvements. Finally, a combined cinematographic and kinetic approach will significantly increase the accuracy of hand contact and hand release identification.

1.7 Summary

Current standard methods of measuring wheelchair propulsion ability for people with different SCI levels have adopted wheel-based measurement systems, such as strain gauge force transducers and the SMART^{Wheel}, and allow for the collection of propulsion kinetics and wheelchair kinematics. In this project, a new method is proposed based on the assumption of propelling a wheelchair with constant velocity on a slope, and by considering different propulsion techniques applied. Important quantities in measuring wheelchair propulsion ability will be measured using a custom designed wheelchair dynamometer, and will include wheelchair mass properties, kinematics, resistance forces, tractive force and power output. Furthermore, a biomechanical model will be developed to determine how body segments interact mechanically to execute motor tasks. After completing the design and validation of the new procedure for measuring manual wheelchair propulsion ability, and in order to simulate wheelchair propulsion under realistic conditions, the effect of SCI level on wheelchair propulsion ability will be quantified, along with demonstrating whether wheelchair propulsion kinetic and kinematics changes result following TROIDS surgery.

1.8 Objectives

The purpose of this project is to develop a new approach to measurement and modeling of wheelchair propulsion for quantifying the effect of SCI level on wheelchair propulsion ability, which has been divided as three chapters.

I. Establishment and validation of a new procedure for measuring manual wheelchair propulsion ability in subjects with SCI

The procedure includes the method evaluation, test rig design, calibration and validation of a new wheelchair dynamometer. Before testing subjects with SCI, the results of able-bodied subjects will be compared with literature to verify the system's validity.

II. Quantifying the effect of SCI level on wheelchair propulsion ability and characterizing wheelchair propulsion kinematics for people with different SCI levels

After determining the mathematical model and test procedure, which can fully investigate the wheelchair propulsion ability, the subjects involved in this study will be divided into different groups depending on the SCI level and the control of muscles, such as triceps and abdominals. Both kinetic data (power output, torque and force) and kinematics (velocity and arm motion) will be analysed to compare with other studies.

III. Demonstrating any improvement in power of wheelchair propulsion and representing wheelchair propulsion kinematics following TROIDS surgery

Due to the importance of triceps function for wheelchair propulsion, the focus will be put on the group of C5/C6 tetraplegia along with TROIDS transfer surgery. The improvements will not only be measured on amplitude, strength and speed of arm movement, but also on propulsion technique.

References

[1] Yves Vanlandewijck, Daniel Theisen and Dan Daly. Wheelchair Propulsion Biomechanics (Implication for Wheelchair Sports). Sports Med 2001; 31 (5): 339-367

[2] L.H. van der Woude, W.H. Bakker, J.W. Elkhuizen, H.E. Veeger and T. Gwinn. Propulsion technique and anaerobic work capacity in elite wheelchair athletes: cross-sectional analysis. Am J Phys Med Rehabil 77 (1998), pp. 222–234.

[3] A.J. Dallmeijer, L.H. van der Woude, A.P. Hollander and H.H. van As. Physical performance during rehabilitation in persons with spinal cord injuries. Med Sci Sports Exerc 31 (1999), pp. 1330–1335.

[4] F.S. Duran, L. Lugo, L. Ramirez and E.E. Lic. Effects of an exercise program on the rehabilitation of patients with spinal cord injury. Arch Phys Med Rehabil 82 (2001), pp. 1349–1354.

[5] R.H. Jebsen, R.B. Trieschmann, M.A. Mikulic, R.B. Hartley, J.A. McMillan and M.E. Snook. Measurement of time in a standardized test of patient mobility. Arch Phys Med Rehabil 51 (1970), pp. 170–175.

[6] R.L. Kirby, J. Swuste, D.J. Dupuis, D.A. MacLeod and R. Monroe. The Wheelchair Skills Test: a pilot study of a new outcome measure. Arch Phys Med Rehabil 83 (2002), pp. 10–18.

[7] T.W. Janssen, C.A. van Oers, H.E. Veeger, A.P. Hollander, L.H. van der Woude and R.H. Rozendal. Relationship between physical strain during standardised ADL tasks and physical capacity in men with spinal cord injuries. Paraplegia 32 (1994), pp. 844–859.

[8] J.F. Lehmann, C.G. Warren, E. Halar, J.B. Stonebridge and B.J. DeLateur. Wheelchair propulsion in the quadriplegic patient. Arch Phys Med Rehabil 55 (1974), pp. 183–186.

[9] M. Taricco, C. Colombo, R. Adone et al. The social and vocational outcome of spinal cord injury patients. Paraplegia 30 (1992), pp. 214–219.

[10] M.N. Sawka, R.M. Glaser, L.L. Laubach, O. Al-Samkari and A.G. Suryaprasad. Wheelchair exercise performance of the young, middle-aged, and elderly. J Appl Physiol 50 (1981), pp. 824–828.

[11] S.A. Morrison, S.L. Melton-Rogers and S.P. Hooker. Changes in physical capacity and physical strain in persons with acute spinal cord injury. Top Spinal Cord Inj Rehabil 3 (1997), pp. 1–15.

[12] T.W. Janssen, A.J. Dallmeijer, D.J. Veeger and L.H. van der Woude. Normative values and determinants of physical capacity in individuals with spinal cord injury. J Rehabil Res Dev 39 (2002), pp. 29–39.

[13] L. Noreau. Relationship of impairment and functional ability to habitual activity and fitness following spinal cord injury. Int J Rehabil Res 16 (1993), pp. 265–275.

[14] A.J. Dallmeijer, L.H. van der Woude, P.A. Hollander and E.L. Angenot. Physical performance in persons with spinal cord injuries after discharge from rehabilitation. Med Sci Sports Exerc 31 (1999), pp. 1111–1117.

[15] Alicia M Koonta, Rory A. Cooper, Michael L. Boninger, Aaron L. Souza, Brian T. Fay. Shoulder kinematics and kinetics during two speeds of wheelchair propulsion. Journal of Rehabitation Research and Development Vol. 39 No. 6 pp 635-650 November/December 2002

[16] Craig J. Newsam, Sreesha S. Rao, Sara J. Mulsroy, JoAnne K. Gronley, Ernest l. Bontrager and Jacquelin Perry. Three dimentional upper extremity motion during manual wheelchair propulsion in men with different level of spinal cord injury. http://www.elsebier.com/locat/gaitpost

[17] Kornelia Kulig, Sreesha S. Rao and Sara J. Mulroy. Shoulder joint kinetics during the push phase of wheelchair propulsion. Clinical Orthopaedics and Related Research Number 354 pp 132-143 March 25 1998

[18] Korelia Kulig, Craig J. Newsam and Sara J Mulroy. The effect of level of spinal cord injury on shoulder joint kinetic during manual wheelchair propulsion. Clinical Biomechanics 16 (2001) pp 744-751 July 2001

[19] Rick N. Robertson, PhD, Michael L. Boninger, MD, Rory A. Cooper, PhD and Sean D. Shimada, MS. Pushrim Forces and Joint Kinetics During Wheelchair Propulsion. Arch Phys Med Rehabil Vol 77, September 1996.

[20] Annet J. Dallmeijer, MSc Luc H. V. van der Woude PhD, H. E. J. (DirkJan) Veeger, PhD and A. Peter Hollander, PhD. Effectiveness of force application in manual wheelchair propulsion in persons with spinal cord injuries. American Journal Of Physical Medicine and Rehabilitation. 1998

[21] Alicia M. Koontz, Rory A. Cooper, Michael L. Boninger, Yusheng Yang, Bradley G. Impink and Lucas H.V. van der Woude. A kinetic analysis of manual wheelchair propulsion during start-up on select indoor and outdoor surfaces. Journal of Rehabilitation Research and Development Vol 42 NO 4, July/August 2005 Pages 447-458

[22] Freehafer AA. Tendon transfers in patients with cervical spinal cord injury. J Hand Surg 1991; 16A: 804-809.

[23] Lamb DW and Chan KM. Surgical reconstruction of the upper limb in traumatic tetraplegia. A review of 41 patients. J Bone Joint Surg 1983;65B:291-298.

[24] O Remy-Neris, J Milcamps, R Chikhi-Keromest, A Thevenon, D Bouttens and S Bouilland. Improved kinematics of unrestrained arm rasing in C5-C6 tetraplegic subjects after deltoid-to-triceps transfer. Unite des blesses medullaires, Centre Calve, Groupe Hopale, Berck sur mer, France. 2003 41, 435-445.

[25] Moberg E. Surgical rehabilitation of the upper limb in tetraplegia. Paraplegia 1990; 28:330-334.

[26] Moberg E. The present state of surgical rehabilitation of the upper limb in tetraplegia. Paraplegia 1987; 25:351-356.

[27] Raczka R, Braun R and Waters RL. Posterior deltoid-to-triceps transfer in quadriplegia. Clin Orthop 1984; 187: 163-167.

[28] Ejeskar A and Dahllof A. Results of reconstructive surgery in the upper limb of tetraplegic patients. Paraplegia 1988; 26: 204-208.

[29] Richard L. Lieber, PhD, San Diego, CA, Jan Friden, MD, PhD, Goteborg, Sweden, Toni Hobbs, BS, Alastair G. Rothwell, MD, Christchurch, New Zealand. Analysis of Posterior Deltoid Function One Year After Surgical Restoration of Elbow Extension. The Journal of Hand Surgery. January 6, 2003.

[30] William D. Memberg, MS; Patrick E. Crago, PhD; Michael W. Keith, MD. Restoration of elbow extension via functional electrical stimulation in individuals with tetraplegia. Journal of Rehabilitation Research & Development. Volume 40 Number 6, November/Decemeber 2003 Pages 477-486

[31] Robert F. Kirsch, Ana Maria Acosta, Eric J. Perreault, and Michael W. Keith. Measurement of Isometric Elbow and Shoulder Moments: Position-Dependent Strength of Posterior Deltoid-to-Triceps Muscle Tendon Transfer in Tetraplegia. IEEE TRANSACTIONS ON REHABILITATION ENGINEERING, VOL. 4, NO. 4, DECEMBER 1996

[32] R.F. Kirsch, A.M. Acosta, E.J. Perreault, W.D. Memberg, M.W. Keith, and P.E. Crago. APPROACHES FOR RESTORING ELBOW EXTENSION IN

TETRAPLEGIA: MUSCLE TENDON TRANSFER AND FUNCTIONAL NEUROMUSCULAR STIMULATION. 18th Annual International Conference of the IEEE Engineering in Medicine and Biology Society, Amsterdam 1996. 2.5.2: FES I1 - Control Strategies

[33] AL Dunkerley, A Ashburn and EL Stack. Deltoid triceps transfer and functional independence of people with tetraplegia. Spinal Cord 2000; 38: 435-441.

[34] J D Steeves, D Lammertse, A Curt, J W Fawcett, M H Tuszynski, J F Ditunno, P H Ellaway, M G Fehlings, J D Guest, N Kleitman, P F Bartlett, A R Blight, V Dietz, B H Dobkin, R Grossman, D Short, M Nakamura, W P Coleman, M Gaviria and A Privat. Guidelines for the conduct of clinical trials for spinal cord injury (SCI) as developed by the ICCP panel: clinical trial outcome measures. Spinal Cord advance online publication 19 December 2006;

[35] Rich Hansen Foundation, About SCI & Links. 26 July 2007. www.rickhansen.com/index.php?option=com_content&task=view&id=67&Itemid=6

[36] Yagesh Bhambhani. Physiology of Wheelchair Racing in Athletes with Spinal Cord Injury. Sports Med 2002; 32 (1): 23-51

[37] L Floris, C Dif and MA Le Mouel. The tetraplegic patient and the environment. Surgical rehabilitation of the upper limb in tetraplegia. Chapter 5.

[38] Clinical information. www.nisu.flinders.edu.au/pubs/bulletin16/bulletin16-Clinical.html

[39] Sandra Connolly, BHScOT, OT Reg (Ont.), JoAnne Aubut, BA, Robert W Teasell MD FRCPC and Tal Jarus, PhD, OTR. Upper Limb Rehabilitation Following Spinal Cord Injury. Spinal cord injury rehabilitation evidence.

[40] KHALID D. MOHAMMED, ALASTAIR G. ROTHWELL, STUARTW. SINCLAIR, SUE M. WILLEMS and ALLAN R. BEAN. UPPER-LIMB SURGERY FOR TETRAPLEGIA. Burwood Hospital Christchurch. THE JOURNAL OF BONE AND JOINT SURGERY. VOL. 74-B, NO. 6, November 1992.

[41] Mark Schmeler, MS, OTR/L, ATP and Mary Ellen Buning, MS, OTR, ATP. Manual Wheelchairs: Set-Up & Propulsion Biomechanics. Schmeler, MR & Buning, ME. October 1999.

[42] Rory A. Cooper. Rehabilitation Engineering (Applied to Mobility and Manipulation)

[43] Margaret A. Finley, PhD, PT; Elizabeth K. Rasch, MS, PT; Randall E. Keyser, PhD; Mary M. Rodgers, PhD, PT. The biomechanics of wheelchair propulsion in individuals with and without upper-limb impairment. Journal of Rehabilitation Research & Development. May/June 2004. Volume 41, Number 3B, Pages 385–394.

[44] Carmen P. DiGiovine, Rory A. Cooper and Michael A Boninger. Dynamic calibration of a wheelchair dynamometer. Journal of Rehabilitation Research and Development Vol. 38 No. 1, January and February 2001

[45] Meyers AR, Anderson JJ, Miller DR, Shipp K, Hoenig H. Barriers, facilitators, and access for wheelchair users: substantive and methodologic lessons from a pilot study of environmental effects. Soc Sci Med. 2002;55:1435-46.

[46] Rory A. Cooper, Senior Member, IEEE, David P. VanSickle, Rick N. Robertson, Member, IEEE, Michael L. Boninger, and Greg J. Ensminger. A Method for Analyzing Center of Pressure During Manual Wheelchair Propulsion. IEEE TRANSACTIONS ON REHABILITATION ENGINEERING, VOL. 3, NO. 4, DECEMBER 1995

[47] Annet J. Dallmeijer, Yvonne J.Kappe, Dirkjan H.E.J. Veeger, Thomas W.J.Jassen and Luc H.V. van der Woude. Anaerobic power output and propulsion technique in spinal cord injured subjects during wheelchair ergometer. Journal of Rehabilitation Research and Development Vol. 31 No. 2, 1994 Pages 120-128

[48] A.D. Moss, N.E. Fowler and V.L. Goosey-Tolfrey. The intra-push velocity profile of the over-ground racing wheelchair sprint start. Journal of Biomechanics 38 (2005) 15-12

[49] Snoek GJ, Ijzerman J, Post MW, Stiggelbout AM, Roach MJ, Zilvold G. Choice based evaluation for the improvement of upper-extremity function compared with other impairments in tetraplegia. Arch Phys Med Rehabil 2005; 86: August, 1623-1630.

[50] Ditunno JF. Predicting recovery after spinal cord injury. A rehabilitation imperative. Arch Phys Med Rehabil 1999; 80: 361-364.

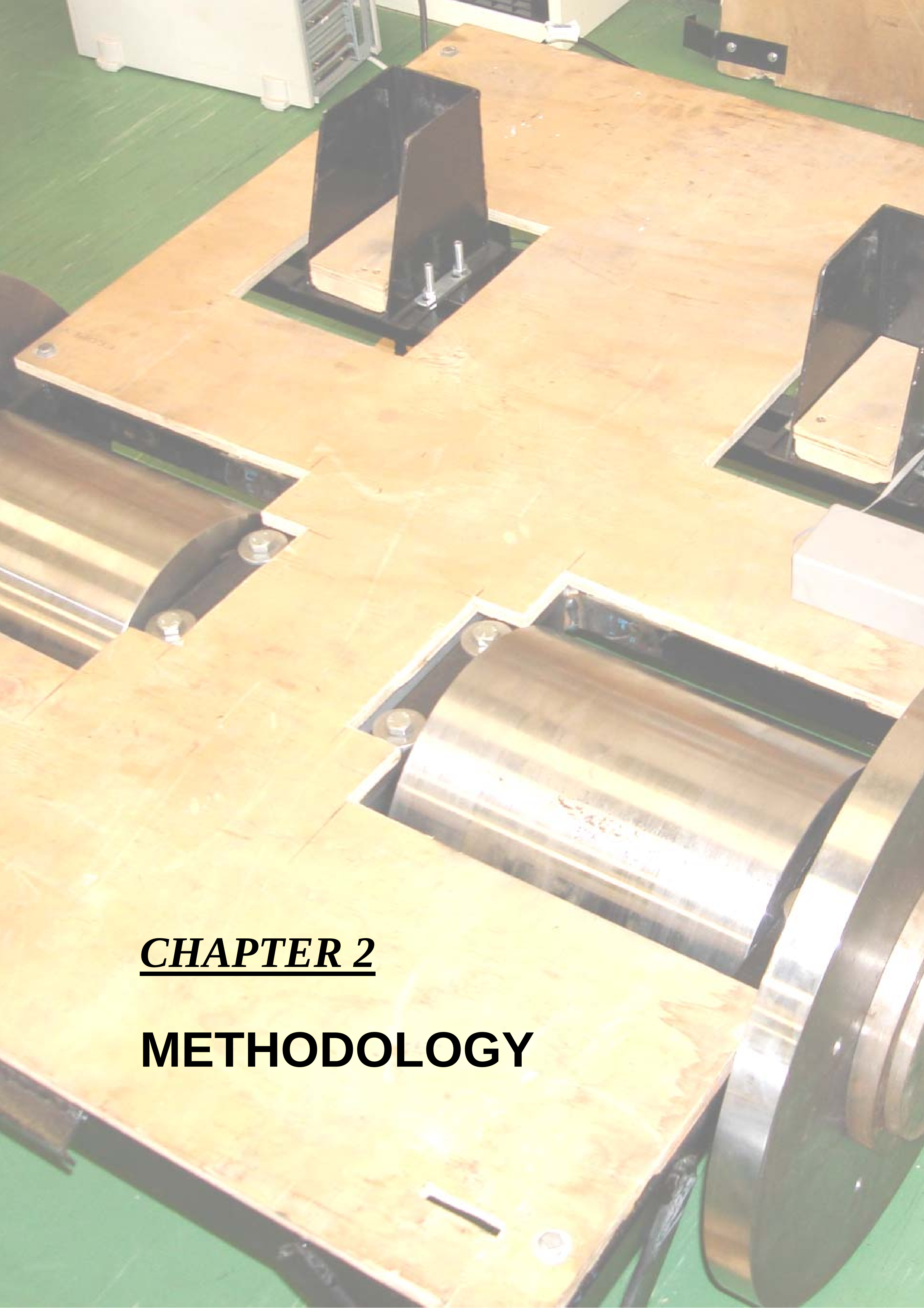

CHAPTER 2

METHODOLOGY

A Procedure for Measuring Manual Wheelchair Propulsion Ability for People with Spinal Cord Injuries

Summary

Purpose: This study evolves a means of measuring manual wheelchair propulsion ability so that the effects of surgical procedures can be objectively evaluated.

Method: Wheelchair propulsion is an important part of daily living for many people with spinal cord injuries (SCI's). Higher injury levels severely restrict the ability of people with SCI's to negotiate obstacles, ramps and uneven surfaces. Seventeen people with SCI's were tested while propelling their wheelchairs. The test involved varying levels of resistance from a self-selected comfortable speed along flat ground to maximum effort up a steep (12:1) ramp. Wheelchair propulsion techniques were captured using a video camera. The criteria for measuring wheelchair propulsion were formulated and wheelchair propulsion measurement methods such as test tracks, dynamometers and instrumented push rims assessed. A new inertia dynamometer was built and calibrated.

Results: From analysis of the video data, the well-documented differences in upper body motion with level of SCI were observed. A significant observation in terms of measuring wheelchair propulsion ability was the variation of techniques used for grasping the push rim. More than 80 percent of the participants in this study used the push rim and tyre together to apply torque to their wheelchair wheels. While some earlier studies have used instrumented push rims (including the SMART^{Wheel}) for people with tetraplegia, these methods would not have given a true indication of propulsion ability for the participants in this study. Wheelchair distance, velocity and acceleration were plotted against time and compared with the literature.

Conclusions: The use of instrumented push rims such as the SMART^{Wheel}, used exclusively, would not be expected to give a true measure of wheelchair propulsion ability for people with tetraplegia. This is because people with tetraplegia generally contact both the push rim and tyre to impart motion to their wheelchair wheels.

Nomenclature

Algebraic symbols	
T_{K_1}	Kinetic energy for occupant and wheelchair (J)
m	Mass of wheelchair and occupant (kg)
$\dot{x}$	Linear wheelchair velocity (m/s)
T_{K_2}	Kinetic energy for one roller (J)
I	Polar mass moment of inertia (kgm^2)
$\dot{\theta}_R$	Angular velocity for roller (rad/s)
m_R	Mass of one roller (kg)
r_R	Radius of roller (m)
I_{req}	Inertia required, which is related to *m* (kgm^2)
F_t	Tractive force (N)
F_{ro}	Rolling resistance force (N)
F_D	Aerodynamic force (N)
g	Gravity (9.81m/s^2)
C_{rr}	Coefficient of rolling resistance
F_N	Normal wheel force at ground (N)
C_D	Drag coefficient
A	Frontal wheelchair area including occupant (m^2)
$\ddot{x}$	Linear wheelchair acceleration (m/s^2)
$\dot{\theta}$	Angular wheelchair velocity (rad/s)
$\ddot{\theta}$	Angular wheelchair acceleration (rad/s^2)
T_W	Torque on wheel (Nm)
Greek symbols	
$\hat{\theta}$	Gradient (rad)
ρ	Air density (1.23 kg/m^3)
Suffixes	
W	Wheel
R	Roller

2.1 Introduction

Most wheelchair users prefer to use a hand rim wheelchair in everyday life, with rims of a relatively large diameter [1]. This type of wheelchair offers many advantages with respect to ease of transportation and flexibility of use in general [1]. Proficient wheelchair use is important in achieving independent mobility. As a result, measuring wheelchair propulsion ability is essential for enabling wheelchair users to deal with the physical barriers they will inevitably encounter in various environments and in making the difference between dependence and independence in daily life. Current methods for measuring wheelchair propulsion ability include the determination of propulsion performance kinetics and wheelchair kinematics (Table 2.1). Methods for acquiring kinematic data are divided into two parts; distance, acceleration and velocity data based on the information gathered from encoders attached on the test rig for example, or from a mobility course and video recordings providing motion analysis data. Additional kinetic data, for example, force and torque, can be measured directly from some sensor devices, such as a SMART^{Wheel} [2-4] or strain gauge transducers [5-6].

Table 2.1 *Summary of methods for measuring wheelchair propulsion*

Kinematics data	**Methods**	**Outputs**
Distance Velocity Acceleration	A scoring system (FIM [7], Mobility course [4])	Performance of activities of daily living
	Ergometer [5-6, 8-14]	Measuring work and power
	Dynamometer [2-3, 15-16]	Not only can measure work and power, but also can measure torque and speed directly as well as apply a load or adding power to the system
Arm positions	Video recordings (with markers attached on subjects)	1D model: Sagittal plane [17-18]
		2D model: Right hand side [14] A “Pan and Tilt” system [19]
		3D model: VICON [5-6] OPTO*TRAK* 3020 [20]
Kinetic data	**Methods**	**Outputs**
Force Torque	Strain gauge force transducer [5-6]	Measuring the magnitude and direction of the forces exerted by the hand on the push-rim
	SMART^{Wheel} [2-4]	Recording three-dimensional push-rim forces and moments directly during the wheelchair propulsion
Synchronization	**Methods**	**Outputs**
Kinematic and Kinetic data	LED counter [21]	Synchronise video data with encoder data

Cooper et al. [16] quantified the kinetics of manual wheelchair propulsion on different surfaces (e.g. a mobility course) [4] whereas Dunkerley et al. [7] described a scoring system (Functional Independence Measure - FIM) for comparing the effectiveness of surgery (e.g. posterior deltoid to triceps transfer in tetraplegic patients) on wheelchair propulsion. Both of them successfully described methods of measuring wheelchair propulsion ability under real environments. Furthermore, for wheelchair motion simulation, some previous reports have focused on the use of a custom-made ergometer and examined the characteristics of a computer-controlled wheelchair ergometer [5-6, 8-14]. These studies concluded that a roller ergometer is capable of predicting wheelchair propulsion ability, thereby allowing direct comparisons between different devices used. Other researches [2-3, 15-16] have exploited dynamic calibration tests for characterizing the properties of a wheelchair dynamometer. Rather than measuring work and power only (as with an ergometer), a dynamometer also can measure torque and speed directly as well as applying a load or adding power to the system [2]. For force and torque measurements, most of the studies [2-4] listed in Table 2.1 used a wheelchair with a SMART^{Wheel} attached to the dynamometer, and an electric motor-load system, which allowed three-dimensional push-rim forces and moments to be recorded directly during wheelchair propulsion. However, these studies were all based on measuring the forces and moments generated by users transmitted only through the push rim, and potentially do not give a true indication of propulsion ability of users using different propulsion techniques, such as contact with only the wheelchair tyre, or combination of push-rim and tyre. Furthermore, the subjects could not use their own wheelchairs during the test procedure, potentially affecting the accuracy of the results. For example, wheelchair seat height has an interrelationship with kinematic parameters, such as velocity, trunk contribution and push angle [22]. . In addition to concerns regarding the test device, the technique of data analysis for evaluating arm motions during wheelchair propulsion must be considered. Most of the studies have been limited to the sagittal plane [17-18] and 2D analysis [14, 19, 21]. To measure arcs of motion in all three planes, 3D kinematic analyses have been developed [5-6, 20].

Due to the abovementioned limitations of current methods for measuring wheelchair propulsion ability, a preliminary study was performed to observe methods of wheelchair propulsion technique. Seventeen subjects with varying levels of spinal cord injury were asked to propel their wheelchairs under different levels of resistance. The subjects movements were captured on video and their propulsion techniques analyzed. The whole procedure included moderate and maximum intensity tests, which simulated propelling a wheelchair from a resting position up to a self-selected comfortable speed on a flat floor and accelerating a wheelchair with maximum effort up a ramp (12:1 slope) respectively. As shown in Table 2.2, 85.7% (28.6% + 57.1%) of tetraplegic subjects used the wedges (gaps between the tires and push rims) to accelerate the wheelchair or grasped both the tires and push-rims (where possible) to propel the wheelchair efficiently under both moderate and maximal test conditions. A similar situation was also observed in T1-T8 paraplegic subjects, where 80% (8 in 10 as shown in Table 2.2) of those tested chose grasping both the tyre and push-rim or the wedges to accelerate the wheelchair, with only two subjects using the push-rims exclusively. This pattern of using wedges to accelerate the wheelchair was not observed in subjects with lower injury levels (T9-T12 and L1). Finally, the test results indicated the pattern of contacting the wheelchair was not changed under moderate versus maximum test intensity.

Table 2.2 *Summary of techniques used to grip wheelchair observed in preliminary study of 17 patients with varying SCI level.*

Injury level	Subjects	Moderate intensity test			Maximum intensity test		
		Push-rims only	**Tires and push-rims**	**Wedges**	**Push-rims only**	**Tires and push-rims**	**Wedges**
C5/C6 tetraplegia	7	14.3%	28.6%	57.1%	14.3%	28.6%	57.1%
T1-T8 paraplegia	4	25%	50%	25%	25%	50%	25%
T9-T12 paraplegia	4	25%	75%	0	25%	75%	0
L1 paraplegia	2	0	100%	0	0	100%	0

One reason for grasping both the tyres and push-rims to propel the wheelchair is that the push-rims provide insufficient friction and surface area for the subjects with lower injury level who can accelerate wheelchair faster as shown in Figure 2.1C. For example, due to the diminished grasp function between thumb and forefingers in people with C5/C6 tetraplegia, the grip adopted for maximum wheel torque in wheelchair propulsion often involves the user wedging their hands between the tires and push-rims (Figure 2.1D) to propel the wheelchair. In this situation, people with a normal grasp often use the tyre and pushrim together to obtain maximum wheel torque, as shown Figure 2.1A. As a result, wheelchair propulsion methods based on the measurements of the push rim forces exclusively, will not give a true indication of propulsion ability for people with different injury levels.

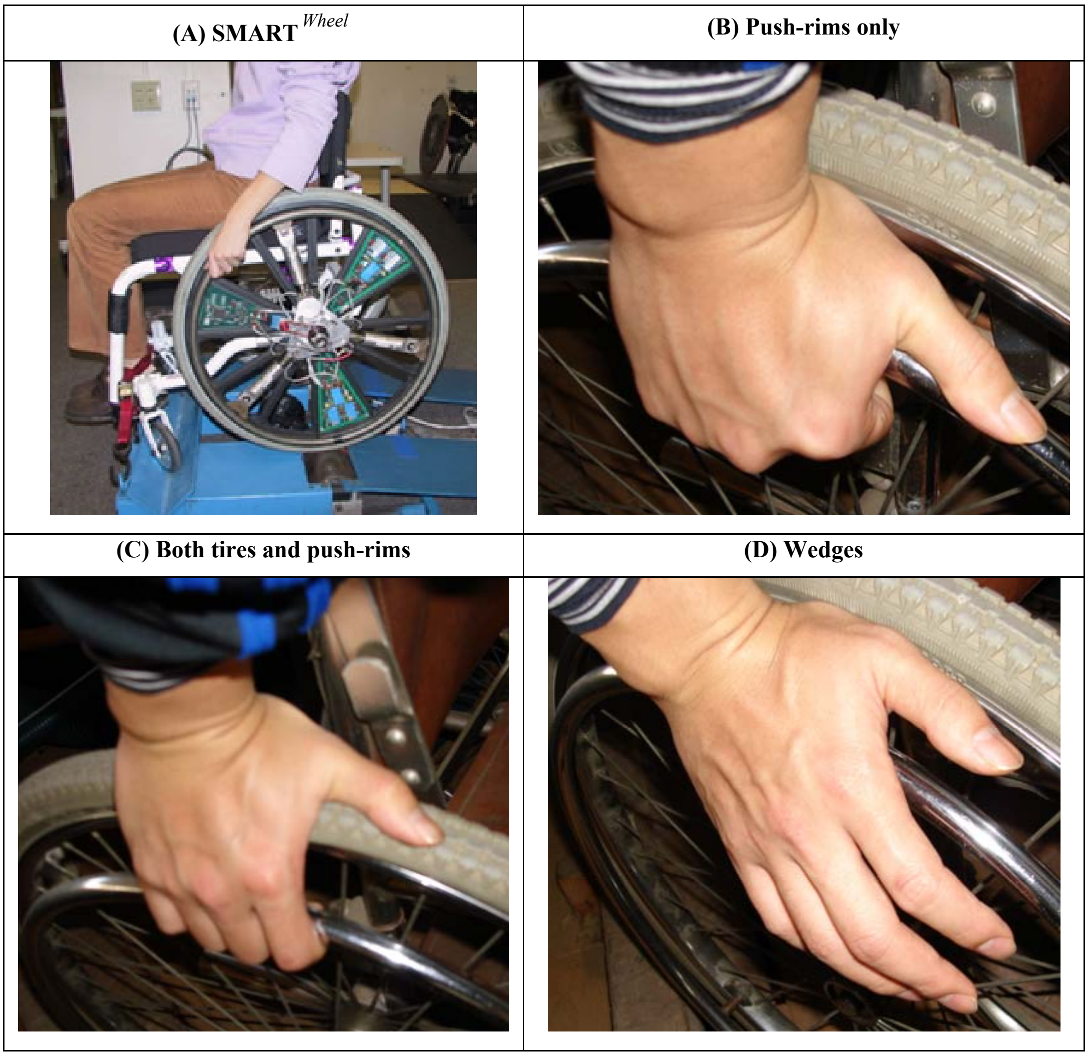

Figure 2.1 *The comparison between the SMART^{Wheel} (A) and three different propulsion techniques observed after the test in this study, namely, propelling push-rims only (B), grasping both tires and push-rims (C) and using wedges (D)*

These observations suggest that a more suitable method for accurately measuring wheelchair propulsion ability needs to be identified. Therefore, the purpose of this study was to develop an improved procedure for kinetic and kinematic evaluation of manual wheelchair propulsion ability, particularly for patients with higher level SCI injury.

2.2 Material and Method

2.2.1 Test rig design

To exclude variation in wheelchair propulsion ability due to hand/wheel grasping techniques, this study adopts the use of a variable inertia dynamometer and video analysis system for measuring kinetic and kinematic data. Using rotary encoders and careful design of dynamometer's roller and flywheel assembly, the wheelchair wheel position can be determined with respect to time. This data can be used to calculate wheel speed, acceleration. Knowing the inertia of the system then allows predictions of the wheel torque, work done and power output for each wheelchair user independent of wheelchair type and design. In addition, the purpose of kinematic video analysis in this study would be to determine the effect of arm function on wheelchair propulsion with varying SCI level. Performance parameters would involve defining propulsion and recovery phase, calculating contacting and release angles and highlighting the contribution of trunk movement. As a result, a 2D analysis was the most effective kinematics system for this study.

The test rig consists of a dynamometer, a rigid frame wheelchair, flywheels, a LED counter, two encoders and two video cameras. The dynamometer includes a plywood deck, two independent steel tubular rollers (one for each wheel), a rectangular hollow section (RHS) steel frame, two anchor points for the front wheelchair castors and a detachable ramp. The rear wheels of the wheelchair sit on the rollers and the front wheels are locked into the caster anchors using the belts. The inertia simulation during level propulsion is achieved by means of removable flywheels which are loaded on the roller shaft and are proportional to the weight of the subject. Rotary encoders are attached to the RHS frame and connected to the inside of the rollers using flexible couplings. The electrical signal from the rotary encoders is processed using a personal computer (PC) to record wheel position data along with time. An LED time counter is also connected to the PC. This counter visible on the video recordings, is used to synchronise video images with the encoder data. The type of the devices used in this manual wheelchair propulsion study can be defined as wheelchair linked to a custom-made dynamometer [2]. The prototype dynamometer as shown in Figure 2.2 designed for measuring wheelchair propulsion capability has been produced and improved from the original design.

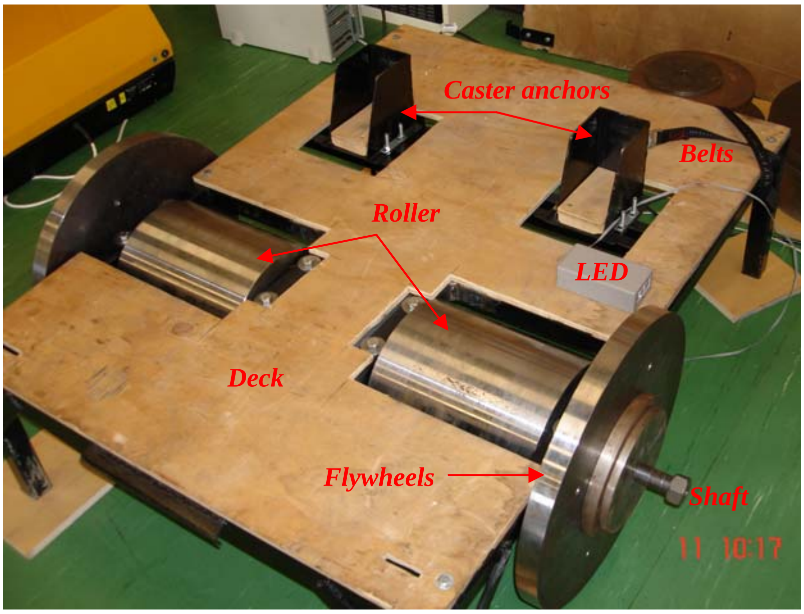

Figure 2.2 *The comparison between the design and prototype of a wheelchair dynamometer*

The rollers were designed based on the combined weight of the participant (minimum 45 kg) and the wheelchair (20 kg). The kinetic energy of a person propelling a wheelchair can be calculated using:

$$T_{K_1} = \frac{m\dot{x}^2}{2} \qquad 2.1$$

For the rollers on the dynamometer, the rotational kinetic energy is of the form:

$$T_{K_2} = \frac{I\dot{\theta}_R}{2} \qquad 2.2$$

Equating (2.1) and (2.2), noting that $\dot{x} = \dot{\theta}_R \, r_R$, and rearranging, the total roller inertia required to simulate the combined weight of the participant and their wheelchair is:

$$I = \frac{m\dot{x}^2}{\dot{\theta}_R{}^2} = m r_R{}^2 \qquad 2.3$$

Initially, the inertia of a solid cylinder roller is:

$$I = \frac{m_R r_R^{\ 2}}{2} \qquad 2.4$$

The roller drums were constructed from thick walled steel tubes with steel end plates and a solid steel shaft. This arrangement was selected to achieve a satisfactorily high initial inertia value (0.7132 kgm^2) and low system weight. Since the radius of the roller is fixed (r_R = 0.1255m), noting that there are two rollers, Equation 2.4 may be written in the simplified form

$$I_{req} = \frac{m\dot{x}^2}{2\dot{\theta}_R^{\ 2}} = 0.00787m \qquad 2.5$$

Seven different sizes of flywheel were manufactured to provide adequate accuracy in matching the inertia with the weight of the subject. Optical shaft encoders (US digital, 1000 counts/revolution) were coupled to a PC using (Labview) software. Encoder data was subsequently analysed in Matlab software (The MathWorks, Inc. USA) to calculate velocity and acceleration versus time.

2.2.2 Dynamic calibration of the dynamometer

The torque required to overcome dynamometer roller bearing friction and windage losses was determined by measuring the deceleration of the rollers during a ‘no load’ coast down test. The deceleration was found to be relatively constant for the test speed range. Also, since bearing friction and windage losses are small in comparison with the input torque, they can be estimated using the following equation:

$T_{Roller\ friction\ and\ windage}$ = Inertia Deceleration

Determining the inertia of the dynamometer to match the inertial characteristics of each subject allowed for the calculation of the torque required to overcome the dynamometer’s inertia and the wheelchair resistance. As for the rotational inertia, the dynamometer was designed by means of removable flywheels positioned on the roller shaft such that they were proportional to the weight of the subject. However, to calculate the force required to propel the tires of the wheelchair running on the rollers, individual coefficients of rolling resistance needed to be determined. Rolling resistance depends on the type of tyre, the tyre pressure, the subject mass and the contacted surface. It was worth noting that the rolling resistance caused the wheelchair to slow by contact between the wheelchair tires with the surfaces as well as propelling the rollers based on the Newton's third law.

A "coast down" test [2] was performed to measure the rolling resistance for the wheelchair on the dynamometer so that the experiments could be compared with normal wheelchair propulsion on a flat surface. This experiment consisted of accelerating the wheelchair with one push on the push rim and then measuring the deceleration of the rollers. In this study, the wheelchair was allowed to coast down in neutral under windless conditions on the roller surface and the time (t_1 and t_2) that elapsed while the wheelchair coasted down by a specific increment of speed was measured from two initial velocities, $\dot{x}_{1i}$ (high speed) and $\dot{x}_{2i}$ (low speed). The information was used to calculate the mean velocities ($\dot{x}_1, \dot{x}_2$) and deceleration rates ($\ddot{x}_1, \ddot{x}_2$). Given the inertia of the roller, flywheels and wheelchair, the equation described speed as a function of time and the friction can be determined. The formulas are illustrated as:

$$F_t = F_{ro} + F_D + m.\ g.\ \sin \hat{\theta} \qquad 2.6$$

$$F_{ro} = C_{rr}\ .\ F_N \qquad 2.7$$

$$F_N = m\ .g \qquad 2.8$$

$$F_{air} = 1/2.\ \rho\ .\ C_D.\ A.\ \dot{x}^2 \qquad 2.9$$

From equations (2.6) to (2.9),

$$C_{rr} = (\ddot{x}_2\ .\ \dot{x}_1^2 - \ddot{x}_1\ .\ \dot{x}_2^2)\ /\ g.\ (\dot{x}_1^2 - \dot{x}_2^2) - \sin \hat{\theta} \qquad 2.10$$

The $\hat{\theta}$ will be zero if the test is on a level surface and the formula will be

$$C_{rr} = (\ddot{x}_2\ .\ \dot{x}_1^2 - \ddot{x}_1\ .\ \dot{x}_2^2)\ /\ g.\ (\dot{x}_1^2 - \dot{x}_2^2) \qquad 2.11$$

Therefore, the coefficient of the frictional resistance tested for the dynamometer was 0.0129 and we ensured subjects had their own coefficients of rolling resistance, which was more accurate for friction calculations and closer to the real situation of a chair rolling on a flat surface.

2.2.3 Test Method

Able-bodied subjects (one male and one female) were asked to propel the wheelchair to a constant velocity with maximum effort from rest [21, 23] and maintain it for thirty seconds on the dynamometer. Flywheels were added to the dynamometer according to the weight of the participants in their wheelchairs. As listed in Table 2.2, four wheelchair users with complete spinal cord injury ranging from C5/C6 to L1/L4 were required to accelerate the wheelchair up to a comfortable self-selected speed [4].

During the test, the participants arm and upper body motion was captured using a SONY AC-L15B video camera. Propulsion kinematics data, such as accelerations (linear and angular), velocities (linear and angular) and torque applied by the subjects, which contributed to calculate the resultant forces and moments of the shoulder and elbow during the propulsion cycle, were calculated in Matlab based on the data gathered from the encoders. The inputs for Matlab calculation are listed as follows: the diameter of the rollers (0.251m), the number of averaged periods for acceleration and velocity for smoothing (600), the number of counts per revolution for the encoder (1000 counts per revolution) and the frequency, or number of times per second, data was collected (1000 times per second). Figure 2.3 displays the whole procedure of the kinetic data calculation in Matlab, which contributed to the kinematics data processed in the spreadsheet.

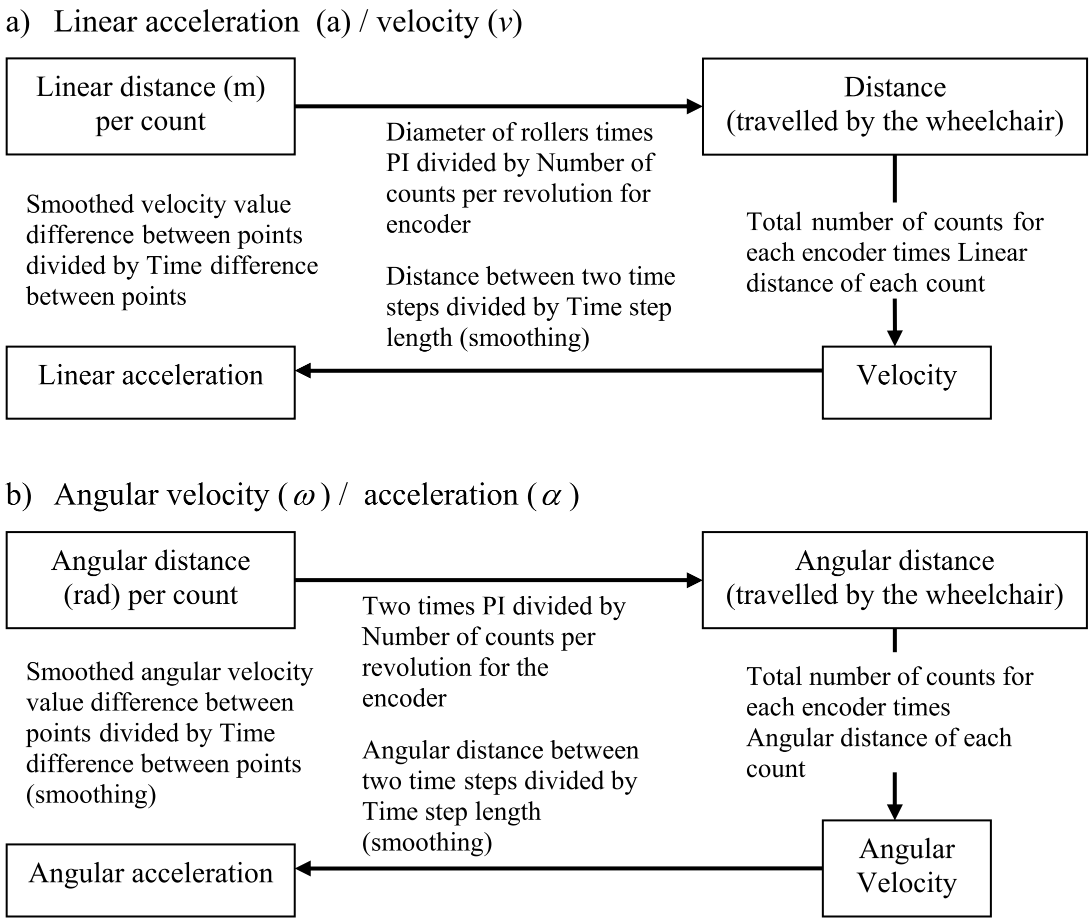

Figure 2.3 *The procedure of the Matlab program calculation*

2.3 Results & Discussion

Figure 2.4 shows a comparison of the distance, velocity and acceleration versus time curves generated from the dynamometer made in this study by able-bodied subjects (A, B and C) to those of Coutts et al [23] (D, E and F) respectively during the procedure of performing a maximum propulsion effort from a standing start. These curves demonstrated that the velocity increased until the acceleration reached a plateau. The maximum acceleration was also observed in the first push. All the curves generated from this test were consistent with the plots of the best individual measured by Coutts et al. The differences in performance noted by Coutts between the track athletes' (solid line) and basketball player' (dash line) in the velocity and acceleration curves (Figure 2.4 E, F) was due to the different propulsion techniques and the wheelchair used [23]. The track wheelchairs had significantly smaller diameter push-rims and larger wheels compared with the basketball players and the normal wheelchair used in this study.

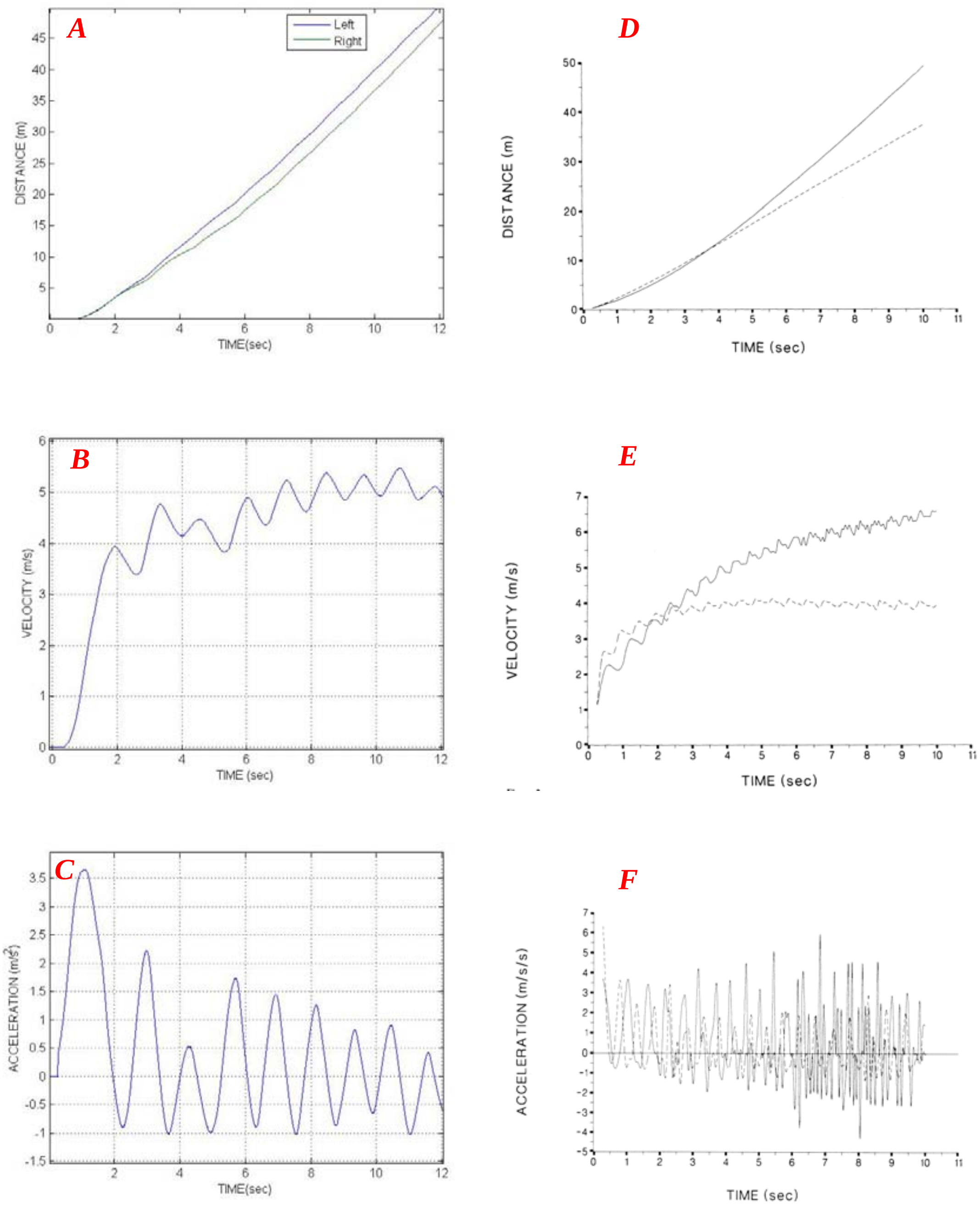

Figure 2.4 *Distance graphs of (A) the dynamometer test, (D) reference [23] test, Velocity graphs of (B) the dynamometer test, (E) reference [16] test and acceleration graphs of (C) the dynamometer test, (F) reference [23] test*

The distance recorded in this study (Figure 2.4A) illustrates the difference between the left and right hands as a result of the rolling resistance being equal on both sides of the dynamometer. This is because the test rig reflects the natural tendency related to having a dominant side of the body. The graphical comparison (Figure 2.4 B and E) between the acceleration curves gathered from the test in this study and the result from Coutts et al [23] indicated that a higher positive acceleration during the first several pushes and this resulted in the velocities increasing rapidly (from rest to 5 m/s in 10 seconds). Furthermore, it demonstrates that the experienced wheelchair users i.e. track and basketball athletes with better upper body strength, have better wheelchair propulsion ability. However, when the positive and negative changes in acceleration are smaller and consistent, this demonstrates that the velocity is becoming constant, which is desirable for further studies, such as kinematic data calculation based on video analysis given the more consistent arm motion during constant velocity. Moreover, the propulsion force and torque applied on the push-rim by the subjects are more even during a single stroke when a constant velocity is achieved as opposed to accelerating from rest. Finally, comparing the graphs from this study (Figure 2.4A, B and C) and the best individual basketball (dash line) and track athletes' (solid line) performance (Figure 2.4D, E and F) from Coutts et al [23] demonstrates that the able-bodied subjects' wheelchair propulsion performance was closer to the basketball player's (solid line), due to the similarity in wheelchair type used.

The velocity curves show that the maximum wheel velocity generally occurs after the hands left the push-rim, which has been described in other studies [19]. Due to the contribution of rolling resistance decelerating the wheelchair during the recovery phase, the velocity keeps going down until the next propulsion phase. Furthermore, other factors, such as windage losses and bearing friction, also contribute to explain why the accelerations are changing from negative to positive during the whole stroke progress. The propulsion and recovery time [16] are measured as well, which are 0.36s and 0.52s respectively when a constant velocity is achieved.

Figure 2.5 illustrates the plot of torque produced from the dynamometer by an able-bodied subject for one particular stroke compared with the literature [24]. Similar torque curves are observed in this study compared with the literature using SMART^{Wheel} [24].

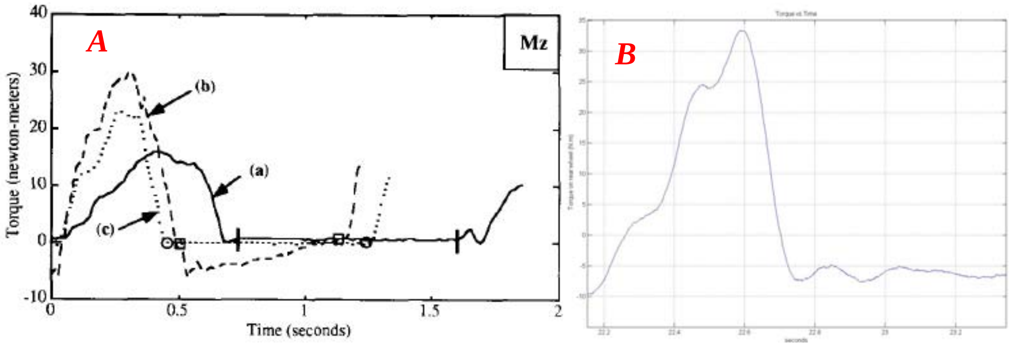

Figure 2.5 *The comparison of torque graphs between (A) literature [24] and (B) test from able-bodied subjects in this study*

Furthermore, depending on injury level, height and weight, four subjects with spinal cord injury from the previous SMART^{Wheel} study [4] were chosen to compare with the results from this study as shown in Table 2.3, whereby the average torque (*T*) of the first seven strokes was calculated. It demonstrates that the inertia dynamometer is capable of accurately measuring people's wheelchair propulsion ability. Significantly higher results calculated in this study compared with SMART^{Wheel} studies indicated that the extra torque applied on the tyre or the wedges has been taken into account. More importantly, it highlights some of the limitations of previous SMART^{Wheel} studies based on measurements taken only via the push-rims. The applied torque changing from negative to positive meant the subjects depended more on the biceps during the pull phase and the triceps play a more important role during the push phase. Finally, for inexperienced users, torque curves (Figure 2.5B) showed an initial negative deflection and a dip in the rising portion of the curve, which was reported to be in agreement with results of previous investigations [25-27].

Table 2.3 *The torque comparison between the literature using SMART^{Wheel} [4] and subjects tested in this study*

SCI level	**Literature**			**Test results**		
	Gender	**Age**	**Weight**	**Gender**	**Age**	**Weight**
C6/C7 tetraplegia	M	54	80.7	M	49	80
T5/T6 paraplegia	M	55	99.8	M	61	98.7
T11/T12 paraplegia	M	53	68.4	M	33	74
L1-L4 paraplegia	M	49	88.4	M	20	79.2

	Strokes						
	1	**2**	**3**	**4**	**5**	**6**	**7**
Literature	25.2(6.7)	22.6(7.0)	20.6(8.8)	17.5(7.9)	13.4(6.3)	14.1(5.4)	12.5(6.0)
Test results	40.9(14.4)	31.9(16.6)	31.3(15.3)	27.7(15.6)	26.4(15.2)	22.7(12.4)	18.7(7.1)

The advantages of using a dynamometer with flywheels to test wheelchair propulsion ability include the independence in type of wheelchair used, which means subjects can use their own wheelchair and more importantly, the test rig is independent of propulsion techniques used. Moreover, a combined cinematographic (LED and video capture) and kinetic (data gathered from the encoders) approach will significantly increase the accuracy of hand contact and hand release identification. The flywheel inertia simulation provides the possibility to increase resistance, which can represent the different components of the wheeling tasks, such as starting, wheeling and sprinting and changes in external conditions also can be achieved. However, a few limitations may affect the accuracy of the results. Firstly, since backward tilting [1] is prevented on most stationary dynamometers, the forces generated on the push rims will be much higher compared with the same task under flat floor conditions, especially during the start of a sprint task. Inertial forces acting on the wheelchair caused by acceleration and deceleration of the trunk and arms are neglected in stationary systems. Furthermore, the changes in air resistance brought about by changes in velocity cannot be considered [19]. Finally, the 2D kinematics measurement system limited the calculation of mechanical efficiency, which is the ratio of external energy production to consumed metabolic energy.

2.4 Conclusion

This study suggests that studies adopting the use of instrumented push rims, such as the SMART^{Wheel}, are not likely to provide a true measure of wheelchair propulsion ability for people with different injury levels. This is because users generally contact both the push rim and tyre to impart motion to their wheelchair wheels. In this study, the analysis of the dynamometer roller position and time data proved to be a valid method for testing the parameters of the custom-made inertia wheelchair dynamometer. Furthermore, the frictional resistance (0.0129) and rolling resistance (C_{rr}=1.179 between the tyre and roller) values obtained allow the results from this study to be compared with other similar studies. Comparison of our results with previous studies by Coutts *et al.* [23] and Cooper *et al.* [4] indicated that the test rig designed and constructed in this study was suitable for comparing people's wheelchair propulsion ability. Additional validity studies are currently being performed in a larger cohort of patients, testing the effects of spinal cord injury on wheelchair propulsion ability and including additional evaluation parameters, such as power output and body motion analysis.

Acknowledgements

The help of the technical staff, in particular, Ken Brown, Paul Wells and Julian Murphy from the Mechanical Engineering Department at the University of Canterbury was greatly appreciated.

References

[1] Yves Vanlandewijck, Daniel Theisen and Dan Daly. Wheelchair Propulsion Biomechanics (Implication for Wheelchair Sports). Sports Med 2001; 31 (5): 339-367

[2] Carmen P. DiGiovine, Rory A. Cooper and Michael A Boninger. Dynamic calibration of a wheelchair dynamometer. Journal of Rehabilitation Research and Development Vol. 38 No. 1, January and February 2001

[3] Rick N. Robertson, PhD, Michael L. Boninger, MD, Rory A. Cooper, PhD and Sean D. Shimada, MS. Pushrim Forces and Joint Kinetics During Wheelchair Propulsion. Arch Phys Med Rehabil Vol 77, September 1996.

[4] Alicia M. Koontz, Rory A. Cooper, Michael L. Boninger, Yusheng Yang, Bradley G. Impink and Lucas H.V. van der Woude. A kinetic analysis of manual wheelchair propulsion during start-up on select indoor and outdoor surfaces. Journal of Rehabilitation Research and Development Volume 42 Number 4, July/August 2005 Pages 447-458

[5] Craig J. Newsam, Sreesha S. Rao, Sara J. Mulsroy, JoAnne K. Gronley, Ernest l. Bontrager and Jacquelin Perry. Three dimentional upper extremity motion during manual wheelchair propulsion in men with different level of spinal cord injury. http://www.elsebier.com/locat/gaitpost

[6] Korelia Kulig, Craig J. Newsam and Sara J Mulroy. The effect of level of spinal cord injury on shoulder joint kinetic during manual wheelchair propulsion. Clinical Biomechanics 16 (2001) pp 744-751 July 2001

[7] AL Dunkerley, A Ashburn and EL Stack. Deltoid triceps transfer and functional independence of people with tetraplegia. Spinal Cord 2000; 38: 435-441.

[8] Veeger HEJ, van der Woude LHV, Rozendal RH. A computerized wheelchair ergometer. Scand J Rehabil Med 1992;24:17-23.

[9] Langbein WE, Robinson CJ, Kynast L, Fehr L. Calibration of a new wheelchair ergometer: the wheelchair aerobic fitness trainer. IEEE Trans Rehabil Eng 1993;1:49-58.

[10] Theisen D, Francaux M, Fayt A. A new procedure to determine external power output during handrim wheelchair propulsion on a roller ergometer: a reliability study. Int J Sports Med 1996;17:564-71.

[11] Forchheimer F, Lundberg Å. Wheelchair ergometer. Scand J Rehabil Med 1986;18:59-63.

[12] Niesing R, Eijskoot F, Kranse R, den Ouden AH, Storm J, Veeger HEJ, et al. Computer-controlled wheelchair ergometer. Med Biol Eng Comput 1990; 28: 329-38.

[13] Kornelia Kulig, Sreesha S. Rao and Sara J. Mulroy. Shoulder joint kinetics during the push phase of wheelchair propulsion. Clinical Orthopaedics and Related Research Number 354 pp 132-143 March 25 1998

[14] Annet J. Dallmeijer, Yvonne J.Kappe, Dirkjan H.E.J. Veeger, Thomas W.J.Jassen and Luc H.V. van der Woude. Anaerobic power output and propulsion technique in spinal cord injured subjects during wheelchair ergometer. Journal of Rehabilitation Research and Development Vol. 31 No. 2, 1994 Pages 120-128

[15] Jarvis S, Rolfe H. The use of an inertial dynamometer to explore the design of children's wheelchairs. Scand J Rehabil Med 1982;14:167-76.

[16] Rory A. Cooper. Rehabilitation Engineering (Applied to Mobility and Manipulation)

[17] Masse LC and Lamontagne M. Kinematics analysis of wheelchair propulsion for three speeds of propulsion. Int Cong Biomech 1989; 12:234.

[18] Masse LC, Lamontagne M and O'Riain MD. Biomechanical analysis of wheelchair propulsion for various seating positions. J Rehab R&D 1992; 29: 12-28.

[19] A.D. Moss, N.E. Fowler and V.L. Goosey-Tolfrey. The intra-push velocity profile of the over-ground racing wheelchair sprint start. Journal of Biomechanics 38 (2005) 15-12

[20] Alicia M Koonta, Rory A. Cooper, Michael L. Boninger, Aaron L. Souza, Brian T. Fay. Shoulder kinematics and kinetics during two speeds of wheelchair propulsion. Journal of Rehabitation Research and Development Vol. 39 No. 6 pp 635-650 November/December 2002

[21] Annet J. Dallmeijer, MSc Luc H. V. van der Woude PhD, H. E. J. (DirkJan) Veeger, PhD and A. Peter Hollander, PhD. Effectiveness of force application in manual wheelchair propulsion in persons with spinal cord injuries. American Journal Of Physical Medicine and Rehabilitation. 1998

[22] Dr. Lue H.V. van der Woude, Dr. Dirk-Jan Veeger, Prof. Dr. Rients N. Rozendal, Prof. Dr. Tony 3. Sargeant. Seat height in handrim wheelchair propulsion. Journal of Rehabilitation Research and Development Vol. 26 No. 4 Pages 31 -50.

[23] Kenneth D. Coutts PhD. Kinematics of sport wheelchair propulsion. Journal of Rehabilitation Research and Development Vol. 27 No. 1 Pages 21-26.

[24] Kimberly T. Asato, Rory A. Cooper, Rick N. Robertson, and J. F. Ster. SMART^{Wheel}: Development and Testing of a System for Measuring Manual Wheelchair Propulsion Dynamics. IEEE TRANSACTIONS ON BIOMEDICAL ENGINEERING, VOL. 40, NO. 12, DECEMBER 1993.

[25] C. E. Brubaker, C. A. McLaurin, I. D. Gibson, and T. H. Soos. Seat position and wheelchair performance. Wheelchair Mobility 1976-1981. W. Stamp, and C. A. McLaurin, Eds. Rehabilitation Engineering Center, University of Virginia, pp. 12-21, 1981.

[26] S. A. Ross and C. E. Brubaker. Electromyographic analysis of selected upper extremity muscles during wheelchair propulsion. in Proc. 2nd Int. Conf. Rehabil. Eng., pp. 7-8, 1984.

[27] W. Lesser. Ergonomische Untersuchung der Gestaltung antreibsrelevanter Einflussgroessen beim Rollstuhl mit Handantrieb. Fortschrtittberichte VDI Verlag, Reihe 17, Biotechnik No. 28, p. 265, 1986.

CHAPTER 3

WHEELCHAIR PROPULSION ABILITY

Quantifying Manual Wheelchair Propulsion Ability vs. Injury Level for People with Spinal Cord Injuries

Summary

Purpose: The purpose of this study was to quantify the effect that spinal cord injury (SCI) level has on manual wheelchair propulsion ability.

Method: Seventeen people with SCI's were tested on a custom-built wheelchair dynamometer. Participants propelled their regular wheelchairs under various loading conditions ranging from a self-selected normal speed test on simulated flat ground to a high resistance maximum effort test. Markers were attached to the participant's arms, neck and head. Two digital video cameras were used to capture upper body motion during wheelchair propulsion. The participant's posture was measured at the following points in the propulsion cycle: on initial contact between the participants hand and the wheelchair rim; at top dead centre; at the hand/rim release point; and during the recovery phase.

Results: The results naturally fitted into four groups of participants as found in earlier studies, namely: C5-C8; T1-T8; T9-T12; L1-S5. Wheelchair displacement, velocity and acceleration measurements were plotted and the propulsion cycle phase information added. Average results for maximum achievable wheelchair speed were 2.83, 6.4, 7.24 and 8.49 m/s respectively for the above groups. Similarly, average power output was calculated as 140.1, 737.1, 755.5 and 959.9 watts. C5-C6 candidates were found to have significantly less elbow movement during wheelchair propulsion than for the other groups.

Conclusions: People with C5/C6 tetraplegia have a significantly reduced capability in terms of wheelchair propulsion when compared with the T1-T8 group. The relative difference between the T1-T8 and T9-T12 and the T9-T12 and L1-S5 groups was much less. This study indicates that arm function is a more important factor in wheelchair propulsion than trunk stability and strength. Anecdotal evidence obtained from post deltoid to triceps surgery subjects suggests that restoration of triceps function improves wheelchair propulsion. To what extent triceps function objectively improves wheelchair propulsion is the subject of ongoing research.

Nomenclature

T_W	Torque on wheel (Nm)
I	Polar mass moment of inertia (kgm^2)
$\ddot{\theta}$	Angular wheelchair acceleration (rad/s^2)
P	Power output (watt)
$\dot{x}$	Linear wheelchair velocity (m/s)
r	Wheel radius (m)
$\dot{\theta}$	Angular wheelchair velocity (rad/s)
F_t	Tractive force (N)
F_r	Radial force (N)
C_f	Coefficient of friction between rubber and steel
F_{res}	Resultant force (N)
S (x_S, y_S)	Shoulder position in mathematical model
E (x_E, y_E)	Elbow position in mathematical model
H (x_H, y_H)	Hand position in mathematical model
T (x_T, y_T)	Trunk position in mathematical model
O (x_C, y_C)	Centre coordinate in mathematical model
θ_S	Shoulder position (^{0})
θ_E	Elbow position (^{0})
θ	Hand position (^{0})
θ_T	Trunk position (^{0})
V_{max}	Peak velocity (m/s)
t_{pv}	Time to peak velocity relative to contact time during one stroke (s)
V_c	Linear wheelchair velocity at point of hand contact (m/s)
V_r	Linear wheelchair acceleration at point of hand release (m/s)
a_{max}	Linear wheelchair acceleration during one stroke (m/ s^2)
T_{max}	Peak torque on wheel (Nm)
P_{max}	Peak power output (w)
PP	Propulsion phase
RP	Recovery phase
ST	Stroke time (s)
θ_c	Contact angle (^{0})
θ_r	Release angle (^{0})
θ_{E-min}	Minimum elbow angle (^{0})
θ_{E-max}	Maximum elbow angle (^{0})
θ_{T-min}	Minimum elbow angle (^{0})
θ_{T-max}	Maximum elbow angle (^{0})

3.1 Introduction

Biomechanical analysis [1-6] of wheelchair propulsion has been widely studied, along with improvements to wheelchair design, such as biomechanical properties [7] and the user interface [8]. Recently, researchers [9-11] have shifted their focus more to the propulsion enhancement of wheelchair users to understand the physical demands on the wheelchair user during propulsion and to find methods to optimize wheelchair propulsion. More importantly, these studies demonstrated that the biomechanics of wheelchair propulsion vary in relation to the subjects' levels of spinal cord injury (SCI) [9]. To evaluate the effect of SCI level on wheelchair propulsion ability, the stationary wheelchair ergometer [6, 9, 12-16, 19] and dynamometer [17-18] systems have become the standardized methods, which can better control and more accurately assess body movements. Moreover, the development of a biomechanical model is also essential and typically has been determined from video recordings using two-dimensional (2D) [9, 20] or three-dimensional (3D) [19] analysis to clarify how the body segments, which includes shoulder, elbow, wrist and trunk, interact mechanically to execute motor tasks. Cooper et al. described the SMART^{Wheel} [21], a commercial force- and torque- sensing push-rim that has been used in several studies [7, 10, 18] to examine 3D propulsion forces, moments, and temporal characteristics over different surfaces and inclines.

However, most investigations of wheelchair propulsion biomechanics have been performed on people with paraplegia [3-4] or wheelchair athletes [11, 22-23]. It has been suggested that the most interesting results could be expected with a study of the biomechanics of people with cervical injury level [24]. Furthermore, given that limited information is available regarding the initial motion and energy required to start a wheelchair from a stationary position, this paper built on the development of a model appropriate for those people using a standard wheelchair [Chapter 2]. The current evaluation methods adopting the use of a SMART^{Wheel} (which records forces and wheel torques applied to the wheelchair rim only) may not provide an accurate measurement of wheelchair propulsion ability in tetraplegic subjects. These subjects tend not to grip or contact the wheelchair rim, but rather take hold of the tyre or "wedge" their hand in the gap between the tyre and wheel to accelerate the wheelchair

[Chapter 2]. As a result, a custom-made inertia dynamometer was used to measure total wheelchair propulsion output. While a majority of previous studies have taken wheelchair propulsion recordings up to a comfortable, self-selected speed, thereby measuring propulsion ability at a moderate intensity level [2, 10, 19], maximum effort measurements will provide more information to quantify and evaluate the effect of SCI level on wheelchair propulsion ability. Finally, the combination of the statistical and visual analysis (adapted from [25]) will lead to an accurate model for estimating the starting and constant phases of wheelchair propulsion.

Therefore, the objectives in this study were to quantity the effect of SCI level on wheelchair propulsion ability and to characterize wheelchair propulsion kinematics for people with SCI's respectively. In order to achieve this, we aim to further develop and describe a kinematics model as well as measure maximum effort under variable rolling resistance conditions.

3.2 Methods

3.2.1 Subjects

This study took place at the Burwood Hospital Spinal Unit over a 6-month period. The inclusion criteria for the potential subjects (adapted from [6]) were: (1) complete tetraplegia or paraplegia; (2) use of a manual wheelchair as a primary mode of mobility; and (3) between 18 and 65 years old. Seventeen male subjects voluntarily participated in this test after giving written informed consent. Based on SCI level, subjects were divided into four groups as described below. Group I (cervical injuries) consisted of subjects with C5-C6 tetraplegia. Depending on the control of abdominal muscles, thoracic level subjects were divided as Group II (T1-T8) and Group III (T9-T12) respectively. Subjects with full upper body control (i.e., lumbar or sacral injuries) were placed in Group IV.

Table 3.1 *Group means and standard deviations of personal data*

Subjects data \ Groups	Group I (n=7)	Group II (n=4)	Group III (n=4)	Group IV (n=2)
Gender	M	M	M (1 Female)	M (1 Female)
Age	38.1 (10.8)	49 (20.9)	32 (11.1)	21 (1.4)
Weight (kg)	88.2 (13.7)	100.1 (22.3)	84.6 (12.9)	80.6 (2.0)
Upper arm Length (cm)	27.1 (2.6)	30.4 (3.6)	27.8 (3.9)	26.4 (1.2)
Forearm Length (cm)	25.2 (1.9)	27.3 (2.5)	26.5 (2.1)	26.0 (0.8)
Duration W/C use (months)	129.6 (106.9)	209.5 (239.3)	85 (82)	35.5 (34.6)

3.2.2 Test procedure

Arm movement analyses were performed with video recordings by tracking the markers attached on the shoulder, elbow and hand (Figure 3.1). In order to investigate the contribution of head and trunk, the marker was also located on the subject as shown in Figure 3.1.

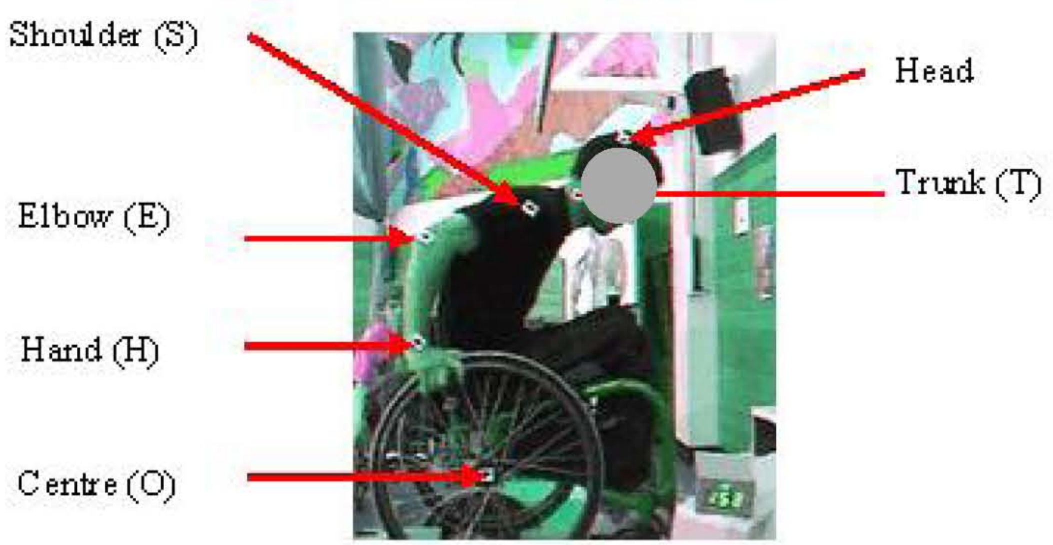

Figure 3.1 *The markers location during the test (The black dots)*

3.2.2.1 Test 1: Rolling resistance test on the dynamometer (Coast down test)

The purpose of this test was to determine each test subject's own coefficient of rolling resistance using their own wheelchair, thereby providing an accurate calculation of friction forces and more closely simulate the real situation. Two pushes were required by accelerating the wheelchair normally and maximally. After reaching a constant speed, the wheelchair was allowed to lose momentum naturally for one run.

3.2.2.2 Test 2: Constant speed test

The purpose of this test was to simulate the everyday occurrence of propelling a wheelchair from rest to a constant speed. Subjects were loaded onto the dynamometer and asked to propel their wheelchair from rest up to a self-selected comfortable speed. They maintained constant speed for approximately 20 seconds. During this time roller drum position data was recorded at 1000 counts/sec time intervals.

3.2.2.3 Test 3: Maximum effort test

The maximum effort test focused on the first three stokes from the start to investigate the propulsion ability. Subjects propelled the hand rim with maximum effort to maximum velocity and maintained it for twenty seconds before returning to a stationary position, with the whole test period lasting approximately 40 seconds.

3.2.2.4 Test 4: Maximum effort high resistance test

The high resistance test involved fitting additional flywheels to the dynamometer. The resistance was equivalent to twice the mass of the user and wheelchair. The purpose of this test was to evaluate a person's ability to ascend a ramp or propel themselves on a high resistance surface.

3.2.3 Data capture

A custom-made wheelchair dynamometer was designed and built at the Department of Mechanical Engineering, University of Canterbury. Two rotary encoders (US digital, 1000 counts/second) were fitted to the inboard end of the dynamometer. These encoders were connected to a personal computer to record the roller position with respect to time. From the position/time data, roller velocity and acceleration can be measured and then power output can be calculated in Matlab (The MathWorks, Inc. USA). Video cameras (SONY AC-L15B) were positioned on each side of the dynamometer at elbow height to capture the participants arm motion during wheelchair propulsion. An LED counter, visible in the video frames, showed the time so that the video can be synchronised with the recorded wheel position data. Figure 1 shows a sample frame from the video recording.

3.2.4 Data analysis

3.2.4.1 Kinetic measurement system

Methods for determining kinetic measurements have been described previously [Chapter 2]. Briefly, wheel torque can be calculated as:

$$T_W = I\ddot{\theta} \qquad 3.1$$

Power output was given by:

$$P = \frac{T_W \dot{x}}{r} = T_W\,\dot{\theta} \qquad 3.2$$

Furthermore, based on the torque applied on the wheel, the tangential forces F_t (Figure 3.2) to propel wheelchair at various positions of propulsion were determined:

$$F_t = \frac{T_W}{r} \qquad 3.3$$

Following that, the other force component F_r (Figure 3.2) was also calculated combined with the C_f tested in this study:

$$F_r = \frac{F_t}{C_f} \qquad 3.4$$

Finally, the resultant force F_{res} (Figure 3.2) for one side only was determined as follows:

$$F_{res} = \sqrt{F_t^2 + F_r^2} \qquad 3.5$$

3.2.4.2 Mathematical model for kinematics

A mathematical model [25], for optimization of wheelchair propulsion was adapted for this study as illustrated in Figure 3.2, and consisted of four segments, namely, shoulder (S), elbow (E), hand (H) and trunk (T). A manual process was employed to process the video data by grabbing frames from the video and marking (illustrated in Figure 3.1), as well as calculating angles for the shoulder joint (θ_S), elbow joint (θ_E), and hand position (θ) respectively (equation 3.6-3.8). The contribution of the trunk (θ_T) [9] was also investigated.

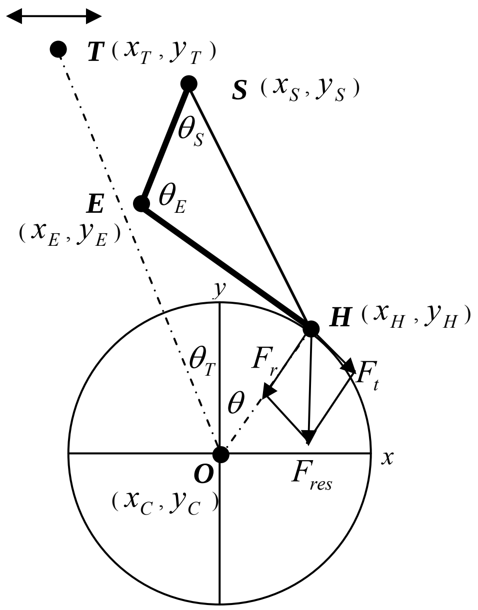

Figure 3.2 *System geometry (adapted from [25])*

$$\theta_S = \mathrm{TAN}^{-1}\frac{(x_S - x_E)}{(y_S - y_E)} + \mathrm{TAN}^{-1}\frac{(x_H - x_S)}{(y_S - y_H)} \qquad 3.6$$

$$\theta_E = \mathrm{TAN}^{-1}\frac{(y_S - y_E)}{(x_S - x_E)} + \mathrm{TAN}^{-1}\frac{(y_E - y_H)}{(x_E - x_H)} \qquad 3.7$$

$$\theta = \mathrm{TAN}^{-1}\frac{x_H - x_C}{y_H - y_C} \qquad 3.8$$

$$\theta_T = \mathrm{TAN}^{-1}\frac{x_T - x_C}{y_T - y_C} \qquad 3.9$$

3.3 Results & Discussion

Data was captured during the first three trials from stationary under the normal and twice-normal resistance tests respectively. As expected, the subjects with a cervical lesion (C5/C6 tetraplegia) had a significantly lower wheelchair velocity (2.83 m/s) and power output (140.1 watts) compared with other subjects with a lower lesion (6.4 m/s and 737.1 watts, 7.24 m/s and 755.5 watts, 8.49 m/s and 959.9 watts in Groups II, III and IV respectively). Furthermore, after increasing the rolling resistance as shown in Table 3.2, the differences noted, such as the maximum velocity (V_{max}) decreasing by 35.8% in Group I versus 26.2% and 24.7% in Group II and III respectively after the first trial from stationary start, demonstrated that people with higher lesion level would be more affected by different external conditions i.e. propelling up a ramp. Finally, it also highlighted that diminished arm function was the major factor in propulsion kinematics under different external conditions simulated.

Table 3.2 *The results of all the kinetic in four groups showing the mean values along with standard deviations in brackets for the 17 subjects tested.*

1st PP	Normal Resistance test				Twice-normal resistance test			
	I	II	III	IV	I	II	III	IV
V_{max} *[m/s]*	1.87(0.8)	3.9(0.7)	4.53(0.4)	5.56(1.5)	1.2(0.5)	2.88(1)	3.41(0.6)	3.75(0.2)
t_{pv} *[s]*	1.49(0.3)	1.11(0.1)	0.93(0.2)	1.19(0.2)	1.96(0.2)	1.29(0.1)	1.04(0.2)	1.09(0.1)
V_r *[m/s]*	1.79(0.8)	3.67(0.7)	3.94(0.4)	5.22(1.2)	1.15(0.5)	2.68(0.8)	3.05(0.7)	3.31(0.3)
T_{max} *[Nm]*	10.9(2.5)	23.5(13)	30.5(10.6)	26.4(4.1)	11.7(3.1)	35.5(9.1)	38.7(10.8)	56(15.7)
P_{max} *[w]*	99.5(32.3)	415.8(49.4)	452.9(32.6)	471.9(66.4)	72.7(29.6)	287.5(33.9)	295.8(41.2)	913.1(65.2)

2nd PP	Normal Resistance test				Twice-normal resistance test			
	I	II	III	IV	I	II	III	IV
V_{max} *[m/s]*	2.42(1)	5.42(0.8)	5.97(0.2)	7.34(1.5)	1.69(0.6)	4.06(1.3)	4.68(1)	4.95(0.1)
t_{pv} *[s]*	0.76(0.1)	0.58(0)	0.5(0.1)	0.47(0)	1.08(0.1)	0.73(0.1)	0.64(0.1)	0.48(0)
V_c *[m/s]*	1.85(0.8)	3.69(0.7)	4.48(0.3)	5.4(1.6)	1.19(0.5)	2.31(0.8)	3.21(0.4)	3.5(0.6)
V_r *[m/s]*	2.34(1)	5.08(0.8)	5.48(0.1)	6.92(1.3)	1.64(0.6)	3.9(1.2)	4.62(1.3)	4.92(0.1)
T_{max} *[Nm]*	7(1.8)	22.4(3.8)	20.3(3.6)	23(0.9)	8.4(3.2)	27(4.9)	25.4(6.6)	51.9(37.3)
P_{max} *[w]*	124.1(51.2)	645(35.2)	699.8(43.7)	872.5(77.7)	94.2(51.9)	523.1(58.2)	506.3(82.8)	1115(65.8)

3rd PP	Normal Resistance test				Twice-normal resistance test			
	I	II	III	IV	I	II	III	IV
V_{max} *[m/s]*	2.83(1.2)	6.4(0.9)	7.24(0.4)	8.49(2)	2.01(0.8)	4.75(1.6)	5.56(1.3)	5.81(0.1)
t_{pv} *[s]*	0.72(0.1)	0.49(0)	0.42(0.1)	0.42(0)	0.98(0.2)	0.6(0)	0.54(0.2)	0.44(0)
V_c *[m/s]*	2.38(1)	5.27(0.8)	5.89(0.2)	7.13(1.7)	1.67(0.6)	3.64(1)	4.52(0.9)	5.1(0.1)
V_r *[m/s]*	2.74(1.1)	6.12(0.9)	6.83(0.4)	8.14(1.9)	1.99(0.8)	4.47(1.3)	5.29(1.2)	5.73(0)
T_{max} *[Nm]*	6.7(1.4)	20.8(1.8)	17.4(2)	19.5(2.1)	8(2.4)	26.3(6.1)	23.3(4.4)	52(39.7)
P_{max} *[w]*	140.1(49.7)	737.1(36.9)	755.5(49.9)	959.9(84.4)	114.9(61.1)	654.9(72.6)	576.3(71.6)	1398(90.5)

3.3.1 Velocity

The reason of choosing velocity is that the reduced propulsive capacity is best demonstrated by the effect of SCI level on propulsion speed [2]. The propulsion phase was divided into five stages, namely, contacting point, first quarter, top dead centre (TDC), third quarter and releasing point as shown in Figure 3.3. The contact (V_c), release (V_r) and maximum (V_{max}) velocity increased with each push in both of the Group I (Figure 3.3A) and Group II subjects (Figure 3.3B) compared with the decrease of the stroke time in the first three pushes. However, Group II accelerated their wheelchair two times faster than Group I (reaching a speed of 4 m/s for T5 subjects versus 1.7 m/s for C5 subjects) after first three trials under the same rolling resistance condition. Furthermore, the V_c was lower than V_{max} of the previous push due to deceleration of the wheelchair during the recovery phase, where the rolling resistance became the only force influencing the wheelchair.

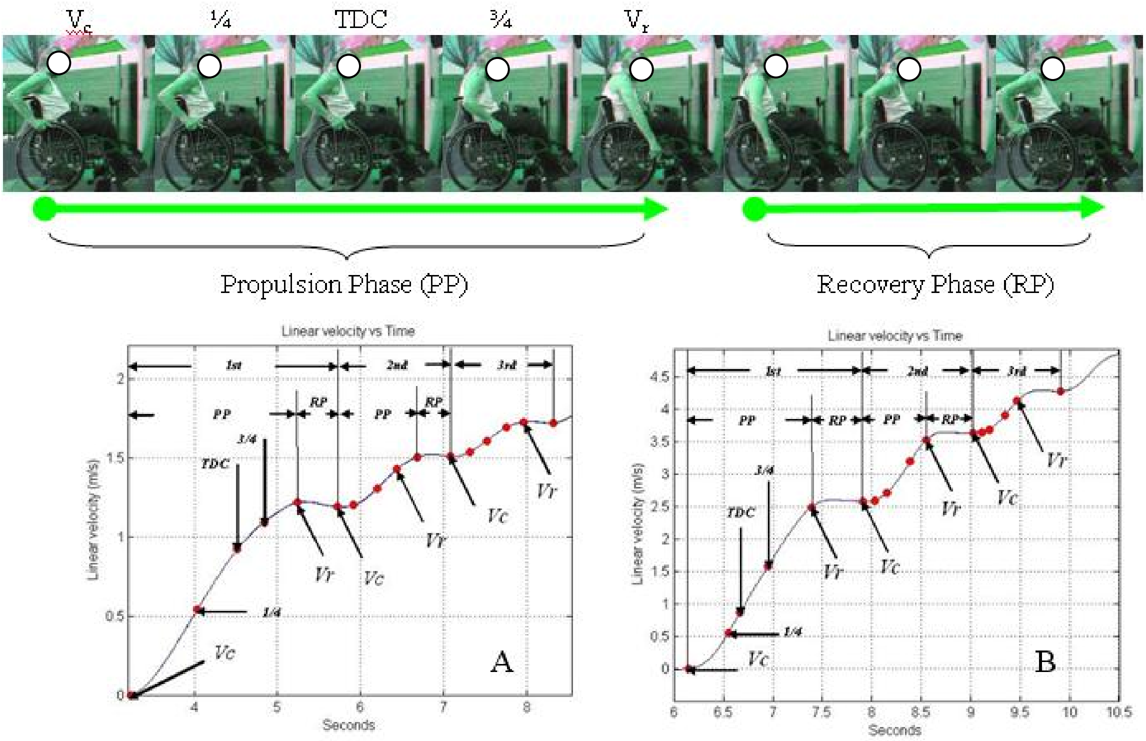

Figure 3.3 *Comparison of the velocity time history curves between Group I (left) and Group II (right) subjects (first three propulsion phases during the maximum resistance test).*

Figure 3.4 shows that T5 paraplegic subjects (Group II) spend less total time on the first three trials and propel the wheelchair at a greater velocity than C5 tetraplegic subjects (Group I). Due to their reduced triceps function, C5 tetraplegia subjects depend more on the pull movement (elbow flexion) and cannot give an impulse during the late push (elbow extension). Furthermore, active triceps during elbow flexion allow the flexor muscles to produce a larger amplitude flexion plus greater acceleration of the forearm than that obtained without triceps activity. This leads to the lower performance in C5 tetraplegia and indicates that triceps function may play a more important role in obtaining a higher velocity during wheelchair propulsion. Triceps function influences the time taken to perform rapid arm movements and thus, is a major parameter in controlling the speed of elbow rotation. As shown in Figure 3.4, T5 paraplegia subjects (Group II) finished the three trials in a shorter period because of the relatively faster elbow flexion and extension. Finally, as indicated by the velocity curve shown in Figure 3.4, a relatively higher slope demonstrates that higher acceleration was achieved resulting from higher force applied on the wheel by T5 paraplegia subjects, thereby increasing their ability to propel the wheelchair faster.

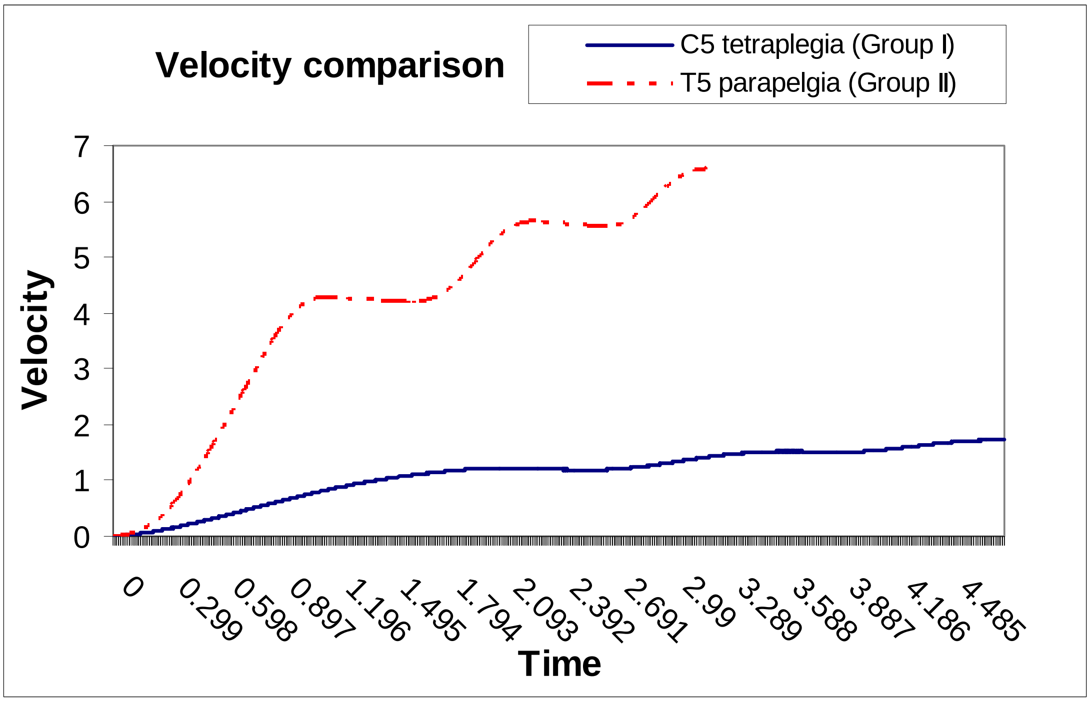

Figure 3.4 *The first three trials velocity comparison between the best performing subjects from Group I and Group II*

The results calculated from Matlab show that peak velocity in one stroke always occurs after release (Figure 3.5), which is in accordance with the time to peak velocity (t_{pv}) listed in Table 3.2 and data from Ross et al [11]. The recovery phase includes the procedure of wheelchair acceleration after releasing and then deceleration until the next stroke starts. As a result, a stronger last push before releasing suggests that a higher velocity can be achieved to optimize wheelchair propulsion, thereby reducing the period of deceleration during recovery phase as shown in Figure 3.5. This was further illustrated in Figure 3.3 whereby group II subjects tended not to lose ground between pushes by the fact that V_r was less than V_c for any given stroke.

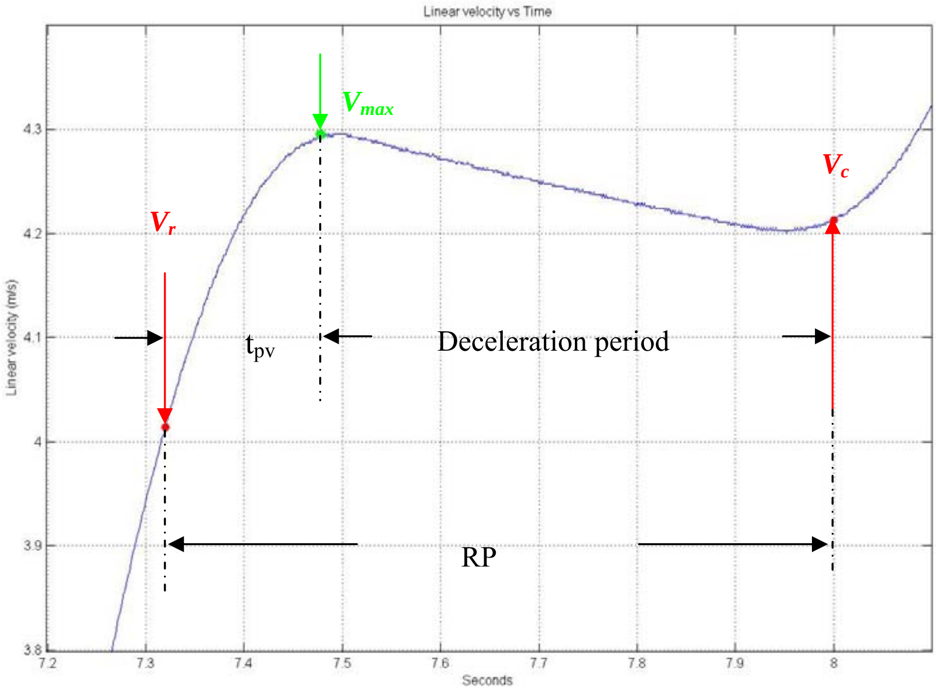

Figure 3.5 *Velocity graph during recovery phase (RP)*

3.3.2 Power output

A certain amount of work is required for the user to move their wheelchair from one place to another. For wheelchair propulsion to be practical, the task of moving must be completed within a reasonable time. Hence, it is useful to measure of the rate at which work can be done, i.e. power output. Figure 3.6 shows a comparison of power output curves for the best performance of a subject in each group. As illustrated in Figure 3.6, subjects with lower lesion injuries produce a much higher and smoother power output curve with a shorter PP time (0.597s for L1 subject versus 0.625, 0.782 and 0.778 for T10, T5 paraplegia and C5 tetraplegia). P_{max} for the C5 tetraplegia (150 watts) was found to be significantly lower than the other three subjects (800 watts for T5, 1050 watts for T10 and 1250 watts for L1 paraplegia). The reason that the highest power output was generated by an L1 subject was likely due to their ability to generate greater torque to accelerate the wheelchair with the aid of full upper body control. More importantly, the differences in power output as listed above were likely related to the muscle control among different SCI level subjects. The largest difference was observed in T5 paraplegia and C5 tetraplegia subjects due to the control of triceps or lack thereof, as illustrated in Figure 3.6.

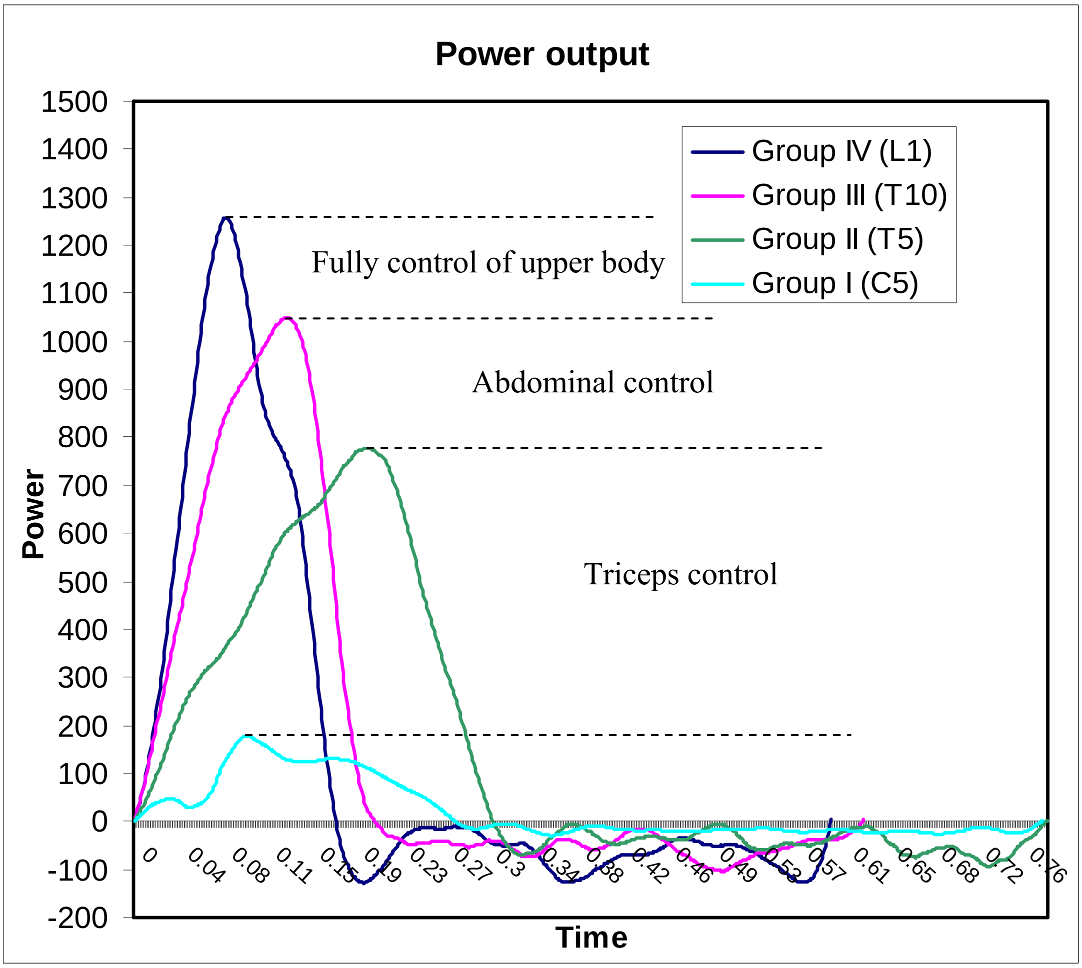

***Figure 3.6** The graphs of power output of the best performing person from each group*

3.3.3 Kinematics from video recordings

The calculated kinematic parameters for normal and twice-normal resistance tests are listed in Table 3.3. The propulsion phase (PP) was higher in Group I (1.3s), when accelerating the wheelchair from stationary up to a constant speed, compared with the other groups (0.98, 0.7 and 1s for Group II, III and IV respectively), which correlated directly with power output curves in Figure 3.4. More importantly, the difference in PP was more obvious after increasing the rolling resistance (1.76 for Group I versus 1.16, 0.88 and 0.87s for Group II, III and IV). When expressed as PP/ST (stroke time), the highest value was observed in Group I, which indicated that they spent the longest time contacting the push-rim to accelerate the wheelchair. Therefore, a higher PP and PP/ST suggested that higher lesion level subjects would encounter more difficulties in overcoming a range of environments and obstacles, which agreed well with the velocity results mentioned previously.

***Table 3.3** The results of all the kinematics in four groups*

1st trial	Normal Resistance test				Twice-normal resistance test			
	I	II	III	IV	I	II	III	IV
PP *[s]*	1.3(0.26)	0.98 (0.11)	0.7(0.24)	1(0.06)	1.76(0.25)	1.16(0.1)	0.88(0.25)	0.87(0.18)
RP *[s]*	0.39(0.04)	0.48(0.14)	0.39(0.17)	0.5(0.14)	0.39(0.06)	0.43(0.13)	0.34(0.1)	0.44(0.06)
PP/ST *[%]*	76.2(5.3)	67.3(7.6)	64.3(6.7)	67(5.1)	81.7(1.3)	73.3(5.7)	71.5(7.9)	66(7.6)
θc *[^{o}]*	-34.3(8.1)	-33.9(7.7)	-26.5(7.8)	-38.1(15.4)	-33.7(11.4)	-26.4(14.8)	-27.8(4.5)	-28.7(2)
θ_r *[^{o}]*	36.4(11.2)	39.8(10.7)	47.8(19.1)	59.5(40.6)	25(9.8)	36(16.9)	37.7(17.1)	64.5(34.6)
$\theta_{E\text{-}min}$ *[^{o}]*	109.6(14.3)	92.7(8.8)	107.5(15.2)	96.9(31)	112.2(14.6)	96.7(9.38)	104.5(16.5)	98.1(32.6)
$\theta_{E\text{-}max}$ *[^{o}]*	132.3(10.4)	127.8(6.6)	136.6(4.9)	151.8(19.7)	134(10)	126.9(5.3)	132.5(6.2)	149.3(21.7)
$\theta_{T\text{-}min}$ *[^{o}]*	-2.4(1.3)	-0.2(3.4)	4.6(4.1)	3(2.5)	-3(2.3)	-0.18(1.6)	2.85(0.8)	8.5(14)
$\theta_{T\text{-}max}$ *[^{o}]*	5.7(5.7)	4.8(3.4)	11.5(3.7)	22.9(18.5)	3.7(4.7)	3.95(2.7)	11.9(3.4)	20.8(20.2)

2nd trial	Normal Resistance test				Twice-normal resistance test			
	I	II	III	IV	I	II	III	IV
PP *[s]*	0.61(0.13)	0.42(0.05)	0.33(0.08)	0.32(0.06)	0.91(0.13)	0.62(0.11)	0.46(0.08)	0.42(0.08)
RP *[s]*	0.42(0.06)	0.45(0.13)	0.38(0.08)	0.48(0.06)	0.42(0.06)	0.47(0.14)	0.36(0.07)	0.4(0)
PP/ST *[%]*	59.1(5.6)	48.9(7.2)	46.5(6.8)	40(7)	68.7(2)	57.5(5.5)	56.1(7.4)	50.9(5.1)
θc *[^{o}]*	-36.2(5.2)	-35(7.8)	-25.5(7.8)	-22.1(8.2)	-33.6(10.1)	-33.9(16.3)	-26.6(1.5)	-24.8(10.4)
θ_r *[^{o}]*	34.5(11.7)	42.5(11.1)	50.4(15.7)	54.7(26)	29.8(4.1)	38.7(9.3)	45(19.6)	53.5(33.6)
$\theta_{E\text{-}min}$ *[^{o}]*	108.6(15.8)	98.8(8.6)	107.2(13.1)	96.8(27.5)	112(14.2)	98.1(10.9)	107.4(14.1)	97.8(31.9)
$\theta_{E\text{-}max}$ *[^{o}]*	134.1(7.6)	130.7(3.1)	136.3(6.4)	146.5(22.8)	134(9.1)	124.8(2.5)	136.6(6.3)	148.4(18.5)
$\theta_{T\text{-}min}$ *[^{o}]*	-0.1(3.7)	0.2(3.6)	5.13(2.8)	12.3(11)	-1.1(3.1)	0.9(2.5)	5.5(3.4)	12(14.9)
$\theta_{T\text{-}max}$ *[^{o}]*	2.6(4.1)	4.8(3.5)	10.8(3.6)	16.1(12.1)	3.4(5.1)	4(3.1)	10.4(3.8)	15.3(15.2)

3rd trial	Normal Resistance test				Twice-normal resistance test			
	I	II	III	IV	I	II	III	IV
PP *[s]*	0.54(0.13)	0.33(0.55)	0.26(0.05)	0.28(0.01)	0.82(0.23)	0.33(0.55)	0.38(0.08)	0.34(0.08)
RP *[s]*	0.39(0.07)	0.43(0.13)	0.32(0.06)	0.42(0.03)	0.42(0.05)	0.43(0.13)	0.34(0.08)	0.42(0.03)
PP/ST *[%]*	57.8(5.3)	44.3(8.2)	45.2(4.5)	40(1.6)	65.6(7.2)	44.3(8.2)	52.8(9.6)	44.4(4.5)
θc *[^{o}]*	-35.2(5.5)	-31.4(7.8)	-25.2(4.5)	-21.1(2)	-34.2(9.5)	-31.4(7.8)	-25.1(4.4)	-23.5(10.6)
θ_r *[^{o}]*	35.1(10.7)	41.6(7.1)	50.4(19.1)	56.9(26.2)	28.6(9.3)	41.6(7.1)	47.2(15.1)	61.4(26.8)
$\theta_{E\text{-}min}$ *[^{o}]*	110(14.9)	101.3(9.8)	103.1(15.5)	100.1(26.6)	114.2(12.1)	101.3(9.8)	105.3(15.9)	97.1(30.7)
$\theta_{E\text{-}max}$ *[^{o}]*	132.8(9.5)	132.1(5.1)	135.5(5.5)	147.9(14.6)	135(7.7)	132.1(5.1)	134.2(8.6)	151.2(23.2)
$\theta_{T\text{-}min}$ *[^{o}]*	-0.2(4.2)	-0.5(4.88)	6.8(3.1)	12.2(12.4)	-0.9(3.3)	-0.5(4.88)	5.7(3.1)	12.7(14.5)
$\theta_{T\text{-}max}$ *[^{o}]*	2.5(4.2)	5.4(4.1)	10(3)	16.8(8.3)	2.7(4.8)	5.4(4.1)	9.7(3.1)	17.1(16.7)

3.3.3.1 Propulsion phase

The range of contact angles was also found to be related to SCI level, ranging from 70^o (Group I) to 116^o (Group IV) as shown in Figure 3.7. This indicated that Group IV subjects had the ability to adjust contact closer to the TDC and release closer to the bottom dead centre (BDC) to increase the contact range of the push-rim, resulting in an increased velocity with each push. More importantly, this also suggested that subjects with lower lesion injuries (e.g. Group IV) had the ability to produce a higher impulse during the late push, resulting in a greater torque and power output with the aid of reaching closer to the BDC. Furthermore, Figure 3.7 illustrated that reduced arm function resulted in a decrease of the movement range of the elbow. Due to the lack of triceps function, elbow angle in Group I subjects remained in a more extended position (approximately 130^o) during the whole propulsion stroke compared with

75.2^o to 164.5^o observed in Group IV, and this movement limitation was reflected in the lower power output and force generated on the wheel. As a result, the greatest difference in kinematics patterns relates to how subjects with tetraplegia positioned the forearm to contact the push rim.

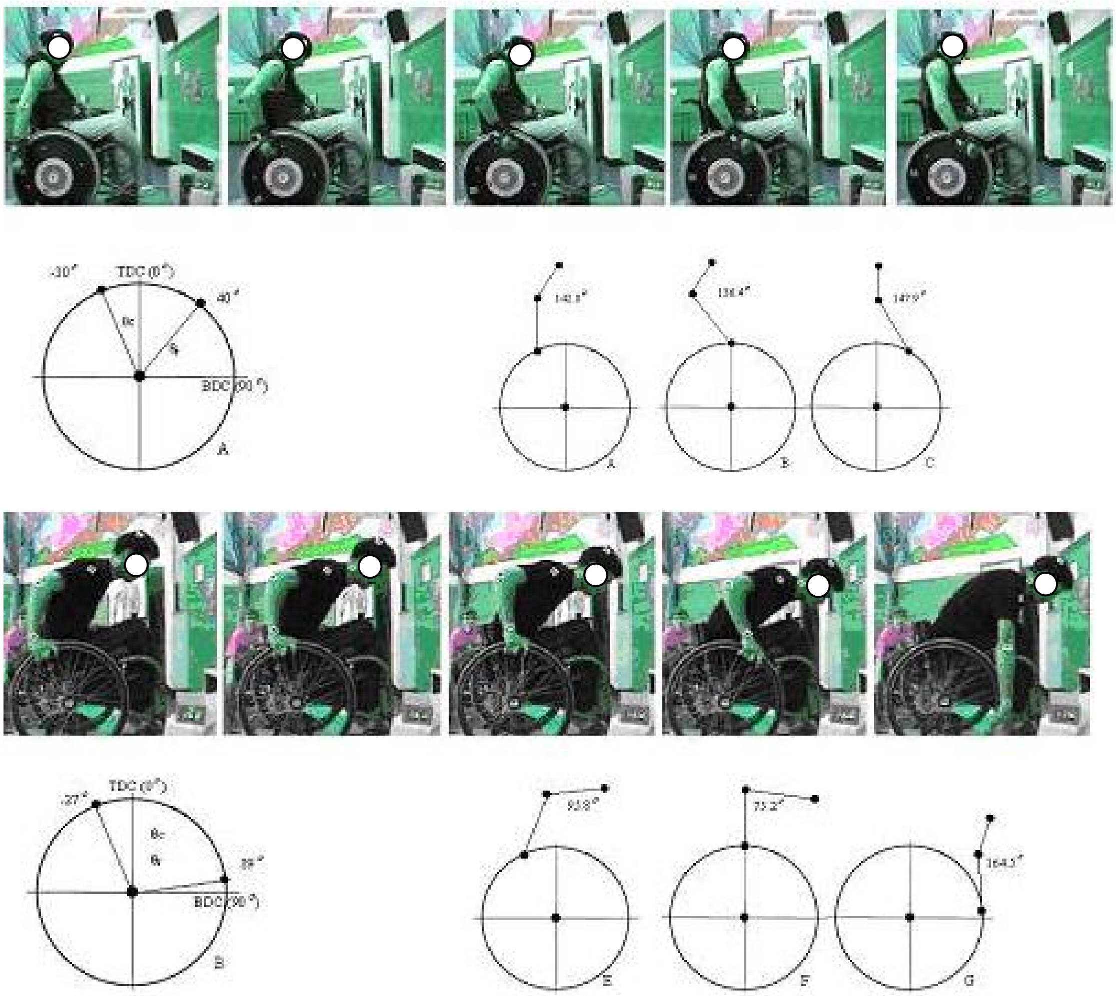

Figure 3.7 *Example of two typical forms of maximum contact and release angle of the elbow for Group I (top) and Group IV subjects (bottom).*

3.3.3.2 Recovery phase

As shown in Figure 3.8, the graphs in the left column illustrating the hand movements of different SCI groups adapted from Annet et al [9], are in agreement with the results found in this study. Due to the lack of triceps control, Group I subjects can not reach to full extension and have to flex their elbows during the recovery phase rather than further extending their elbows as observed in the other groups. The control of the abdominal muscles further helps Group III and IV subjects to lean forward and push the wheel closer to the BDC and thereby generate a stronger impulse before releasing as well as reduce the contact time with the wheel when the velocity is increasing.

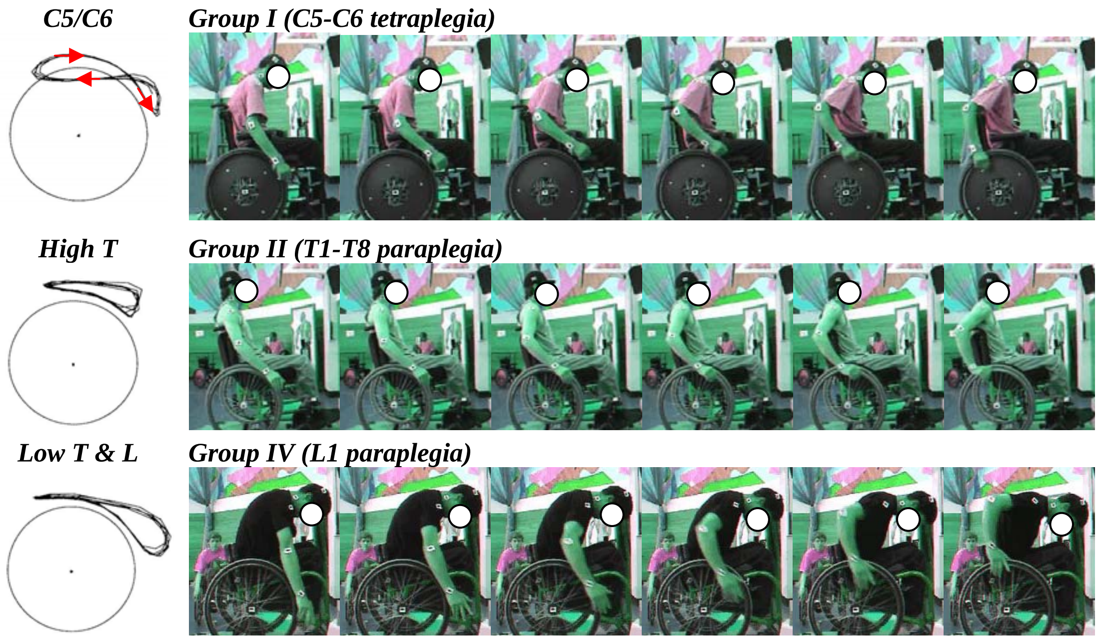

Figure 3.8 *The graphs of the hand movement in different groups*

Due to the lack of triceps control, Group I subjects' elbows remain at more fixed angle compared with other groups where elbow angle changes significantly, particularly during the last quarter of the propulsion phase (Figure 3.9). This suggests that Group I subjects cannot generate a strong impulse before releasing as the other groups of subjects do. When the velocity increases, the Group I subjects have to depend more on the pull phase (elbow flexion) to accelerate the wheelchair. The elbow movement patterns also help to explain the lower torque and power output generated by Group I subjects with cervical spinal cord lesion.

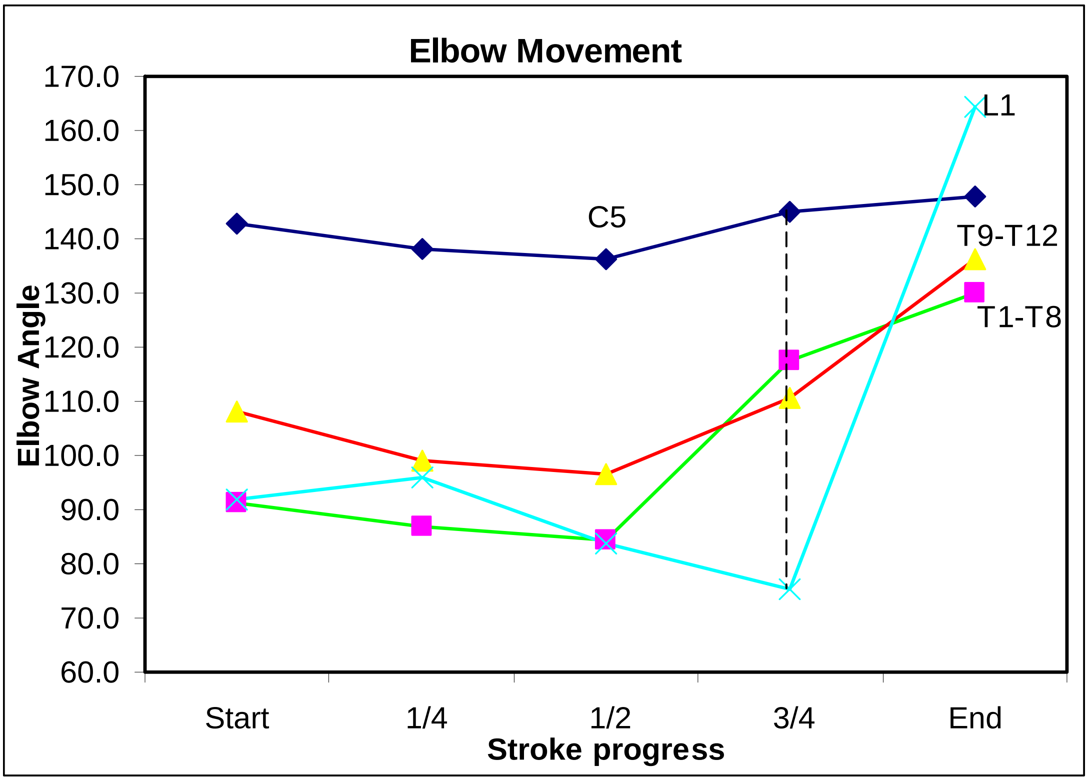

Figure 3.9 *The graph of the elbow movement in four groups*

3.3.4 Trunk contribution

Different movement patterns of the upper body, including trunk and arm, also result in the different performances in the four groups. As shown in Table 3.3 and Figure 3.10, the trunk movements are small for all the subjects after the 1st trial. The difference is that Group I subjects depend more on the backrest of the wheelchair compared with Group III and IV subjects with abdominal muscle control who tend to lean more forward.

Figure 3.10 *Trunk movement comparisons in all groups*

3.4 Conclusion

In this study, an alternative kinetic and kinematics test procedure is described to measure wheelchair propulsion in SCI subjects using a custom-made wheelchair dynamometer. A reduced propulsive capacity is best demonstrated by the effect of SCI level on propulsion speed, e.g. 2.83 m/s for Group I versus 6.4, 7.24 and 8.49 m/s for Group II, III and IV respectively after first three trials from a stationary start.

Furthermore, subjects with cervical spinal cord lesion (Group I) show a dramatically lower peak power output (140.1 watts) than the subjects with a thoracic or lumbar lesion (737.1, 755.5 and 959.9 watts for Group II, III and IV respectively). Finally, based on kinematics analysis (i.e. contact and release angle, elbow angle and hand movement patterns), 1.5 times greater contact angle range and 5.5 times greater elbow angle range during the propulsion phase are observed in Group IV compared with Group I, C5/C6 tetraplegia subjects differ significantly from subjects with a lower SCI level, as observed by the lowest wheelchair propulsion performance in Group I. The results of this study quantify the effect of SCI level on wheelchair propulsion ability at different intensity conditions (normal and twice-normal resistance), characterize wheelchair propulsion kinematics for people with SCI's, and indicate that arm function is a more important factor in wheelchair propulsion than trunk stability and strength. Given that triceps function appears to be important for wheelchair propulsion, we are currently investigating the effectiveness of the posterior deltoid to triceps transfer surgery to further study the role of triceps function during propulsion and recovery phase in C5/C6 tetraplegia.

Acknowledgements

I would like to thank all the subjects from the Burwood Hospital Spinal Injury Unit, Christchurch, New Zealand.

References

[1] Sie I, Waters R L, Adkins R and Gellman H. Upper extremity pain in the post rehabilitation spinal cord patient. Arch. Phys. Med. Rehab. 73 44-8 1992

[2] Korelia Kulig, Craig J. Newsam and Sara J Mulroy. The effect of level of spinal cord injury on shoulder joint kinetic during manual wheelchair propulsion. Clinical Biomechanics 16 (2001) pp 744-751 July 2001

[3] Kornelia Kulig, Sreesha S. Rao and Sara J. Mulroy. Shoulder joint kinetics during the push phase of wheelchair propulsion. Clinical Orthopaedics and Related Research Number 354 pp 132-143 March 25 1998

[4] Alicia M Koonta, Rory A. Cooper, Michael L. Boninger, Aaron L. Souza, Brian T. Fay. Shoulder kinematics and kinetics during two speeds of wheelchair propulsion. Journal of Rehabitation Research and Development Vol. 39 No. 6 pp 635-650 November/December 2002

[5] Hwai-Ting Lin, Fong-Chin Su, Hong-Wen Wu and Kai-Nan An. Muscle forces analysis in the shoulder mechanism during wheelchair propulsion. Proc. Instn Mech. Engrs Vol. 218 Part H: J. Engineering in Medicine. 2004

[6] F.C.T. van der Helm and H. E. J. Veeger. J. Quasi-static analysis of muscle forces in the shoulder mechanism during wheelchair propulsion. Biomechanics Vol. 29. No. 1 pp 39-52 1996

[7] Carmen P. DiGiovine, Rory A. Cooper and Michael A Boninger. Dynamic calibration of a wheelchair dynamometer. Journal of Rehabilitation Research and Development Vol. 38 No. 1, January and February 2001

[8] Rory A. Cooper. Rehabilitation Engineering (Applied to Mobility and Manipulation)

[9] Annet J. Dallmeijer, Yvonne J.Kappe, Dirkjan H.E.J. Veeger, Thomas W.J.Jassen and Luc H.V. van der Woude. Anaerobic power output and propulsion technique in spinal cord injured subjects during wheelchair ergometer. Journal of Rehabilitation Research and Development Vol. 31 No. 2, 1994 Pages 120-128

[10] Alicia M. Koontz, Rory A. Cooper, Michael L. Boninger, Yusheng Yang, Bradley G. Impink and Lucas H.V. van der Woude. A kinetic analysis of manual wheelchair propulsion during start-up on select indoor and outdoor surfaces. Journal of Rehabilitation Research and Development Volume 42 Number 4, July/August 2005 Pages 447-458

[11] A.D. Ross, N.E. Fowler and V.L. Goosey-Tolfrey. The intra-push velocity profile of the over-ground racing wheelchair sprint start. Journal of Biomechanics 38 (2005) 15-22

[12] Veeger HEJ, van der Woude LHV, Rozendal RH. A computerized wheelchair ergometer. Scand J Rehabil Med 1992;24:17-23.

[13] Langbein WE, Robinson CJ, Kynast L, Fehr L. Calibration of a new wheelchair ergometer: the wheelchair aerobic fitness trainer. IEEE Trans Rehabil Eng 1993;1:49-58.

[14] Theisen D, Francaux M, Fayt A. A new procedure to determine external power output during handrim wheelchair propulsion on a roller ergometer: a reliability study. Int J Sports Med 1996, 17:564-71.

[15] Forchheimer F, Lundberg Å. Wheelchair ergometer. Scand J Rehabil Med 1986, 18:59-63.

[16] Niesing R, Eijskoot F, Kranse R, den Ouden AH, Storm J, Veeger HEJ, et al. Computer-controlled wheelchair ergometer. Med Biol Eng Comput 1990; 28:329-38.

[17] Jarvis S, Rolfe H. The use of an inertial dynamometer to explore the design of children's wheelchairs. Scand J Rehabil Med 1982;14:167-76.

[18] Rick N. Robertson, PhD, Michael L. Boninger, MD, Rory A. Cooper, PhD and Sean D. Shimada, MS. Pushrim Forces and Joint Kinetics During Wheelchair Propulsion. Arch Phys Med Rehabil Vol 77, September 1996.

[19] Craig J. Newsam, Sreesha S. Rao, Sara J. Mulsroy, JoAnne K. Gronley, Ernest l. Bontrager and Jacquelin Perry. Three-dimensional upper extremity motion during manual wheelchair propulsion in men with different level of spinal cord injury. http://www.elsebier.com/locat/gaitpost

[20] Annet J. Dallmeijer, MSc Luc H. V. van der Woude PhD, H. E. J. (DirkJan) Veeger, PhD and A. Peter Hollander, PhD. Effectiveness of force application in manual wheelchair propulsion in persons with spinal cord injuries. American Journal Of Physical Medicine and Rehabilitation. 1998

[21] Kimberly T. Asato, Rory A. Cooper, Rick N. Robertson, and J. F. Ster. SMART^{Wheel}: Development and Testing of a System for Measuring Manual Wheelchair Propulsion Dynamics. IEEE TRANSACTIONS ON BIOMEDICAL ENGINEERING, VOL. 40, NO. 12, DECEMBER 1993

[22] Yagesh Bhambhani. Physiology of Wheelchair Racing in Athletes with Spinal Cord Injury. Sports Med 2002; 32 (1): 23-51

[23] Kenneth D. Coutts PhD. Kinematics of sport wheelchair propulsion. Journal of Rehabilitation Research and Development Vol. 27 No. 1 Pages 21-26.

[24] Margaret A. Finley, PhD, PT; Elizabeth K. Rasch, MS, PT; Randall E. Keyser, PhD; Mary M. Rodgers, PhD, PT. The biomechanics of wheelchair propulsion in individuals with and without upper-limb impairment. Journal of

Rehabilitation Research & Development Volume 41, Number 3B, Pages 385–394, May/June 2004

[25] Lan-Yuen Guo, K D Zhao, Fong-Chin Su and Kai-Nan An. Moment generation in wheelchair propulsion. Proc. Instn Mech. Engrs Vol. 217 Part H: J. Engineering in Medicine. 2003

CHAPTER 4

TROIDS EVALUATION

Evaluation of posterior deltoid to triceps transfer surgery in C5/C6 tetraplegia on manual wheelchair propulsion

Summary

Purpose: The aim for this study was to demonstrate any change in torque, velocity and power output of wheelchair propulsion and to characterize wheelchair propulsion kinematics following the TROIDS surgery in a group of C5/C6 tetraplegia subjects.

Method: The tests studied were self-chosen normal and maximal velocity under normal resistance and maximally accelerated start under twice-normal resistance condition on an inertia custom-made dynamometer. Twelve male subjects voluntarily participated in this test were grouped as: complete C6 tetraplegia (Group I: no elbow extension), complete C6 tetraplegia (Group II: TROIDS for elbow extension) and C7 tetraplegia (Group III: retained active triceps for elbow extension). Subjective information was gathered from all the post-surgery subjects using a questionnaire.

Results: The effect of triceps function on wheelchair propulsion was highlighted by the best performance in Group III subjects, including the highest power output (399.3 and 449.5 watts) and maximum velocity (4.7 and 3.32m/s) attained under normal and twice-normal resistance tests respectively. More importantly, the improvements in torque, power output and velocity, approximately 14.3%, 8.2% and 8.6 % respectively, were observed in Group II compared with Group I subjects following the normal resistance test and a similar trend was also found during the twice-normal resistance, which was due to the aid of triceps restoration on wheelchair propulsion during the push phase. Finally, the important result of Group II subjects naturally moving their arms in a “circular” pattern without any sort of training, which was more similar to Group III subjects, demonstrated that a better arm movement pattern during the recovery phase chosen following TROIDS surgery.

Conclusions: These observations indicate the extent of which triceps function improves wheelchair propulsion by highlighting the test performance differences in all three groups. The restoration of triceps by TROIDS not only allowed active elbow extension, but also increased the amplitude and strength as well as the speed of arm movement. The results also point to TROIDS allows a real push phase and a better arm movement pattern during both propulsion and recovery phase under normal and extreme conditions.

Nomenclature

V_c	Linear wheelchair velocity at point of hand contact (m/s)
1/4	First quarter of propulsion phase
TDC	Top dead center
3/4	Third quarter of propulsion phase
V_r	Linear wheelchair acceleration at point of hand release (m/s)
F_t	Tractive force (N)
m	Mass of wheelchair and occupant (kg)
g	Gravity (9.81m/s^2)
C_{rr}	Coefficient of rolling resistance
ρ	Air density (1.23 kg/m^3)
C_D	Drag coefficient
A	Frontal wheelchair area including occupant (m^2)
V_1	Linear wheelchair velocity on dynamometer under normal resistance test
a_1	Linear wheelchair acceleration on dynamometer under normal-resistance test
V_2	Wheelchair velocity on dynamometer under twice normal resistance test (m/s)
a_1	Wheelchair acceleration on dynamometer under twice normal-resistance test (m/s)
$O\,(x_C\,,\,y_C)$	Centre coordinate in four-bar linkage model
$S\,(x_S\,,\,y_S)$	Shoulder position in four-bar linkage model
$E\,(x_E\,,\,y_E)$	Elbow position in four-bar linkage model
$H\,(x_H\,,\,y_H)$	Hand position in four-bar linkage model
$T\,(x_T\,,\,y_T)$	Trunk position in four-bar linkage model
θ_S	Shoulder position (^{0})
θ_E	Elbow position (^{0})
θ	Hand position (^{0})
T_{max}	Peak torque on wheel (Nm)
P_{max}	Peak power output (watt)
V_{max}	Peak velocity (m/s)
t_{pv}	Time to peak velocity relative to contact time during one stroke (s)
V_c	Linear wheelchair velocity at point of hand contact (m/s)
V_r	Linear wheelchair velocity at point of hand release (m/s)
PP	Propulsion phase (s)
RP	Recovery phase (s)
θ_c	Contact angle (^{0})
θ_r	Release angle (^{0})
$\theta_{E\text{-}max}$	Maximum elbow angle (^{0})
$\theta_{E\text{-}min}$	Minimum elbow angle (^{0})
$\theta_{s\text{-}max}$	Maximum shoulder angle (^{0})
$\theta_{s\text{-}min}$	Maximum shoulder angle (^{0})
$\theta_{T\text{-}max}$	Maximum shoulder angle (^{0})
$\theta_{T\text{-}min}$	Maximum shoulder angle (^{0})

HC	Hand contact
HR	Hand release
V_{pull}	Elbow flexion velocity (m/s)
$t_{start\text{-}TDC}$	Time to TDC relative to contact time during one stroke (s) (s)
$V_{release}$ *(m/s)*	Elbow extension velocity (m/s)
$t_{TDC\text{-}End}$ *(s)*	Time to release relative to TDC during one stroke (s) (s)

4.1 Introduction

Wheelchair propulsion is an important part of daily living for many people with spinal cord injury (SCI). Higher injury levels severely restrict the ability of people with SCI to negotiate obstacles, ramps and uneven surfaces. Individuals with complete injuries at the C5/C6 level have severe loss of upper limb function. They typically have good preservation of shoulder abduction and external rotation, elbow flexion and variable wrist extension but little or no voluntary control of elbow extension and no hand function. Management options include the Deltoid to Triceps transfer (TROIDS) surgery [1-3] or a mechanical orthosis [4, 5] that provides passive elbow extension. The TROIDS surgery involves detaching the posterior deltoid muscle, which remains under voluntary control, and transferring it to the distal triceps tendon via a free tendon graft, e.g., tibialis or hamstrings.

Following a prolonged rehabilitation programme the TROIDS transfer enables a tetrapelgic person to actively extend and control the elbow against gravity plus assisting in transfers, reaching above shoulder height, driving and wheelchair mobility skills. For evaluating recovery of elbow extension following TROIDS surgery, most studies [7, 9-13] have focused on the area of elbow extension in many daily life activities, such as arm raising, driving, swimming and writing [14]. For example, Remy-Neris et al. [9] described a procedure for measuring straight-arm raising and hand-to-nape-of-neck movement by testing 16 tetraplegia and Rabischong et al. [11] quantified maximal torque when locking arm and forearm in position in C6 tetraplegia subjects who had received TROIDS surgery. Other evaluations of the TROIDS transfer surgery have relied on interview or questionnaires [7-8], which are not specific to subjects with tetreplegia. However, until recently, few investigations have focused on a systematic functional quantification of the wheelchair propulsion mechanics in tetraplegia subjects pre-and post-TROIDS transfer surgery [15]. We have previously described the design and validation of a wheelchair dynamometer [Chapter 2] as well as kinetic and kinematic models describing wheelchair propulsion [Chapter 3] in subjects with varying SCI levels. These studies demonstrated that the test rig and test methods were capable of accurately measuring a person's propulsion ability.

While some evidence suggests that TROIDS surgery might improve wheelchair propulsion ability, no previous studies have related directly to functional outcomes. As a result, the aim for this study was to demonstrate any change in torque, velocity and power output of wheelchair propulsion and to characterize wheelchair propulsion kinematics following the TROIDS transfer surgery in a group of C5/C6 tetraplegia subjects.

4.2 Methods and Materials

4.2.1 Subjects

The inclusion criteria for the potential subjects (adapted from [9]) were (i) complete tetraplegia, (ii) use of a manual wheelchair as the primary mode of mobility, and (iii) between 18 and 65 years old. Twelve male subjects (Table 4.1) voluntarily participated in this test after giving written informed consent. Two complete C6 tetraplegia subjects with no active elbow extension and no hand function, but preserved shoulder abduction, external rotation, elbow flexion and variable wrist extension were classified as Group I. Four complete C6 tetraplegia who had undergone the TROIDS at times ranging from 8 to 15 year after surgery were taken as Group II. Six C7 tetraplegia subjects with active triceps for elbow extension as well as wrist extensor and hand control were classified as Group III.

Table 4.1 *Group means and standard deviations of personal data*

Groups / Subjects data	Group I (n=2)	Group II (n=4)	Group III (n=5)
Gender	M	M	M
Age	21 (2.8)	33.8 (3)	44 (10)
Weight (kg)	70 (14.1)	86.9 (21.2)	87.8 (6.8)
Upper arm Length (cm)	27 (0.7)	24.9 (1.8)	29.6 (0.9)
Forearm Length (cm)	24.7 (3.3)	25.2 (1.2)	26.1 (2)
Duration W/C use (months)	8 (8.5)	178.5 (36.1)	137.8 (127)
Time after surgery (months)	-	117 (46.3)	-

4.2.2 Test rig

A custom-made wheelchair dynamometer (Figure 4.1) was designed and built at the Department of Mechanical Engineering, University of Canterbury. The wheelchair was rigidly fixed to the dynamometer with the rear wheels sitting on two independent rollers. The rollers have a mass moment of inertia of 0.7132 kg-m^2. Additional flywheels (solid steel discs) can be fixed to the outboard end of the rollers to achieve a required mass moment of inertia. Two rotary encoders (US digital, 1000 counts per revolution) were fitted to the inboard end of the dynamometer. These encoders were connected to a personal computer to record the roller position with respect to time. From the position/time data, roller velocity and acceleration can be measured. Video cameras were positioned on each side of the dynamometer at elbow height to capture the participants arm motion during wheelchair propulsion. An LED counter, visible in the video frames, shows the time so that the video can be synchronised with the recorded wheel position data.

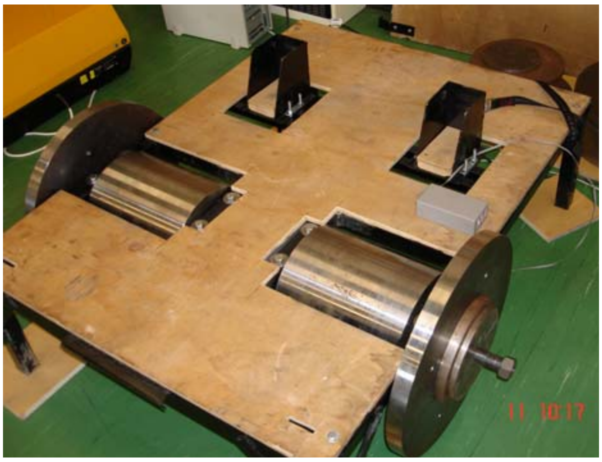

Figure 4.1 *The wheelchair Dynamometer*

4.2.3 Test procedure

The test involved varying levels of exertion from a self-selected comfortable speed test along flat ground to maximum acceleration test from rest and a maximum acceleration test with twice-normal resistance. The twice-normal resistance test achieved by adding addition inertia to the rollers equal to the participants weight. The twice-normal resistance test was used to simulate a persons ability to negotiate a high resistance surface or a steep ramp. Finally, subjective information was gathered from all the post-surgery subjects using a questionnaire, which explored two questions adapted from [15].

- Question 1: Has the TROIDS surgery made a difference to your ability to carry out day-to-day tasks?
- Question 2: Has the TROIDS surgery enabled you to participate in any new activities?

4.2.4 Data analysis

The kinematics data analysis involved calculating the wheelchair distance, velocity and acceleration based on the number of pulses gathered from the roller drum and the corresponding time recordings. Arm position was determined by analysing the video recordings to determine arm positions by tracking markers as shown in Figure 4.2A. For the kinetic data, for example, force, torque and power output, were calculated in Matlab (The MathWorks, Inc. USA) and relied on the data gathered from the encoders mounted on the test rig. A four-bar linkage model [16], which consisted of four segments, namely, upper arm, lower arm, hand to wheel axel and shoulder to wheel axle, for optimization of wheelchair propulsion, was adapted for this study in Figure 4.2B.

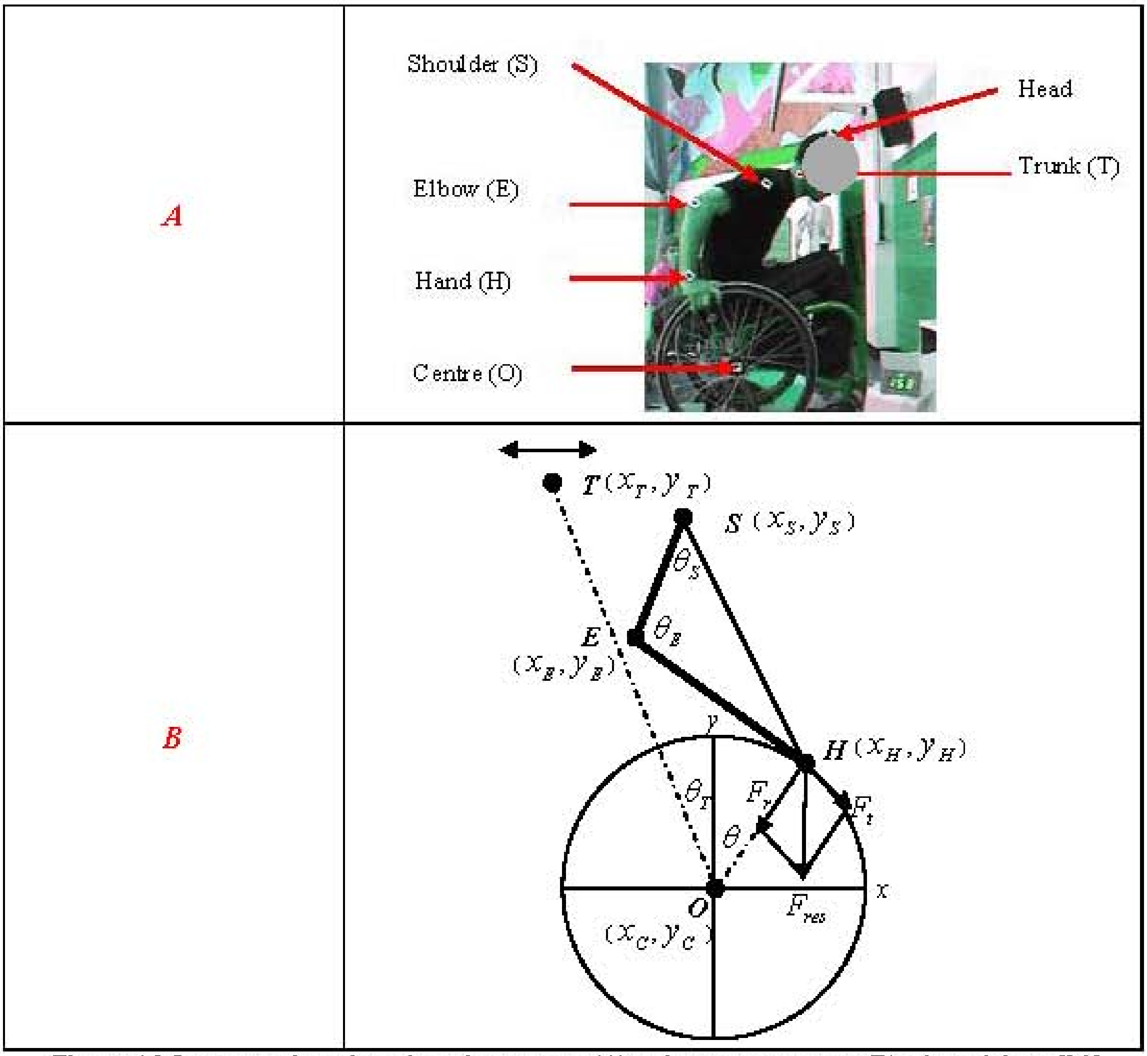

Figure 4.2 *Location of markers for video capture (A) and system geometry (B) adapted from [16]*

Wheelchair propulsion includes the recovery phase as well as actual propulsion (Figure 4.3). The propulsion (or force) phase is a closed chain event, during which the hand is in contact with the rim. It consists of pull and push segments, and begins with when the hands contacting the top of the rim or at a point just behind the top dead centre (TDC). The phase ends when the hands leave the rim, usually when the arms are extended. The propulsion phase (PP) is divided into: contact, first quarter, TDC, third quarter and release. The recovery phase (RP) is an open chain event during which no force is exerted on the push-rim. Four segments are involved; follow through, retrieval, pre-impact and pre-load (Figure 4.3).

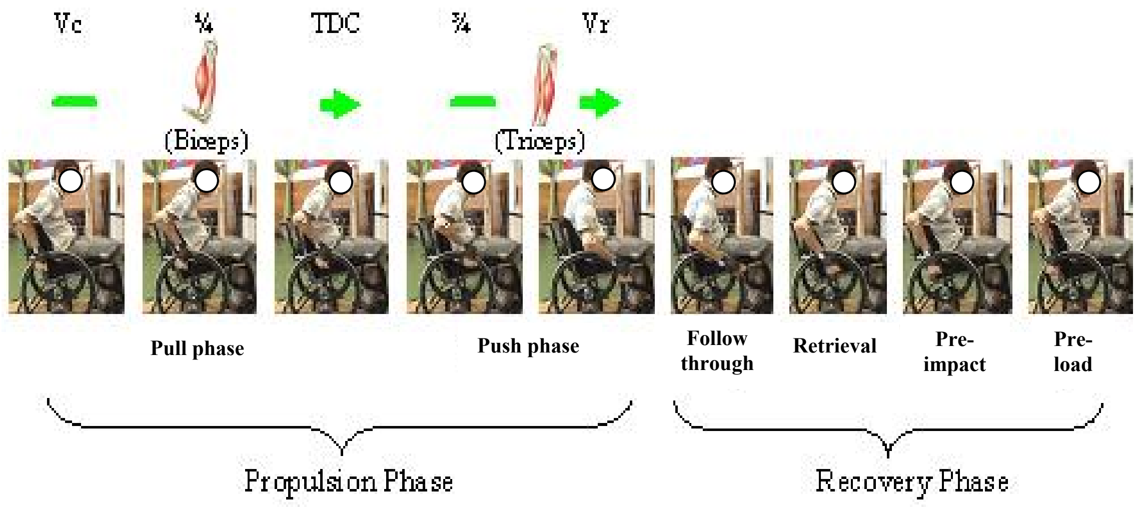

Figure 4.3 *The phases of wheelchair propulsion*

4.3 Results

The first three pushes were analysed given that they are the instances when the resistance is highest, and therefore, give an indication of a person's ability to negotiate difficult situations such as a ramp or rough surfaces. Further justification for measuring the first three push cycles in this study was that the first push is the push from a stationary start, and the second push is the first push in which the subject contacts the push-rim when the wheelchair is in motion. Push three demonstrates the transition period of moving to the steady-state propulsion, which provides information for the constant speed propulsion analysis.

The comparisons of the results listed in Table 4.2, i.e. maximum torque (T_{max}) and power output (P_{max}), demonstrated the important role of the triceps during wheelchair propulsion. The effect of triceps function on wheelchair propulsion was highlighted by the best performance in Group III subjects, including the highest power output (399.3 and 449.5 watts) and maximum velocity (4.7 and 3.32m/s) attained under normal and twice-normal resistance tests respectively (Table 4.2 and 4.3). More importantly, the improvements in torque, power output (Table 4.2) and velocity (Table 4.3), approximately 14.3%, 8.2% and 8.6 % respectively, were observed in Group II compared with Group I subjects following the normal resistance test and a similar trend was also found during the twice-normal resistance. As a result, the increases in both of kinetic (torque and power output) and kinematics (velocity) data illustrated the improvement of propulsion ability by the triceps restoration after TROIDS transfer surgery in Group II subjects.

Table 4.2 *The kinetic test results*

1st cycle	Normal Resistance test			Twice-normal resistance test		
	I	II	III	I	II	III
T_{max} *[Nm]*	**5** (9.4)	**7.5** (14.8)	**14.7** (23.9)	**5.9** (13.3)	**8.4** (19.5)	**21.6** (12.8)
P_{max} *[w]*	**54.6**(35.4)	**83.8** (65.2)	**234.7** (33.3)	**43.1** (43.3)	**66.1** (43.5)	**220.2** (22.5)
2nd cycle	**Normal Resistance test**			**Twice-normal resistance test**		
	I	II	III	I	II	III
T_{max} *[Nm]*	**4.9** (10.3)	**4.3** (5.9)	**13.2** (29.7)	**5.6** (20.5)	**6.4** (13.5)	**21.3** (22.8)
P_{max} *[w]*	**90.1** (51.9)	**90.7** (65.2)	**340.1** (43.7)	**67** (67.4)	**85.3** (54.3)	**42.2** (73.2)
3rd cycle	**Normal Resistance test**			**Twice-normal resistance test**		
	I	II	III	I	II	III
T_{max} *[Nm]*	**36.3** (12.7)	**41.5** (3.8)	**102.9** (19.7)	**55.4** (13.1)	**58.1** (11.5)	**184.2** (20.2)
P_{max} *[w]*	**88.2** (77.9)	**95.5** (48.6)	**399.3** (68.6)	**86.8** (70.6)	**97.9** (59.4)	**449.5** (76.9)

Table 4.3 *The kinematics test results gathered from encoders*

1st cycle	Normal Resistance test			Twice-normal resistance test		
	I	II	III	I	II	III
V_{max} *[m/s]*	**1.75** (0.31)	**2.11** (1.19)	**3.31** (0.85)	**1.12** (0.84)	**1.1** (0.5)	**2.26** (0.75)
t_{pv} *[s]*	**1.71** (0.15)	**1.42** (0.3)	**1.01** (0.19)	**2.18** (0.48)	**2.02** (0.2)	**1.43** (0.28)
V_r *[m/s]*	**1.68** (0.35)	**2.03** (1.15)	**3.12** (0.62)	**1.09** (0.8)	**1.05** (0.5)	**2.13** (0.67)
2nd cycle	**Normal Resistance test**			**Twice-normal resistance test**		
	I	II	III	I	II	III
V_{max} *[m/s]*	**2.44** (0.41)	**2.62** (1.32)	**4.23** (0.75)	**1.81** (0.92)	**1.51** (0.55)	**3.08** (0.88)
t_{pv} *[s]*	**0.92** (0.07)	**0.76** (0.09)	**0.57** (0.03)	**1.44** (0.66)	**1.09** (0.19)	**0.8** (0.12)
V_c *[m/s]*	**1.74** (0.29)	**2.08** (1.18)	**3.18** (0.73)	**1.07** (0.9)	**1.07** (0.47)	**2.17** (0.64)
V_r *[m/s]*	**2.38** (0.49)	**2.56** (1.3)	**4.03** (0.77)	**1.75** (0.94)	**1.47** (0.54)	**2.98** (0.88)
3rd cycle	**Normal Resistance test**			**Twice-normal resistance test**		
	I	II	III	I	II	III
V_{max} *[m/s]*	**2.71** (0.21)	**2.96** (1.45)	**4.97** (0.77)	**2.26** (1.02)	**1.77** (0.65)	**3.4** (0.67)
t_{pv} *[s]*	**0.78** (0.05)	**0.69** (0.19)	**0.56** (0.06)	**1.14** (0.47)	**0.98** (0.21)	**0.72** (0.13)
V_c *[m/s]*	**2.42** (0.4)	**2.56** (1.35)	**4.17** (0.78)	**1.8** (0.92)	**1.48** (0.56)	**2.76** (0.65)
V_r *[m/s]*	**2.66** (0.27)	**2.89** (1.43)	**4.7** (0.81)	**2.24** (0.99)	**1.76** (0.63)	**3.32** (0.69)

Further analysis of video recordings not only demonstrated the different techniques of propelling wheelchair between Group I, II and III in both propulsion and recovery phase, but also illustrated the reasons for the different performances observed in all three groups depending on the mechanics of wheelchair propulsion. Characteristics of upper body movement, such as arm and trunk, during sub-maximal and maximal velocity were addressed. In Table 4.4, the highest PP and RP observed in Group I subjects resulted in the longest time spent in propelling the wheelchair. Furthermore, during the normal resistance test, the greatest contact angles (θ_c in Table 4.4) were observed in Group I (35.4^o) versus 31.7^o in Group II and 26.6^o in Group III. Group I subjects also had dramatically greater shoulder extension angles ($\theta_{s\text{-}max}$ in Table 4.4) at initial contact than the other two groups (70^o in Group I versus 60^o in Group II and III on average). Therefore, the results demonstrated that subjects without active elbow extension (Group I) depended more on the pull phase (relatively higher shoulder and elbow extension during the pull phase) for accelerating the wheelchair, which was further verified by a similar trend during twice-normal resistance test.

In terms of trunk motion, the first push was unique during the propulsion phase ($\theta_{T\text{-}min}$ and $\theta_{T\text{-}max}$ in Table 4.4) because the largest movement always occurred during the start. For the second push, the peak flexion of the trunk was observed at first contact, continuing throughout the whole propulsion phase, and was opposite to the trunk motion compared with the first push. However, in push three, the range of trunk motion was reduced and this indicated it was a velocity-dependent factor. Given the limited abdominal control, C5/C6 tetraplegia subjects in all groups relied little on trunk movements to contribute to wheelchair propulsion. The difference was observed in Group II subjects who depended more on the backrest of the wheelchair compared to Group III (highest trunk flexion was found in Group III in Table 4.4) who tended to lean more forward. Furthermore, while similar trunk movement was expected between Groups I and II, some Group I subjects relied on their wheelchair belt to better control upper body balance and leaning forward may have influenced the difference in $\theta_{T\text{-}max}$ (Table 4.4) values observed.

***Table 4.4** The kinematics test results captured from video recordings*

1st cycle	Normal Resistance test			Twice-normal resistance test		
	I	II	III	I	II	III
PP *[s]*	**1.51** (0.09)	**1.18** (0.25)	**0.85** (0.17)	**1.93** (0.44)	**1.82** (0.19)	**1.26** (0.18)
RP *[s]*	**0.52** (0.11)	**0.37** (0.03)	**0.4** (0.12)	**0.72** (0.39)	**0.44** (0.08)	**0.4** (0.12)
PP/CT *[%]*	**74.4** (4.8)	**75.7** (4.1)	**68.1** (9.9)	**73.5** (11.9)	**80.4** (4)	**76.2** (5.6)
θc *[°]*	**-31.2** (15.3)	**-40** (10.4)	**-29.4** (18.5)	**-39** (11.4)	**-43.5** (12.1)	**-32.2** (11.9)
θ_r *[°]*	**44.9** (5.6)	**34.1** (7.8)	**46.7** (4.6)	**19.1** (7.4)	**24.2** (11.1)	**41.7** (8.5)
$\theta_{E\text{-}min}$ *[°]*	**105** (5.2)	**108** (14.6)	**111.3** (10.6)	**100** (10.3)	**108.6** (15.9)	**110.5** (10.4)
$\theta_{E\text{-}max}$ *[°]*	**132.3** (1.2)	**132.6** (10.4)	**141.2** (8.7)	**129.3** (2.2)	**137.3** (10.8)	**137.1** (6.3)
$\theta_{S\text{-}min}$ *[°]*	**24.2** (1.4)	**26.8** (6.2)	**24.7** (6.2)	**30.3** (8.2)	**24.9** (3.2)	**25.2** (5.4)
$\theta_{S\text{-}max}$ *[°]*	**71.5** (6.7)	**63.8** (16.2)	**60.8** (12.5)	**62.9** (7.1)	**64** (21.9)	**57.9** (10.3)
$\theta_{T\text{-}min}$ *[°]*	**1.5** (2)	**-2** (2.2)	**1.4** (4.3)	**1.1** (1.5)	**-3** (3)	**0.7** (2.5)
$\theta_{T\text{-}max}$ *[°]*	**8.7** (5.4)	**3.5** (2.6)	**9.6** (3.4)	**7.5** (2.4)	**2.5** (4)	**8.3** (2)
2nd cycle	Normal Resistance test			Twice-normal resistance test		
	I	II	III	I	II	III
PP *[s]*	**0.77** (0.14)	**0.62** (0.1)	**0.41** (0.09)	**1.36** (0.45)	**0.9** (0.15)	**0.65** (0.13)
RP *[s]*	**0.63** (0.16)	**0.37** (0.07)	**0.38** (0.15)	**0.52** (0.08)	**0.42** (0.07)	**0.39** (0.13)
PP/CT *[%]*	**55.5** (6.1)	**62.6** (3.7)	**53.1** (5.3)	**71.4** (5.3)	**67.7** (5.3)	**63.3** (6.7)
θc *[°]*	**-41.4** (9.1)	**-39.7** (3.6)	**-19** (26)	**-35.9** (6.7)	**-39.3** (10.4)	**-30.3** (16.1)
θ_r *[°]*	**39.9** (10.8)	**35.8** (12.6)	**44.4** (8.3)	**29.5** (8.1)	**27.7** (3.2)	**39.7** (5.8)
$\theta_{E\text{-}min}$ *[°]*	**101.7** (7.6)	**108.8** (15.6)	**107.8** (6.2)	**102.7** (6.2)	**109.4** (15.8)	**111.8** (10.7)
$\theta_{E\text{-}max}$ *[°]*	**132** (5.2)	**132.7** (7.3)	**139** (12)	**129.7** (7.1)	**134.6** (9.3)	**139.1** (13.1)
$\theta_{S\text{-}min}$ *[°]*	**30.2** (5.2)	**26.8** (3.5)	**22.3** (6)	**22.1** (5.8)	**24.9** (5.2)	**23.1** (6.2)
$\theta_{S\text{-}max}$ *[°]*	**72** (1.4)	**58.8** (6)	**66** (12.1)	**64.7** (2.2)	**56.8** (10.3)	**61.2** (10.4)
$\theta_{T\text{-}min}$ *[°]*	**1.5** (2.7)	**-2** (1.4)	**4.5** (6)	**-0.5** (2.7)	**-2.5** (1.8)	**1** (3.2)
$\theta_{T\text{-}max}$ *[°]*	**6.2** (5.8)	**0.8** (2.5)	**8.1** (6.2)	**5.4** (4.6)	**0.8** (2.5)	**6.9** (3.7)
3rd cycle	Normal Resistance test			Twice-normal resistance test		
	I	II	III	I	II	III
PP *[s]*	**0.64** (0.12)	**0.5** (0.17)	**0.36** (0.06)	**1.12** (0.42)	**0.82** (0.23)	**0.53** (0.11)
RP *[s]*	**0.61** (0.12)	**0.33** (0.07)	**0.4** (0.18)	**0.56** (0.07)	**0.4** (0.04)	**0.37** (0.13)
PP/CT *[%]*	**51.1** (3.7)	**59.8** (5.8)	**49.1** (7.5)	**65.3** (7.1)	**66.5** (6.9)	**59.8** (5.7)
θc *[°]*	**-35.4** (7.7)	**-31.7** (8.8)	**-26.6** (17.8)	**-39.1** (12.4)	**-39.6** (8.3)	**-28.3** (15.5)
θ_r *[°]*	**36.3** (11.1)	**34.6** (9.8)	**46** (5.9)	**33.3** (2.5)	**26.5** (6.6)	**40.3** (8.4)
$\theta_{E\text{-}min}$ *[°]*	**105.2** (0.7)	**103.9** (18.5)	**105.8** (5.8)	**102.5** (8.1)	**110.4** (15.6)	**113.3** (11.3)
$\theta_{E\text{-}max}$ *[°]*	**128.7** (6.8)	**128.4** (9.8)	**138.5** (9.2)	**132.1** (4.5)	**134.4** (7.5)	**140.2** (12.1)
$\theta_{S\text{-}min}$ *[°]*	**30.3** (6.7)	**30.4** (4.7)	**23.9** (6.4)	**26** (4.7)	**26.5** (3.7)	**22.9** (6.7)
$\theta_{S\text{-}max}$ *[°]*	**72.8** (4.7)	**60.1** (7.6)	**69.8** (13.5)	**66.4** (1.2)	**61.8** (9.8)	**61.2** (12.4)
$\theta_{T\text{-}min}$ *[°]*	**3.3** (3.1)	**-2.6** (1.7)	**4.7** (5.9)	**1.7** (1.4)	**-2.8** (1.2)	**3.1** (4.2)
$\theta_{T\text{-}max}$ *[°]*	**7.3** (4.4)	**0.8** (2.5)	**7.9** (6.7)	**7.5** (0.07)	**0.3** (2.3)	**6.5** (4.2)

All four of the post-surgery subjects gave positive response by answering "yes" to questions 1 and 2 stated earlier. They reported improvements in lifting the arms, control and stability. For the wheelchair propulsion, one subject had insufficient strength and balance to use a manual wheelchair prior to TROIDS surgery and cited improved wheelchair propulsion as his greatest gain following the TROIDS surgery.

4.4 Discussion

Complete C5/C6 tetraplegia subjects without active triceps function had a significantly reduced capability in terms of wheelchair propulsion compared with incomplete C7 tetraplegia subjects with triceps function. The results indicated that arm function was a more important factor in wheelchair propulsion than trunk stability and strength. Briefly, during the push phase, the lack of voluntary elbow extension against gravity limited subjects with C5/C6 tetraplegia to push down on their wheelchair rim, and due to their lack of abdominal control, could not lean forward and reach as close as to bottom dead centre (BDC) during the late push phase. The relatively weak push phase because of the paralyzed triceps was concluded as the reason of lower power output and velocity attained in complete C5/C6 tetraplegia (Group I and II subjects) compared with incomplete C7 tetraplegia (Group III subjects). It is important to note that, for this study, limited numbers of pre and post-TROIDS surgery subjects could be recruited over six month duration of the tests given the current trend for C5/C6 tetraplegia subjects to adopt the use of electric wheelchairs (offered by healthcare providers) as opposed to a manual wheelchair following SCI, and that these numbers were significantly lower than expected from other years. However, some evidence obtained from Group II subjects following TROIDS surgery suggested that triceps function improves wheelchair propulsion. To what extent triceps function objectively improves wheelchair propulsion is discussed below.

4.4.1 Power output

The worst performances in generating power output were chosen in each group to highlight the influence of triceps function during normal resistance wheelchair propulsion. Comparison of power output curves among all the groups (Figure 4.4) illustrated that subjects with triceps function (Group III) generated more steady and consistent power output in the shortest time (0.96s for Group III subject versus 1.08s and 1.56s for Group II and I respectively). P_{max} for the subjects with triceps (1032 watts) were 2 to 3.5 times greater than the other two groups (442 watts for Group II and 295 watts for Group I).

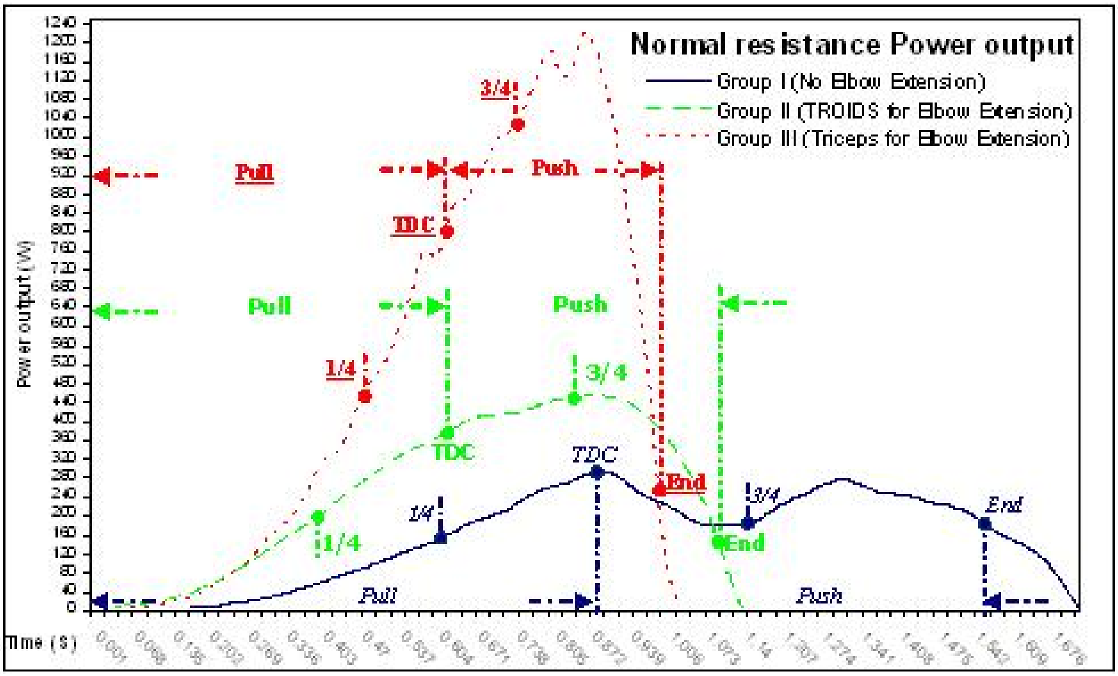

***Figure 4.4** The graphs of first propulsion power output in Group I (No Elbow Extension), Group II (TROIDS for Elbow Extension) and Group III (Triceps for Elbow Extension) under normal resistance*

Following twice-normal resistance tests (Figure 4.5), the peak power outputs were 582 watts (Group III), 207 watts (Group II) and 124 watts (Group I). The propulsion times were 1.4s for Group III versus 1.84s and 2.44s for Group II and I respectively, as shown in Figure 4.5. The Group III subjects were still the best performers and correlated with the normal-resistance tests (Figure 4.4). Increasing resistance significantly influenced the time taken to switch from elbow flexion to elbow extension (TDC in Figure 4.5) as observed in power output curves in Groups I and II. As shown in Figure 4.4 and 4.5, a dramatic increase in duration of the pull phase was observed in both Groups I and II, whereas curves for Group III remained relatively unchanged. However, the relatively stable proportion of pull and push phase observed in Group III subjects suggested that their propulsion technique did not change with increasing resistance due to the better control of both biceps and triceps.

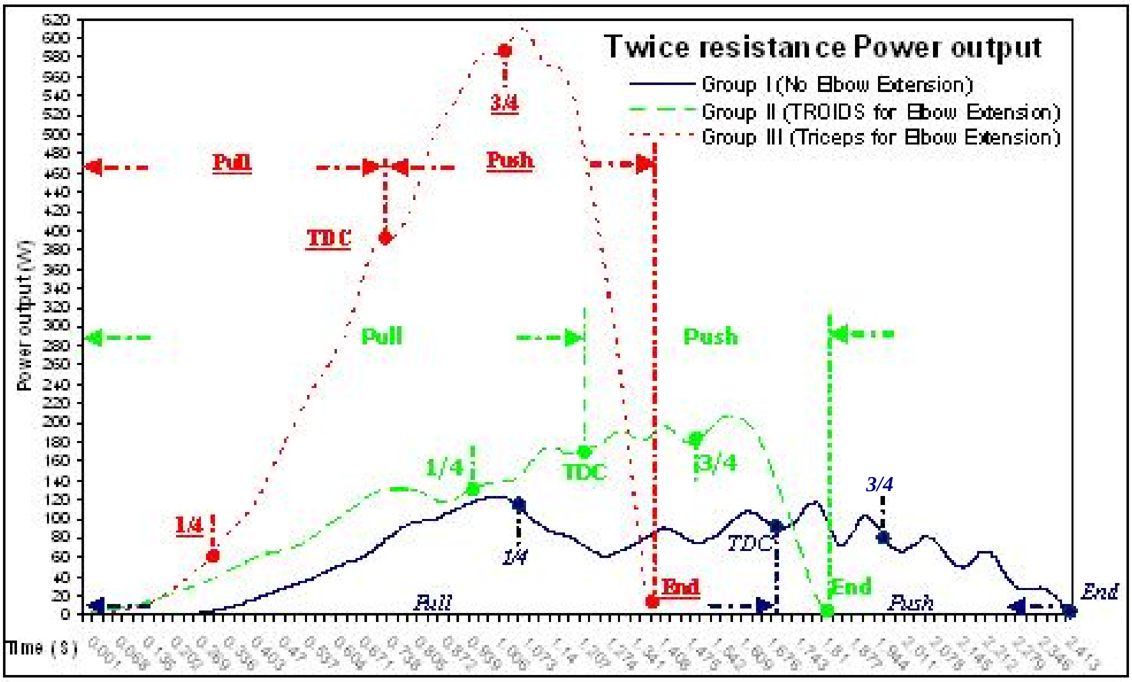

Figure 4.5 *The graphs of first propulsion power output in Group I (No Elbow Extension), Group II (TROIDS for Elbow Extension) and Group III (Triceps for Elbow Extension) under twice-normal resistance*

A higher P_{max} generated under both resistance tests demonstrated a significant improvement in wheelchair propulsion ability after the triceps restoration following TROIDS in Group II subjects compared with Group I. During the pull phase, the restoration of triceps allowed a greater amplitude of flexion and greater acceleration of the forearm than that obtained without triceps activity, resulting in a much higher power output in Group II (330 watts) than Group I (120 watts) subjects (Figure 4.4). However, this advantage was not as significant (120 versus 100 watts) during the twice-normal resistance test (Figure 4.5), and represented a limitation of the triceps restoration following TROIDS under these more extreme conditions. However, additional positive trends were observed during the push phase in both Figure 4.4 and 4.5. A further increase of power output by the aid of triceps restoration was noticed in Group II during the late push phase that was more similar to the results of Group III subjects, indicating that elbow extension contributed to a higher power output. In contrast, the maximum power output occurring at the end of pull phase (TDC in Figure 4.4 and 4.5) proved that Group I subjects were unable to keep accelerating the wheelchair during the push phase due to a lack of triceps function. Furthermore, there was greater fluctuation in power output in Group I subjects during the push phase in the twice normal-resistance test, illustrating that these subjects struggled to push the wheelchair under these more extreme conditions compared with Group II subjects. Although both Group II and I were more dependent on the pull phase, the comparisons illustrated that the restoration of triceps resulted in faster and smoother power output in both of the pull and push phase. As a result, the significant improvement of wheelchair propulsion ability after TROIDS transfer surgery was demonstrated by the difference of both amplitude and pattern of peak power output generation between Group II and I.

4.4.2 Velocity

The reason of measuring velocity is that the reduced propulsive ability is best demonstrated by the triceps function on propulsion speed. The velocity curves (Figure 4.6) of twice normal-resistance test show Group III subjects (with the aid of triceps) can accelerate the wheelchair 1.5 to 1.9 times faster (5.69m/s) than the other two groups after approximately twenty seconds from stationary (2.95m/s, 3.7 m/s for Group I and II respectively) by the aid of triceps.

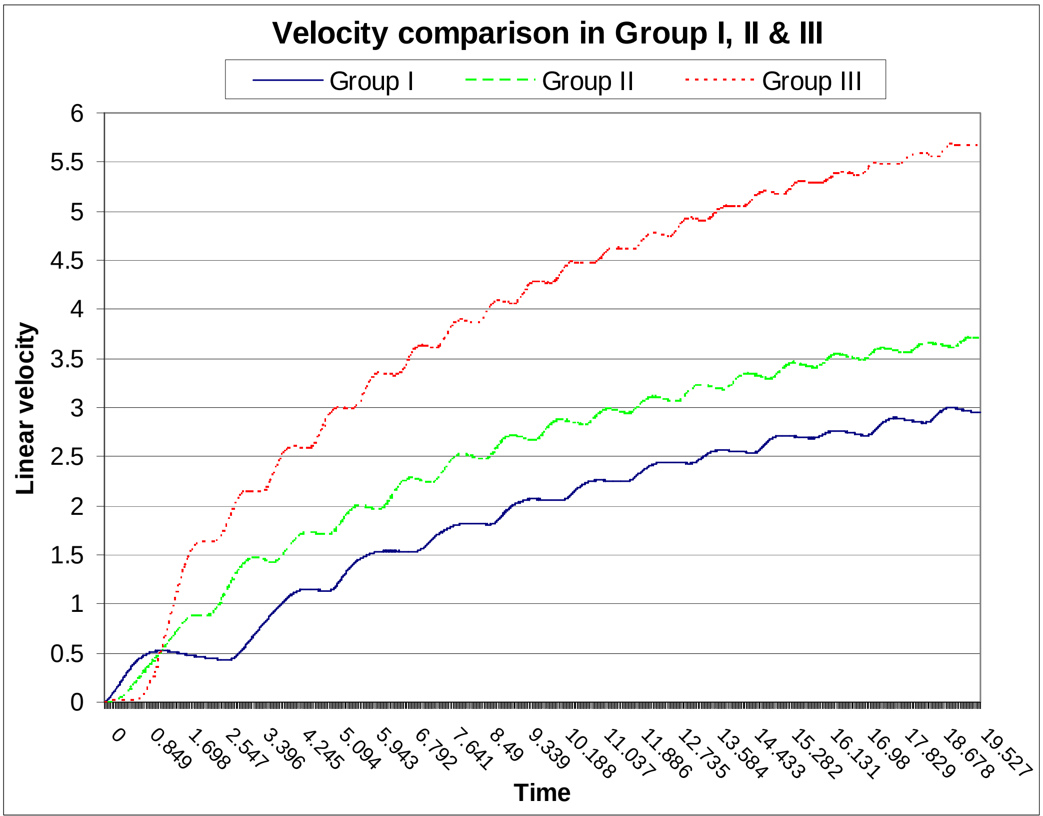

Figure 4.6 *The velocity graphs of twice-normal resistance test in Group I, II & III*

During the normal resistance test, the highest velocity of 2.8m/s was attained by Group III subjects (versus 2.2m/s and 1.9m/s in Group II and I respectively) in the shortest propulsion time (Figure 4.7), correlating well with the results of power output (Figure 4.4). Due to the lack of triceps control, the slope decreased during the push phase in Group I subjects. However, a further increase in velocity during push phase was found in both Group II and III. The different slope changes represented that a switch in muscular activity from biceps to triceps helped achieve a greater velocity during the push phase in Group II and III subjects.

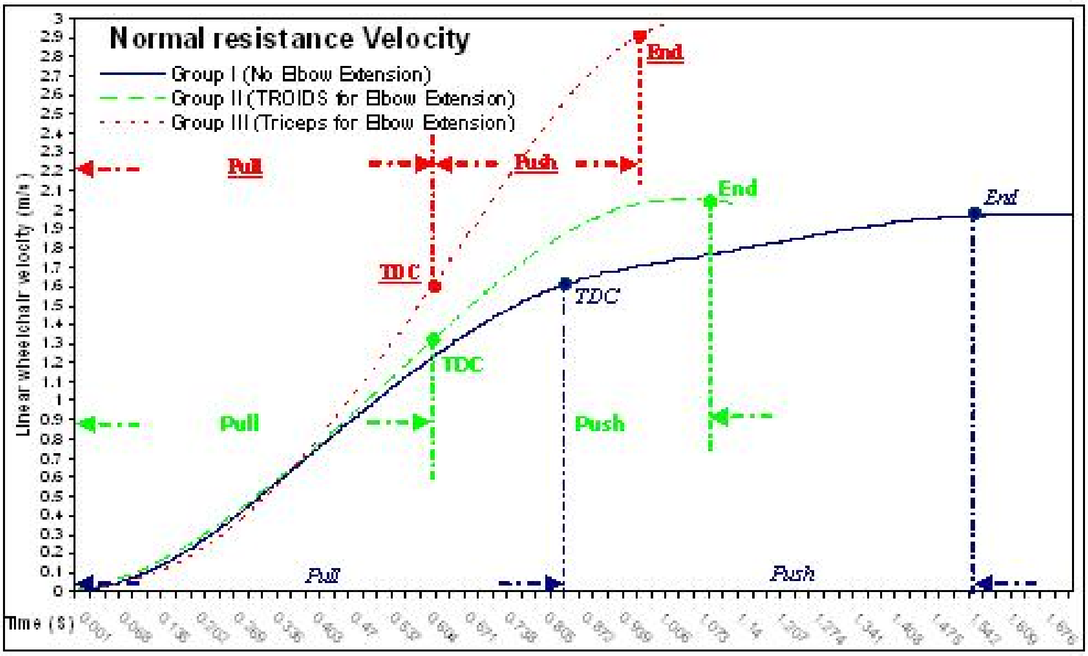

Figure 4.7 *The velocity graphs in Group I, Group II and Group III under normal resistance*

During twice-normal resistance test, the velocities attained after first push from stationary were 1.53, 0.88 and 0.52 m/s for Group III, II and I respectively. Based on the shapes of velocity graphs, a decrease in slope was only observed in Group I (Figure 4.8), illustrating that the maximum acceleration occurred at the early pull phase. Compared to a slight increase of velocity in the normal resistance test, a plateau was found after the pull phase in Group I during the twice-normal resistance test, demonstrating that lack of triceps function limits a higher velocity being attained during the push phase. Furthermore, similar to power output curves (Figure 4.5), it showed that the effect of triceps function on wheelchair propulsion ability was more obvious under these more extreme conditions. Even in instances where biceps function might be affected after TROIDS transfer surgery [18], thereby limiting performance during the pull phase, the higher velocity gained by a stronger push with the aid of triceps proved that TROIDS surgery improved the ability of wheelchair propulsion for complete C5/C6 tetraplegia.

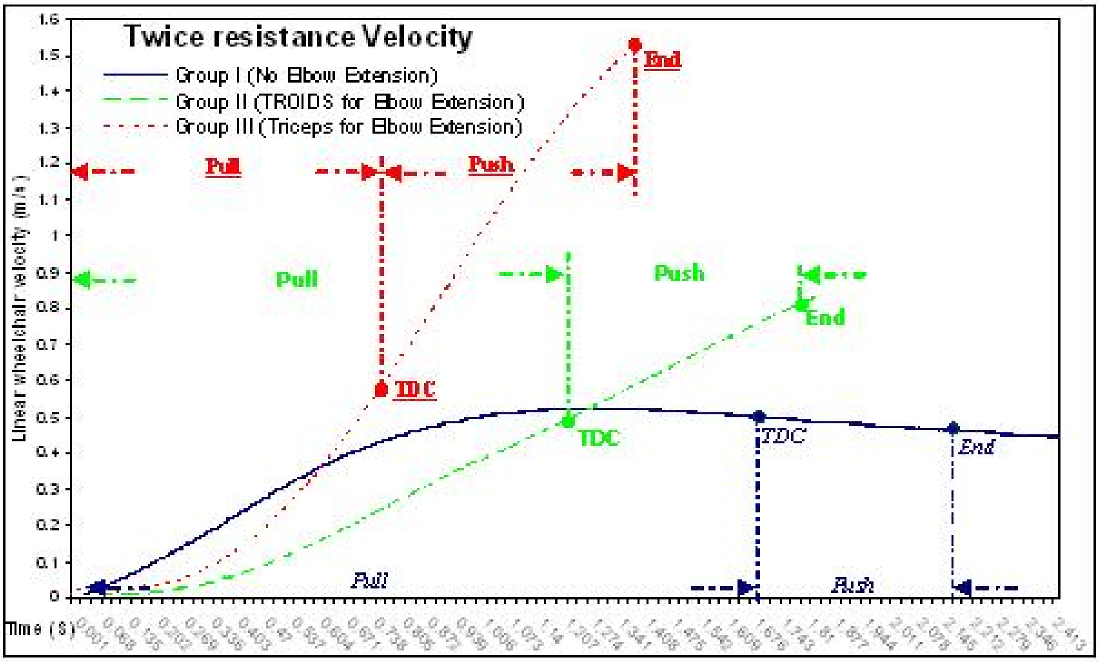

Figure 4.8 *The velocity graphs in Group I, Group II and Group III under twice-normal resistance*

4.4.3 Arm movements

Generally, wheelchair users always contact the push-rims closer to the TDC and release closer to the BDC to propel the wheelchair efficiently. During the start of the propulsion phase, the hands approach TDC and then continue further down the rim to complete the stroke. This propulsion technique was observed in Group III as shown in Figure 4.9C. In order to achieve the maximum efficiency, Group III subjects always end the pull phase at the first quarter of the whole propulsion phase in one stroke in order to gain more time for pushing.

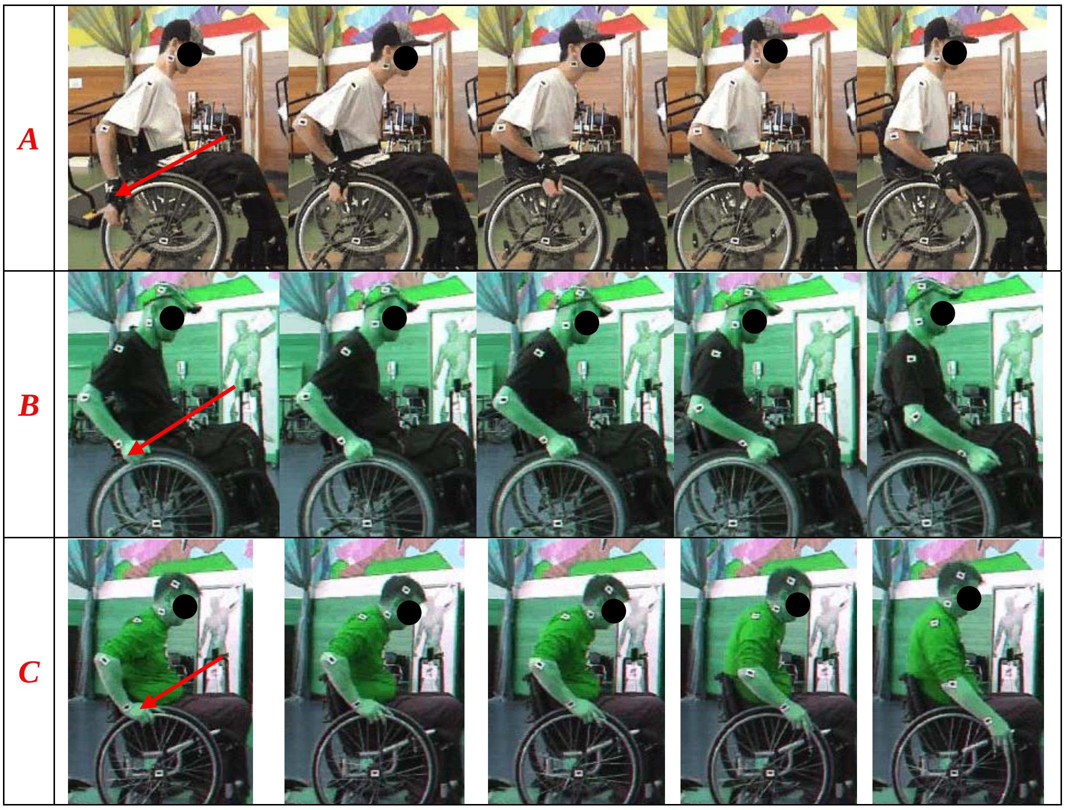

Figure 4.9 Comparisons of elbow movements during propulsion phase in Group I (A), Group II (B) and Group III (C) gathered from video recordings. Arrow indicates the start position of the PP.

For Group II subjects in Figure 4.9B, flexion increased from the initial pull phase until the hands reached the top of the wheel where peak flexion occurred. The push phase showed a rapid motion toward extension as the hand continued to follow the path of the wheel. However, the maximum elbow extension occurred at the start rather than at release in Group I (Figure 4.9A). The reason was that with limited elbow extension, Group I subjects had to depend more on the pull phase, which was also demonstrated in Figure 4.10A and B. The comparison of elbow movements between normal and twice-normal resistance tests demonstrated that wheelchair propulsion ability was highly affected under these more extreme conditions in the Group I subjects compared with Groups II and III. Comparing elbow extension during the late push phase in Group I, the elbow remained in more flexion throughout the entire propulsion cycle of the twice-resistance test and resulted in the lowest performance in Group I. Furthermore, for the subjects without elbow extension (Group I), if hand placement was far behind TDC then there was danger of damaging the joint capsule of the shoulder through the effects of the combined movement of internal rotation and shoulder extension.

A

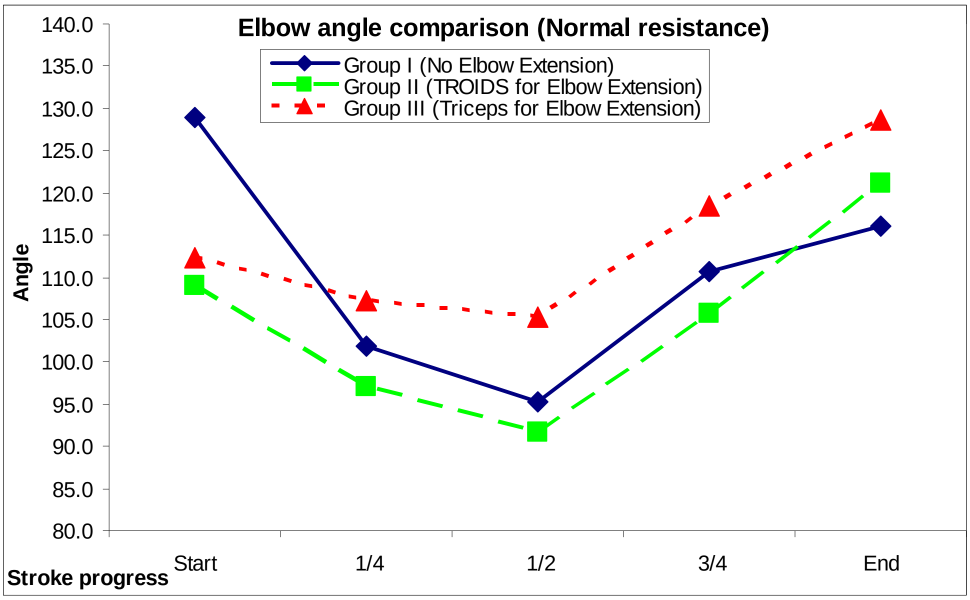

B

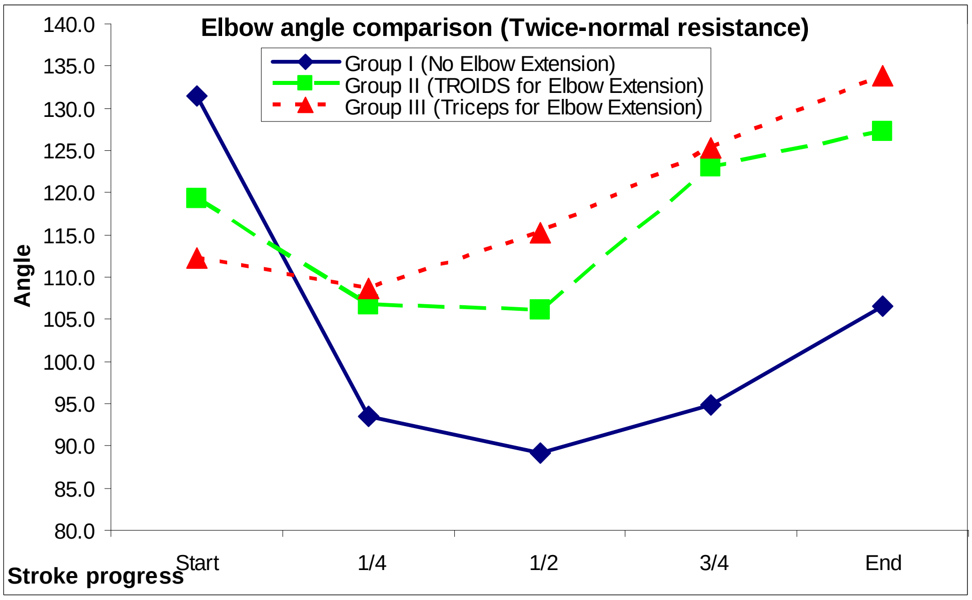

Figure 4.10 *Comparisons of elbow angle in each group during wheelchair propulsion under normal (A) and twice-normal resistance (B).*

The diminished grasp function between thumb and fingers resulted in less effective propulsion mainly because Group I subjects had to increase the radially directed push-rim forces to maintain hand contact. Although elbow extension was observed (Figure 4.10A and B), it was due to relatively larger shoulder movements. During the late push, Group I subjects (Figure 4.9A) leaned further back to allow the arms to follow the path of the wheel by rotating shoulders rather than increasing elbow extension voluntarily, thereby providing a stronger push similar to Group II (Figure 4.9B) and III subjects (Figure 4.9C). Some improvements were observed not only for an intended push by the aid of triceps restored in Group II during the push phase, but also for the better use of shoulders during the whole propulsion phase, which was starting in a position of extension and progressed to flexion to aid wheelchair propulsion. Therefore, the similar propulsion phase between Group II and III illustrated that the restoration of triceps by TROIDS transfer surgery improved wheelchair propulsion ability.

During the propulsion phase (solid line in Figure 4.11A and B) the arm moved in a closed chain, thus the individual propulsion style of the wheelchair user is primarily determined by the recovery phase (dash line in Figure 4.11A and B) since the arms are free to choose any path to return to the push rims. Two arm movement patterns during recovery phase were classified as "anti-clock circular" (A) and "circular" (B) as shown in Figure 11 after the video editing in all the groups. The circular pattern was considered more efficient because it included lifting the arms off the wheel and counter-balancing inertia of the arms for stretching muscles and increasing contractile force. The whole procedure guaranteed the muscles were all activated in the recovery phase to prepare for the impact on the push rims (Figure 4.11D and E). However, rather than continuing elbow extension after the hands left the push-rims (Figure 4.11B), some subjects flexed their elbows up to TDC (Figure 4.11A). For the subjects without elbow extension, an "anti-clock circular" pattern was the most commonly observed propulsion technique. All Group I subjects (Figure 4.11C) chose the "anti-clock circular" pattern compared with 75% of Group II subjects (Figure 4.11D) who adopted a "circular" pattern similar to Group III. Moreover, using the shoulders only to drive arms back to the push-rims as shown in Figure 4.11C, resulted in a less effective energy stored in the arms during the recovery phase.

Thus, the important result observed in Group II subjects following TROIDS surgery was that they naturally adopted a "circular" arm motion pattern more similar to Group III subjects without any training or input from clinicians or physiotherapists. This demonstrated that an imporved arm movement pattern during the recovery phase was chosen following TROIDS surgery. More importantly, improved arm function enhanced wheelchair propulsion ability following TROIDS transfer surgery and was comparable to the natural arm movements of subjects with a lower level SCI injury.

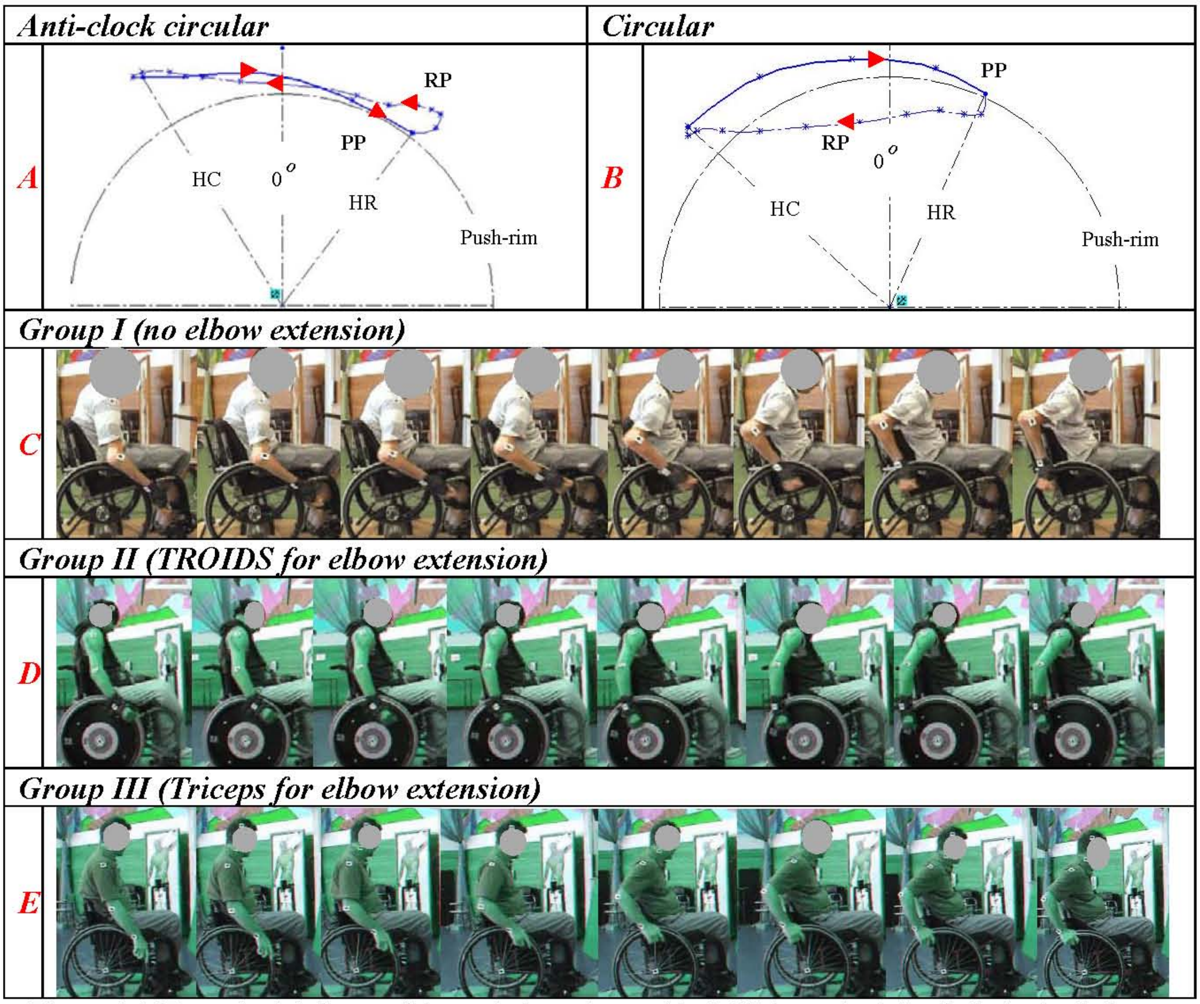

Figure 4.11 Two wheelchair propulsion technique observed in C5/C6 tetraplegia "anti-clock circular" pattern (A), "circular" pattern (B) and arm movement comparisons during recovery phase in Group I (C), Group II (D) and Group III (E) gathered from video recordings

We expected that triceps function would affect the time of the arm movement (Table 4.5) and was thus a major parameter in controlling the speed of elbow flexion. After comparing the elbow flexion and extension velocity and the propulsion time ($t_{\text{start-TDC}} + t_{\text{TDC-End}}$) as illustrated in Table 4.5, (0.36 m/s, 0.47 m/s and 0.64 s for Group I vs 0.38 m/s, 0.55m/s and 0.51s for Group II and 0.71m/s, 1.3m/s and 0.37s for Group III), the lack of active contraction of the triceps is responsible for the slower elbow flexion velocity and prolongs the propulsion and recovery time. This resulted in the lowest performance in the group of subjects without triceps. Moreover, Group II and III subjects had the ability to increase the elbow flexion and extension velocity by the aid of triceps compared with Group I subjects increasing the elbow flexion velocity only during the different resistance tests. Finally, the improvements in Group II proved that the restoration of triceps allowing elbow extension increased not only the amplitude and strength, but also the speed of the arm movement.

Table 4.5 *The elbow velocity comparisons in three groups*

Group I	*Constant effort*						*Maximum effort*					
	1st trial		2nd trial		3rd trial		1st trial		2nd trial		3rd trial	
V_{pull} (m/s)	**0.06**	(0.05)	**0.19**	(0.1)	**0.22**	(0.13)	**0.14**	(0.03)	**0.31**	(0.2)	**0.36**	(0.26)
$t_{start\text{-}TDC}$ (s)	**1.13**	(04)	**0.44**	(0.17)	**0.36**	(0.11)	**0.67**	(0.3)	**0.36**	(0.14)	**0.28**	(0.12)
$V_{release}$ (m/s)	**0.27**	(0.04)	**0.41**	(0.1)	**0.47**	(0.11)	**0.3**	(0.06)	**0.46**	(0.17)	**0.47**	(0.24)
$t_{TDC\text{-}End}$ (s)	**0.69**	(0.08)	**0.55**	(0.02)	**0.43**	(0.02)	**0.67**	(0.09)	**0.41**	(0.05)	**0.36**	(0)
Group II	*Constant effort*						*Maximum effort*					
	1st trial		2nd trial		3rd trial		1st trial		2nd trial		3rd trial	
V_{pull} (m/s)	**0.07**	(0.03)	**0.18**	(0.04)	**0.22**	(0.07)	**0.08**	(0.03)	**0.25**	(0.06)	**0.38**	(0.2)
$t_{start\text{-}TDC}$ (s)	**1.02**	(0.23)	**0.40**	(0.08)	**0.31**	(0.11)	**0.77**	(0.19)	**0.29**	(0.05)	**0.21**	(0.06)
$V_{release}$ (m/s)	**0.3**	(0.08)	**0.43**	(0.18)	**0.48**	(0.22)	**0.36**	(0.16)	**0.49**	(0.2)	**0.55**	(0.29)
$t_{TDC\text{-}End}$ (s)	**0.48**	(0.03)	**0.34**	(0.07)	**0.34**	(0.07)	**0.46**	(0.1)	**0.34**	(0.07)	**0.3**	(0.08)
Group III	*Constant effort*						*Maximum effort*					
	1st trial		2nd trial		3rd trial		1st trial		2nd trial		3rd trial	
V_{pull} (m/s)	**0.20**	(0.09)	**0.47**	(0.21)	**0.58**	(0.20)	**0.28**	(0.10)	**0.57**	(0.30)	**0.71**	(0.34)
$t_{start\text{-}TDC}$ (s)	**0.63**	(0.10)	**0.24**	(0.04)	**0.19**	(0.05)	**0.59**	(0.10)	**0.19**	(0.05)	**0.17**	(0.02)
$V_{release}$ (m/s)	**0.54**	(0.11)	**0.80**	(0.07)	**0.97**	(0.12)	**0.74**	(0.29)	**0.87**	(0.08)	**1.30**	(0.04)
$t_{TDC\text{-}End}$ (s)	**0.40**	(0.04)	**0.28**	(0.04)	**0.23**	(0.02)	**0.32**	(0.07)	**0.25**	(0.06)	**0.20**	(0.04)

4.5 Conclusion

These observations indicate the extent of which triceps function improves wheelchair propulsion by highlighting the test performance differences in all three groups. The restoration of triceps by TROIDS not only allowed active elbow extension, but also increased the amplitude and strength as well as the speed of arm movement. The results also point to TROIDS allows a real push phase and a better arm movement pattern during both propulsion and recovery phase under normal and extreme conditions. This advantage is not obvious under the extreme conditions and the huge difference comparing with triceps for elbow extension represent the limitation of the restoration of triceps.

Acknowledgements

The authors would like to thank all the subjects from Burwood Hospital.

References

[1] S. H. Lacey, R. G. Wilber, P. H. Peckham, and A. A. Freehafer. "The posterior deltoid to triceps transfer: A clinical and biomechanical assessment," J. Hand Surg., vol. 11A, pp. 542–547, 1986.

[2] Richard L. Lieber, PhD, San Diego, CA, Jan Friden, MD, PhD, Goteborg, Sweden, Toni Hobbs, BS, Alastair G. Rothwell, MD, Christchurch, New Zealand. Analysis of Posterior Deltoid Function One Year After Surgical Restoration of Elbow Extension. The Journal of Hand Surgery. 2003, 28A: 288-293.

[3] KHALID D. MOHAMMED, ALASTAIR G. ROTHWELL, STUARTW. SINCLAIR, SUE M. WILLEMS and ALLAN R. BEAN. UPPER-LIMB SURGERY FOR TETRAPLEGIA. Burwood Hospital Christchurch. THE JOURNAL OF BONE AND JOINT SURGERY. VOL. 74-B, NO. 6, November 1992.

[4] M. Margaret Wierzbicka, PHD and Allen W. Wiegner, PHD. Orthosis for improvement of arm function in C5/C6 tetraplegia. Journal of prosthetics and orthotics 1996 Vol. 8. Num. 3.

[5] Allen W. Wiegner, Senior Member, IEEE, and M. Margaret Wierzbicka. Mechanical Compensation for Weak Triceps in CYC6 Tetraplegia. IEEE TRANSACTIONS ON REHABILITATION ENGINEERING, VOL. 1, NO. 2. JUNE 1993

[6] P. E. Crago, W. D. Memberg, M. K. Usey, M. W. Keith, R. F. Kirsch, G. J. Chapman, M. A. Katorgi and E. J. Perreault. An elbow extension neuroprothesis for individuals with tetraplegia. IEEE TRANSACTIONS ON REHABILITATION ENGINEERING, VOL. 6, NO. 1, MARCH 1998.

[7] Freehafer AA. Tendon transfers in patients with cervical spinal cord injury. J Hand Surg 1991; 16A: 804-809.

[8] Lamb DW and Chan KM. Surgical reconstruction of the upper limb in traumatic tetraplegia. A review of 41 patients. J Bone Joint Surg 1983;65B:291-298.

[9] O Remy-Neris, J Milcamps, R Chikhi-Keromest, A Thevenon, D Bouttens and S Bouilland. Improved kinematics of unrestrained arm rasing in C5-C6 tetraplegic subjects after deltoid-to-triceps transfer. Unite des blesses medullaires, Centre Calve, Groupe Hopale, Berck sur mer, France. 2003 41, 435-445.

[10] Moberg E. Surgical rehabilitation of the upper limb in tetraplegia. Paraplegia 1990; 28:330-334.

[11] Moberg E. The present state of surgical rehabilitation of the upper limb in tetraplegia. Paraplegia 1987; 25:351-356.

[12] Raczka R, Braun R and Waters RL. Posterior deltoid-to-triceps transfer in quadriplegia. Clin Orthop 1984; 187: 163-167.

[13] Ejeskar A and Dahllof A. Results of reconstructive surgery in the upper limb of tetraplegic patients. Paraplegia 1988; 26: 204-208.

[14] Sandra Connolly, BHScOT, OT Reg (Ont.), JoAnne Aubut, BA, Robert W Teasell MD FRCPC and Tal Jarus, PhD, OTR. Upper Limb Rehabilitation Following Spinal Cord Injury. Spinal cord injury rehabilitation evidence.

[15] AL Dunkerley, A Ashburn and EL Stack. Deltoid triceps transfer and functional independence of people with tetraplegia. Spinal Cord 2000; 38: 435-441.

[16] Lan-Yuen Guo, K D Zhao, Fong-Chin Su and Kai-Nan An. Moment generation in wheelchair propulsion. Proc. Instn Mech. Engrs Vol. 217 Part H: J. Engineering in Medicine. 2003

[17] Ross SA and Brubaker CE. Electromyographic analysis of selected upper extremity muscles during wheelchair propulsion. Proceedings of the second RESNA conference on rehabilitation engineering. 1984, Ottawa 7-8.

[18] Mulcahey MJ, Lutz C, Kozin SH, Betz RR. Prospective evaluation of biceps to triceps and deltoid to triceps for elbow extension in tetraplegia. Rehabilitation Services and Clinical Research, Shriners Hospitals for Children, Philadelphia, PA, USA. J Hand Surg. 2003 Nov; 28(6):964-71.

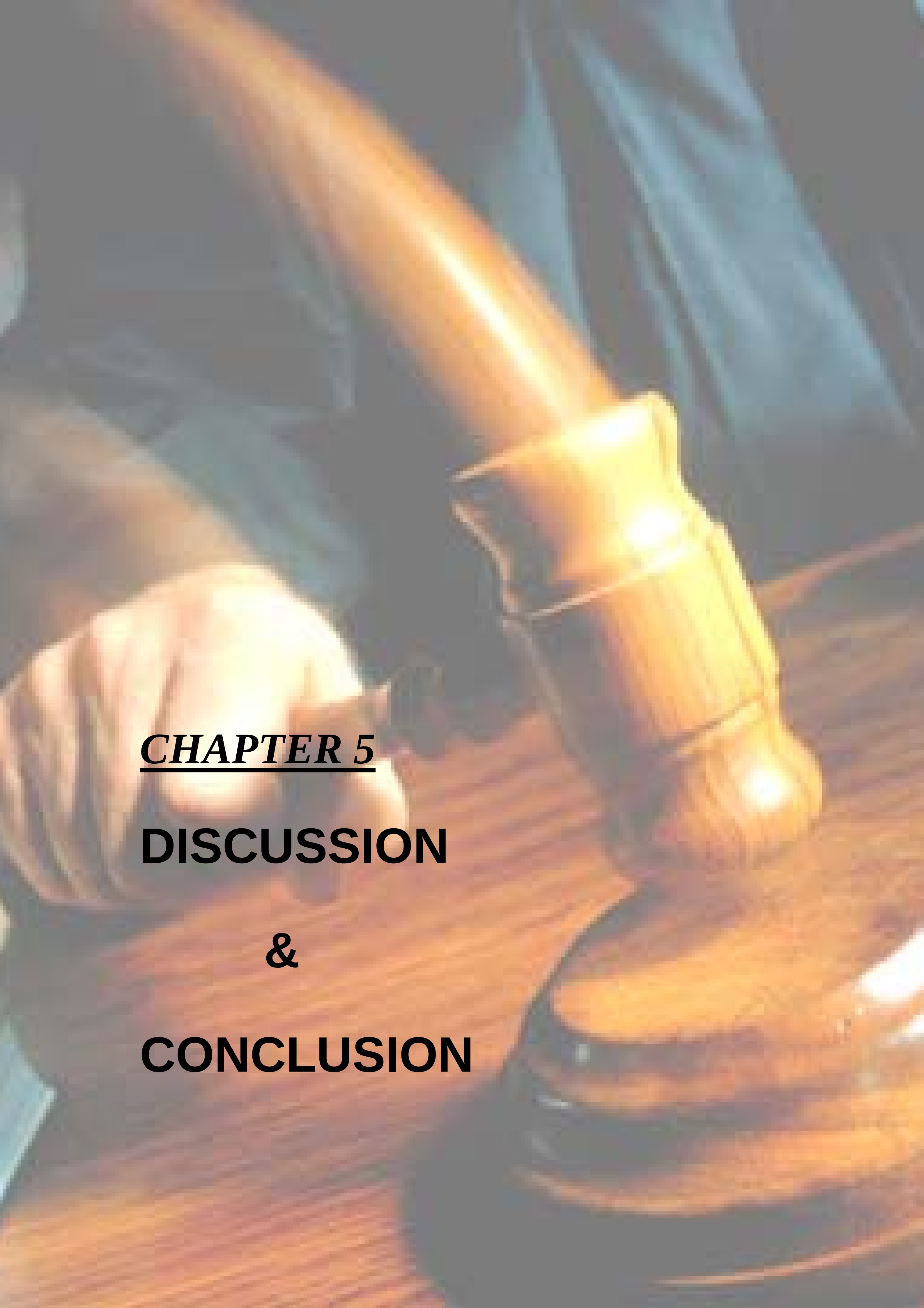

CHAPTER 5

DISCUSSION

&

CONCLUSION

5.1 Discussion

The selected method for measuring wheelchair propulsion ability was based on a significant observation concerned with the variation of techniques used for contacting the push rim, namely, using push rims only, grasping both push rims and tyres, and contacting wedges between push rims and tyres. The wheelchair dynamometer was calibrated after identifying all the important quantities in measuring wheelchair propulsion ability, which include wheelchair mass properties, kinematics, resistance forces (tyre contact losses, aerodynamic drag and mechanical losses) and tractive force. Furthermore, the analysis of the distance, acceleration, velocity and torque curves by comparing the results in literature [1-2] using the SMART^{Wheel}, provided a valid method for testing the parameters of an inertia custom-made wheelchair dynamometer. Once the test rig was constructed, the test procedure was designed which could represent different components of wheelchair propulsion activities, namely, starting and wheeling (Test 1: a self-selected comfortable speed), sprinting (Test 2: maximum effort with normal resistance) and changing resistance (Test 3: maximum effort with twice normal resistance). Due to asymmetries during wheelchair propulsion in the arm movement pattern of wheelchair users, the range of shoulder, elbow and hand movements and selected timing parameters, including cycle time and time spent in contact with the hand rim (propulsion phase), were obtained from both left and right sides. The functional status of people with SCI was assessed by calculating the linear velocity and power output during the maximum effort tests. These parameters were found to be the most important predictor of physical strain during wheelchair propulsion. A higher level of injury means a smaller active muscle mass, which will in turn result in a reduced endurance capacity. The lower values in the subjects with cervical spinal cord injury are in accordance with several previous studies [3-6], which reported that endurance capacity is strongly determined by SCI. The mechanics of wheelchair propulsion have indicated that greater speed is associated with greater stroking frequency and reductions in stroke, push and recovery times. The individuals with higher levels of SCI consistently achieved or selected lower velocities with decreased stroke frequency and increased contact time than those with lower levels of SCI. As expected, age was found to reduce a person's ability to propel a wheelchair when measured on the inertia dynamometer. However, the reduced wheelchair propulsion capability due to SCI influenced physical capacity to a larger extent than age. Diminished arm function was considered the major factor in the noted differences in propulsion kinematics.

Observations of people with and without active triceps function demonstrated that the contributions of triceps in enabling a person to propel a wheelchair was demonstrated by investigating whether or not TROIDS transfer surgery can improve wheelchair propulsion ability. The restoration of triceps for C5/C6 tetraplegia allowed a larger amplitude of arm flexion and extension, which resulted in a further increase of power output and velocity during the push phase compared with the maximum values observed in groups without elbow extension (i.e. without triceps). These subjects may be susceptible to joint capsule damage in the shoulders through the effects of the combined movement of internal rotation and shoulder extension. More importantly, TROIDS enabled an improved propulsion technique to be adopted without any training, and was likely due to activation of all available muscles during the recovery phase to prepare the hands for impact on the push rims. Furthermore, individuals with C5/C6 tetrapelgia generate increased medial forces to provide the needed friction for maintaining a grip on the hand rim. The people with TROIDS transfer surgery in the current study propelled with patterns of reduced contact time with the hand rim, further constraining the user-wheelchair interface and possibly allowing for a larger percentage of tangential force application. The current study has shown that TROIDS transfer surgery allows a person with C5/C6 tetrapelgia to propel their wheelchair with higher stroke frequency, power output and velocity, which resulted in a more effective wheelchair propulsion technique. This indicated that TROIDS transfer surgery allows a person with C5/C6 tetrapelgia to adopt a more efficient balance with their efforts, directing the majority of the force application toward forward motion of the wheelchair.

5.2 Conclusion

Insight into the manual wheelchair propulsion has been achieved through a combination of experimental data collection under realistic conditions with a fundamental mathematical modelling approach. Through a synchronised system measuring kinetic and kinematic data of the arm movement patterns, insight has been gained into the manual wheelchair propulsion of people with different SCI levels. Furthermore, insight into the mechanism of manual wheelchair propulsion was sought through mathematical modelling and simulation. Along with the objectives, the conclusions are represented as follows:

I. A custom-made inertia dynamometer with flywheels is capable of measuring wheelchair propulsion ability under different propulsion techniques

- The distance curve illustrated the difference between the two hands.
- The maximum velocity always occurs after the hands leave the push-rim.
- Relatively higher torque compared with previous SMART^{Wheel} data indicated the extra torque applied on the tyre or the wedges has been measured.

II. Wheelchair propulsion ability is strongly determined by SCI level.

- Subjects with paraplegia (T1-S5) performed better on the inertia dynamometer than subjects with tetraplegia (C5/C6). Subjects with tetraplegia experienced significantly higher levels of strain during task performance than subjects with paraplegia.
- People with C5/C6 tetraplegia have a significantly reduced capability in terms of wheelchair propulsion when compared with the T1-T8 group. The relative difference between the T1-T8 and T9-T12 and the T9-T12 and L1-S5 groups was much less.
- Arm function is a more important factor in wheelchair propulsion than trunk stability and strength.

III. Improvements in wheelchair propulsion following TROIDS surgery include amplitude, strength, speed of arm movements and propulsion technique chosen.

- TROIDS allows a real push phase and a better arm movement pattern during both propulsion and recovery phase under normal and extreme conditions.

- Subjects with motor incomplete lesions performed better than subjects with motor complete lesions.
- The path the arm takes during the recovery phase differs between people with and without triceps function

References

[1] Kenneth D. Coutts PhD. Kinematics of sport wheelchair propulsion. Journal of Rehabilitation Research and Development Vol. 27 No. 1 Pages 21-26.

[2] Kimberly T. Asato, Rory A. Cooper, Rick N. Robertson, and J. F. Ster. $SMART^{Wheel}$: Development and Testing of a System for Measuring Manual Wheelchair Propulsion Dynamics. IEEE TRANSACTIONS ON BIOMEDICAL ENGINEERING, VOL. 40, NO. 12, DECEMBER 1993.

[3] Korelia Kulig, Craig J. Newsam and Sara J Mulroy. The effect of level of spinal cord injury on shoulder joint kinetic during manual wheelchair propulsion. Clinical Biomechanics 16 (2001) pp 744-751 July 2001.

[4] Annet J. Dallmeijer, Yvonne J.Kappe, Dirkjan H.E.J. Veeger, Thomas W.J.Jassen and Luc H.V. van der Woude. Anaerobic power output and propulsion technique in spinal cord injured subjects during wheelchair ergometer. Journal of Rehabilitation Research and Development Vol. 31 No. 2, 1994 Pages 120-128.

[5] Craig J. Newsam, Sreesha S. Rao, Sara J. Mulsroy, JoAnne K. Gronley, Ernest l. Bontrager and Jacquelin Perry. Three-dimensional upper extremity motion during manual wheelchair propulsion in men with different level of spinal cord injury. http://www.elsebier.com/locat/gaitpost

[6] Annet J. Dallmeijer, MSc Luc H. V. van der Woude PhD, H. E. J. (DirkJan) Veeger, PhD and A. Peter Hollander, PhD. Effectiveness of force application in manual wheelchair propulsion in persons with spinal cord injuries. American Journal Of Physical Medicine and Rehabilitation. 1998

CHAPTER 6

FUTURE WORK

6.1 Future work

This study successfully measured wheelchair propulsion ability for people with different SCI levels. However, additional improvements could be applied to further improve the performance of the wheelchair dynamometer and test procedure, as outlined below.

Firstly, mechanical efficiency is the ratio of external energy production to consumed metabolic energy, which was not calculated in this study because of limitations of the 2D kinematics measurement system. Subjects with TROIDS transfer surgery in this study used propulsion patterns with reduced hand contact time with the rim, further constraining the user-wheelchair interface and possibly allowing for a larger percentage of tangential force application. As a result, a 3D mathematical model is needed for further analysis of kinematics and muscular activity patterns.

Furthermore, with respect to test procedure design, when a person is able to perform a certain wheelchair skill but requires a disproportionately long period of time to do it, the performance of this skill will probably not be practicable in the person's daily life, which is not indicated in this study. In order to improve the test rig design, a braking resistance could be designed to provide a more realistic simulation.

Finally, a training program, which is also constrained by strength capability and muscle function, could help people with C5/C6 tetraplegia to adopt a "circular" arm movement pattern, which is superior to the "anti-clockwise" technique. This will rely on exploring the differences in stroke mechanics and muscle activation during level and uphill propulsion. When pushing a wheelchair up an incline, the weight of the wheelchair plus user has a component that is parallel to the inclined surface and serves as a resistance to the forward motion of the wheelchair. It is apparent that this information would be useful for instructional purposes and the design of training programs.

APPENDICES A - MATLAB CODE

A1: Distance Calculation

```
data = data;        % name imported txt file data.
Dia = 0.251;        % Diameter of dynamometer rollers
ave = 300;          %number of averaged periods for acceleration and
speed for smoothing
Enc = 1000;         % Number of counts per revolution for the encoder
Rate = 1000;        % number of times per second data is collected
%%%%%%% initial calculations %%%%%%%%
dt = 1/Rate;        % time between measurements
tandis = Dia * pi / Enc
time = data*[1;0;0];         %this section breaks the data into 3
matrices one for the time in seconds and one each wheel
n=length(time);
% Code to convert to led counts. Activate if want time axis to change
% counts on counter instead of seconds.
% time = [1:n];
% time = time/4;
% Resets varibles so no influance from prior calculations
A = 0;
B=0;
A=data*[0;1;0];         % wheel counts from the encoders.
B=data*[0;0;1];         % Encoder A is left wheel, encoder B is right.
AbsA = A - A(1);    %The encoders do not start at zero, this makes the
AbsB = B - B(1);          % first value of the encoders the zero point
Abs  = [AbsA,AbsB];
Abs = Abs * tandis;
%%%%This section calculates and plots the distance time.%%%%%%%%%%%%%
DisL = AbsA * tandis;      %Calculates the distance by left wheel (m)
DisR = AbsB * tandis;      %calculates the distance traveled by right
Dis = [DisL,DisR];           % matrix of both distances
% figure (1)
% plot(time,Dis)                  % plots distance against time.
% ylabel('distance (m)')
% xlabel('time (s)')
% title('Distance Vs Time')
% legend('Left','Right')
```

A2: Velocity Calculation

```
vel = 0;
for i = 2:n;
    vel(i,1) = (Abs(i,1)-Abs(i-1,1))/dt;
end
% plot(time,vel)                % At this stage it is possible to plot
%  ylabel('velocity (m/s)')          % the unsmoothed velocity.
%  xlabel('time (s)')
%  title('Velocity')
for i = 0.5*ave:n-0.5*ave;                      % smoothing velocity
    total = 0;
    for j = 1:ave;
        total = total + vel(i+j-0.5*ave,1);
    end
    velave(i,1) = total/ave;
end
time1 = time(1:n-ave);
velave = velave(1:n-ave,1);
figure (2)
plot(time1,velave)
```

```
grid on
ylabel('Linear velocity (m/s)')
xlabel('Seconds')
title('Linear velocity vs Time')
```

A3: Acceleration Calculation

```
accel = 0;
for i = 2:n-ave;
    acc(i,1) = (velave(i,1)-velave(i-1,1))/dt;
end
%plot(time,acc)      % can plot unsmoothed acceleration at this stage
for i = 0.5*ave:n-ave-ave;
    total = 0;                            %smoothing acceleration
    for j = 1:ave;
        total = total + acc(i+j-0.5*ave,1);
    end
    accel(i,1) = total/ave;
end
time2 = time(1:n-ave-ave);
figure (3)
plot(time2,accel)
grid on
ylabel('Linear accelaration (m/s^2)')
xlabel('Seconds')
title('Linear accelaration vs Time')
```

A4: Torque Calculation

```
I = 2.6889;                  % From spreadsheet
T = 0;
for i = 2:n-2*ave;
    T(i,1) = Aaccelavg(i,1)* I * Wdia / Rdia;    % torque
end
Tw = 0;
for i = 0.5*ave:n-2.5*ave;
    total = 0;                            %smoothing acceleration
    for j = 1:ave;
        total = total + T(i+j-0.5*ave,1);
    end
    Tw(i-0.5*ave+1,1) = total/ave;
end
time3 = 0;
time3 = time(0.5*ave:n-2.5*ave);
figure (3)
plot(time3,Tw)
grid on
ylabel('Torque on rear wheel (N.m)')
xlabel('seconds')
title('Torque vs Time')
```

A5: Power Calculation

```
p = 0;
for i = 2:n-3*ave;
    p(i,1) = Tw(i,1)* Avelavg(i,1);    % power
```

```
end
P = 0;
for i = 0.5*ave:n-3.5*ave;
    total = 0;                              %smoothing acceleration
    for j = 1:ave;
        total = total + p(i+j-0.5*ave,1);
    end

    P(i-0.5*ave+1,1) = total/ave;
end
time4 = 0;
time4 = time(0.5*ave:n-3.5*ave);
figure (4)
plot(time4,P)
grid on
ylabel('Power output (w)')
xlabel('seconds')
title('Power output VS Time')
```

A6: Video Capture

```
Numframes= GetMovieFrame( 'KMAR.avi',1);
[original,analysed] = FonctionThresholdwheelchair
('image/N100image.jpg');
figure, imshow(original),figure, imshow(analysed);
% get the frame of a movie and save it as a jpg file
function [NumFrame] = GetMovieFrame ( movie,StepBetween2frame )
%movie='Movie 002.avi';StepBetween2frame=400;
fileinfo = aviinfo(movie);
mov = aviread(movie);
NumFrame=0;
for cpt = 1 : StepBetween2frame : fileinfo.NumFrames
NumFrame = NumFrame + 1;
[MovieFrame,Map] = frame2im(mov(cpt));
SaveAsJPG (MovieFrame,'image',NumFrame);
end;
% Save an image as a JPG file in the image directory
function [NumFrame] = SaveAsJPG ( image, name , indice )
indice= num2str(indice);
name=['image/N',indice,name,'.jpg'];
imwrite(image, name,'jpg');
% Find the White dot
function [frame,Scaling] = FonctionThresholdwheelchair ( image )
frame=imread(image);
frameGRAY = rgb2gray(frame);
%******************smooth
%frameGRAY = smooth (frameGRAY);
%frameBW = im2bw(frame,0.8);
taille= size (frameGRAY);
Imax=0;
Imin=255;
%******************lighting equalisation***************************
%Definition of the analized window
Left= 1;
Right= 320;
Up= 1;
Down= 240;
a=0;
                        for x = Up :1: Down
```

```
                           b=0;
                           a=a+1;
                                for y = Left :1: Right
                                    b=b+1;
                                    small(a,b) = frameGRAY(x,y);
                                    frame(Up,:,1)=255;
                                    frame(Down,:,1)=255;
                                    frame(:,Left,1)=255;
                                    frame(:,Right,1)=255;
                                end;
                        end;
%figure, imshow (frame), title ('section of image going to be
analysed');
%figure, imshow (small), title ('avant');
small= im2double(small);
Imax = max( max(small));
Imin = min( min(small));
%disp(['Imin =',num2str(Imin),]);
%disp(['Imax =',num2str(Imax),]);
Scaling =(9/(Imax-Imin))* small +((Imax-10*Imin)/(Imax-Imin));
%qwerty=round(qwerty(:,:));
%*****thresholding*****
sizeScaling = size (Scaling);
for m= 1 : sizeScaling(1,1)
for n= 1 : sizeScaling(1,2)
%if (Scaling(m,n)<8.1)
if (Scaling(m,n)<7)
    Scaling(m,n)= 0;
else
    Scaling(m,n)= 1;
end;
end;
end;
% Test if the sticker is present on each analyzed frame of the movie
clear all; close all; clc;
NumFrame = GetMovieFrame ( 'archive/Cinepak012.avi',1);
%Initialisation of the white dot position
%initialisation is needed only if there is more than one dot in the
first
%frame after image processing
%Position Cinepak006
Xbefore = 58;
Ybefore = 177;
%Position Cinepak003
Xbefore = 28;
Ybefore = 71;
%for cpt = 1: 6
for cpt = 1: NumFrame
disp (cpt);
name = ['image/N',num2str(cpt),'image.jpg'];
[original,analysed] = FonctionThreshold (name);
ImageClearBorder = ClearObject ( analysed );
[ImageFinal, Xbefore ,Ybefore]  = labelisation ( ImageClearBorder,
Xbefore, Ybefore );
[x,y]= find (ImageFinal==1);
ImageFinal2= zeros(size(ImageFinal));
ImageFinal2( find (ImageFinal==1) ) =255;
SizeOriginal = size (original);
FinalFullSize = FullSize (ImageFinal2, SizeOriginal);
[Xround,Yround] = ReturnDotPosition (FinalFullSize);
%FinalFullSize( Xround-10 : Xround+10, Yround:Yround) =255;
```

```
%FinalFullSize( Xround:Xround, Yround-10:Yround+10) =255;
original  = FunctionTestGrimacingSquareScale ( original , Xround ,
Yround , cpt);
% Draw the green cross
original( Xround-15:Xround+15, Yround:Yround,1) =0;
original( Xround:Xround, Yround-15:Yround+15,1 ) =0;
original( Xround-15:Xround+15, Yround:Yround,2 ) =255;
original( Xround:Xround, Yround-15:Yround+15,2 ) =255;
original( Xround-15:Xround+15, Yround:Yround,3 ) =0;
original( Xround:Xround, Yround-15:Yround+15,3 ) =0;
Double = TwoImage2One (original ,FinalFullSize);
%SaveAsJPG (original,'original',cpt);
%SaveAsJPG (analysed,'zanalysed',cpt);
%SaveAsJPG (ImageClearBorder,'zclearborder',cpt);
%SaveAsJPG (ImageFinal,'zfinal',cpt);
%SaveAsJPG (grimacing,'zgrimacing',cpt);
SaveAsJPG (Double,'zzDouble',cpt);
%var = genvarname(['imframe',num2str(cpt)]);
%eval([var ' = image']);
end;
%film = image2movie ( 'zanalysed' ,NumFrame);
```

APPENDICES B - TEST RESULTS

B1: Anthropometric data

Group I C5-C7 Tetraplegia

1. (Pre-surgery C5/C6 tetraplegia)

Gender	Age	Weight	Upper arm length	Forearm length	Duration W/C use	Disability Status
M	23	80	26.5	22.3	14	C6 ASIA A
M	19	60	27.5	27	2	C6 ASIA A

2. (Post-surgery C5/C6 tetraplegia)

Gender	Age	Weight	Upper arm length	Forearm length	Duration W/C use	Time after surgery	Disability Status
M	33	70	24	24.8	168	120	C6 ASIA A
M	35	111.5	23.8	24.3	210	180	C6 ASIA A
M	30	95	27	26.5	132	96	C5 ASIA A
M	37	67			204	72	C6 ASIA A

3. (Incomplete C7 tetraplegia)

Gender	Age	Weight	Upper arm length	Forearm length	Duration W/C use	Disability Status
M	44	96	28.7	26.4	300	C7 ASIA C
M	53	85	29.5	24	78	C7 ASIA C
M	49	80	30.5	28	5	C7 ASIA D
M	30	90			168	C7 ASIA A
M	41	96				C7 ASIA A
M	19	60	27.3	25.5	7	C7 ASIA B

Group II T1-T8 Paraplegia

Gender	Age	Weight	Upper arm length	Forearm length	Duration W/C use	Disability Status
M	62	84.5	29.5	24	492	T5
M	18	85	27.1	28.8	18	T6
M	61	98.7	29.5	27	324	T5
M	55	132	35.6	29.5	4	T5

Group III T9-T12 Paraplegia

Gender	Age	Weight	Upper arm length	Forearm length	Duration W/C use	Disability Status
M	16	74	29.6	28.2	10	T10
M	33	74	32.4	26	156	T11/T12
M	40	100.3	24.2	28.1	156	T9
F	39	90	25	23.8	18	T11/T12

Group IV L&S Paraplegia

Gender	Age	Weight	Upper arm length	Forearm length	Duration W/C use	Disability Status
M	20	79.2	27.2	26.5	60	L1
F	22	82	25.5	25.4	11	L1

B2: C5-C7 Tetraplegia

Maximum effort with normal resistance

Stroke Progress	V_{max} *[m/s]*	t_{pv} *[s]*	V_c *[m/s]*	V_r *[m/s]*	a_{max} *[m/s²]*	t_{pa} *[s]*	T_{max} *[Nm]*	F_{t-max} *[N]*	F_{r-max} *[N]*	$F_{res-max}$ *[N]*	P_{max} *[w]*
1st trial	1.535	1.809	0	1.433	1.148	0.78	10.5	211.1	179.1	276.9	116.9
2nd trial	2.147	0.863	1.532	2.027	1.174	0.474	10.2	214.4	181.8	281.1	200
3rd trial	2.563	0.746	2.132	2.471	0.9638	0.371	8.7	181.2	153.7	237.6	218.5

Stroke Progress	PP *[s]*	RP *[s]*	PP/CT *[%]*	θc *[°]*	θ_r *[°]*	θ_{E-min} *[°]*	θ_{E-max} *[°]*	θ_{T-min} *[°]*	θ_{T-max} *[°]*	θ_{s-min} *[°]*	θ_{s-max} *[°]*
1st trial	1.56	0.4	79.59	-33.7	50.4	110.2	133.0	-0.7	6.2	25.6	65.5
2nd trial	0.64	0.48	57.14	-31.1	52.3	99.8	138.0	1.7	5	25.5	70.7
3rd trial	0.52	0.48	52.00	-26.9	49.1	104.6	136.5	3.1	5.7	23.6	67.9

Maximum effort with twice-normal resistance

Stroke Progress	V_{max} *[m/s]*	t_{pv} *[s]*	V_c *[m/s]*	V_r *[m/s]*	a_{max} *[m/s²]*	t_{pa} *[s]*	T_{max} *[Nm]*	F_{t-max} *[N]*	F_{r-max} *[N]*	$F_{res-max}$ *[N]*	P_{max} *[w]*
1st trial	1.709	1.835	0	1.653	1.235	1.226	12.3	259.5	220.1	340.2	107.7
2nd trial	2.458	0.979	1.703	2.416	1.227	0.504	13.3	284.9	241.7	373.6	173.7
3rd trial	2.986	0.807	2.447	2.939	1.104	0.392	11.9	246.3	208.9	323.0	214.6

Stroke Progress	PP *[s]*	RP *[s]*	PP/CT *[%]*	θc *[°]*	θ_r *[°]*	θ_{E-min} *[°]*	θ_{E-max} *[°]*	θ_{T-min} *[°]*	θ_{T-max} *[°]*	θ_{s-min} *[°]*	θ_{s-max} *[°]*
1st trial	1.64	0.4	80.39	-25.9	26.6	109.8	129.4	0	5.8	23.1	56.3
2nd trial	0.84	0.44	65.63	-28.8	32.5	109.3	136.4	1.4	8.6	20.1	66.9
3rd trial	0.64	0.48	57.14	-24.9	36	109.9	136.3	2.7	7.5	22.5	67.3

Maximum effort with normal resistance

Stroke Progress	V_{max} *[m/s]*	t_{pv} *[s]*	V_c *[m/s]*	V_r *[m/s]*	a_{max} *[m/s²]*	t_{pa} *[s]*	T_{max} *[Nm]*	F_{t-max} *[N]*	F_{r-max} *[N]*	$F_{res-max}$ *[N]*	P_{max} *[w]*
1st trial	1.974	1.603	0	1.927	2.471	0.406	36.67	122.2	103.7	160.3	295.3
2nd trial	2.728	0.969	1.948	2.723	1.761	0.504	35.11	117.0	99.3	153.5	533.8
3rd trial	2.86	0.82	2.699	2.849	0.6133	0.527	18.19	60.6	51.4	79.5	330.6

Right

Stroke Progress	PP *[s]*	RP *[s]*	PP/CT *[%]*	θc *[°]*	θ_r *[°]*	θ_{E-min} *[°]*	θ_{E-max} *[°]*	θ_{T-min} *[°]*	θ_{T-max} *[°]*	θ_{s-min} *[°]*	θ_{s-max} *[°]*
1st trial	1.4	0.6	70.00	-14.8	39.3	99.8	133.0	3.1	10.8	22.9	70.2
2nd trial	0.92	0.6	60.53	-45	34.8	95.2	129.0	5.3	11.5	29.2	73.4
3rd trial	0.76	0.64	54.29	-42	30.3	105.2	123.6	6.2	8.7	30.4	73.2

Left

Stroke Progress	PP *[s]*	RP *[s]*	PP/CT *[%]*	θc *[°]*	θ_r *[°]*	θ_{E-min} *[°]*	θ_{E-max} *[°]*	θ_{s-min} *[°]*	θ_{s-max} *[°]*
1st trial	1.56	0.56	73.58	-45	45	105.0	131.0	24.0	78.8
2nd trial	0.76	0.8	48.72	-48.1	32.7	110.0	128.9	35.8	71.8
3rd trial	0.64	0.72	47.06	-37.2	29.5	105.9	126.1	36.9	77.2

Maximum effort with twice-normal resistance

Stroke Progress	V_{max} *[m/s]*	t_{pv} *[s]*	V_c *[m/s]*	V_r *[m/s]*	a_{max} *[m/s²]*	t_{pa} *[s]*	T_{max} *[Nm]*	F_{t-max} *[N]*	F_{r-max} *[N]*	$F_{res-max}$ *[N]*	P_{max} *[w]*
1st trial	0.5257	2.52	0	0.5178	0.6659	1.64	40.14	133.8	113.5	175.4	124.3
2nd trial	1.157	1.91	0.4363	1.091	0.5783	0.63	27.27	90.9	77.1	119.2	193.5
3rd trial	1.54	1.47	1.143	1.535	0.6045	0.54	36.87	122.9	104.2	161.2	368.5

Right

Stroke Progress	PP *[s]*	RP *[s]*	PP/CT *[%]*	θc *[°]*	θ_r *[°]*	θ_{E-min} *[°]*	θ_{E-max} *[°]*	θ_{T-min} *[°]*	θ_{T-max} *[°]*	θ_{s-min} *[°]*	θ_{s-max} *[°]*
1st trial	2.44	0.6	80.26	-46.2	11.9	89.2	131.5	2.1	9.2	37.4	69.5
2nd trial	1.6	0.6	72.73	-42	35.7	101.9	130.4	-2.4	2.1	24.1	62.5
3rd trial	1.36	0.6	69.39	-47.4	31	93.8	127.3	0.7	7.4	29.4	65.5

Left

Stroke Progress	PP *[s]*	RP *[s]*	PP/CT *[%]*	θc *[°]*	θ_r *[°]*	θ_{E-min} *[°]*	θ_{E-max} *[°]*	θ_{s-min} *[°]*	θ_{s-max} *[°]*
1st trial	1.72	1.16	59.72	-45	18.7	101.0	127.1	37.3	67.3
2nd trial	1.64	0.52	75.93	-36.9	20.4	96.9	122.2	31.6	65.2
3rd trial	1.36	0.6	69.39	-45	32.9	103.8	132.6	31.5	64.9

Maximum effort with normal resistance

Stroke Progress	V_{max} *[m/s]*	t_{pv} *[s]*	V_c *[m/s]*	V_r *[m/s]*	a_{max} *[m/s²]*	t_{pa} *[s]*	T_{max} *[Nm]*	F_{t-max} *[N]*	F_{r-max} *[N]*	$F_{res-max}$ *[N]*	P_{max} *[w]*
1st trial	1.822	1.68	0	1.724	1.831	0.808	14.1	270.4	229.3	354.6	90.3
2nd trial	2.226	0.767	1.882	2.153	0.8061	0.466	6.3	125.8	106.7	165.0	95.2
3rd trial	2.526	0.784	2.211	2.413	0.8236	0.483	6.6	133.6	113.3	175.1	120.3

Stroke Progress	PP *[s]*	RP *[s]*	PP/CT *[%]*	θc *[°]*	θ_r *[°]*	θ_{E-min} *[°]*	θ_{E-max} *[°]*	θ_{T-min} *[°]*	θ_{T-max} *[°]*	θ_{s-min} *[°]*	θ_{s-max} *[°]*
1st trial	1.4	0.32	81.40	-31.9	26.1	106.6	124.7	-2.2	0.9	29.2	59.1
2nd trial	0.6	0.32	65.22	-38	29.5	100.6	125.6	-3.2	-1.3	28.5	60.4
3rd trial	0.56	0.28	66.67	-36.4	24.2	104.0	125.6	-2.7	-1.3	29.1	60.2

Maximum effort with twice-normal resistance

Stroke Progress	V_{max} *[m/s]*	t_{pv} *[s]*	V_c *[m/s]*	V_r *[m/s]*	a_{max} *[m/s²]*	t_{pa} *[s]*	T_{max} *[Nm]*	F_{t-max} *[N]*	F_{r-max} *[N]*	$F_{res-max}$ *[N]*	P_{max} *[w]*
1st trial	1.225	2.052	0	1.217	0.8762	0.719	14.8	432.7	367.0	567.3	76.4
2nd trial	1.522	1.077	1.191	1.506	0.5169	0.542	5.5	320.8	272.1	420.7	58.3
3rd trial	1.732	0.931	1.509	1.727	0.3855	0.411	6.6	285.8	242.4	374.8	80.3

Stroke Progress	PP *[s]*	RP *[s]*	PP/CT *[%]*	θc *[°]*	θ_r *[°]*	θ_{E-min} *[°]*	θ_{E-max} *[°]*	θ_{T-min} *[°]*	θ_{T-max} *[°]*	θ_{s-min} *[°]*	θ_{s-max} *[°]*
1st trial	2	0.48	80.65	-34.9	35.5	103.9	127.8	-4.1	-2.2	28.1	58.3
2nd trial	0.96	0.4	70.59	-34	23.6	102.4	124.7	-4.4	-2.2	29.2	59.6
3rd trial	0.88	0.36	70.97	-38.8	21	106.0	126.0	-4.1	-2.2	29.8	63.0

Maximum effort with normal resistance

Stroke Progress	V_{max} *[m/s]*	t_{pv} *[s]*	V_c *[m/s]*	V_r *[m/s]*	a_{max} *[m/s²]*	t_{pa} *[s]*	T_{max} *[Nm]*	F_{t-max} *[N]*	F_{r-max} *[N]*	$F_{res-max}$ *[N]*	P_{max} *[w]*
1st trial	0.7517	1.668	0	0.7123	0.7973	0.524	11.3	221.4	187.8	290.4	75.9
2nd trial	1.083	0.89	0.7149	1.062	0.8323	0.467	5.8	118.2	100.3	155.0	71
3rd trial	1.243	0.91	0.9725	1.214	0.7535	0.480	6.9	148.2	125.7	194.3	97.1

Stroke Progress	PP *[s]*	RP *[s]*	PP/CT *[%]*	θc *[°]*	θ_r *[°]*	θ_{E-min} *[°]*	θ_{E-max} *[°]*	θ_{T-min} *[°]*	θ_{T-max} *[°]*	θ_{s-min} *[°]*	θ_{s-max} *[°]*
1st trial	1.48	0.4	78.72	-47.7	30.8	131.7	147.8	-4.4	2.7	19.4	44.3
2nd trial	0.8	0.44	64.52	-44.4	27.6	136.5	145.1	-2.1	-0.3	20.5	52.2
3rd trial	0.76	0.4	65.52	-42.3	30.8	135.6	145.7	-2.4	-0.5	22.8	52.4

Maximum effort with twice-normal resistance

Stroke Progress	V_{max} *[m/s]*	t_{pv} *[s]*	V_c *[m/s]*	V_r *[m/s]*	a_{max} *[m/s²]*	t_{pa} *[s]*	T_{max} *[Nm]*	F_{t-max} *[N]*	F_{r-max} *[N]*	$F_{res-max}$ *[N]*	P_{max} *[w]*
1st trial	0.5599	2.219	0	0.5415	0.5169	0.633	12.1	235.5	199.7	308.8	57.3
2nd trial	0.8437	1.14	0.5467	0.8306	0.5169	0.600	7.5	155.6	131.9	204.0	65.9
3rd trial	1.009	1.28	0.8043	1.004	0.4118	0.570	7.6	153.6	130.3	201.5	79.1

Stroke Progress	PP *[s]*	RP *[s]*	PP/CT *[%]*	θc *[°]*	θ_r *[°]*	θ_{E-min} *[°]*	θ_{E-max} *[°]*	θ_{T-min} *[°]*	θ_{T-max} *[°]*	θ_{s-min} *[°]*	θ_{s-max} *[°]*
1st trial	2	0.4	83.33	-53.1	17.7	136.7	150.7	-6.1	2.9	20.8	48.2
2nd trial	1.04	0.44	70.27	-50.8	28.2	136.9	147.5	-2.9	0.2	18.8	47.9
3rd trial	1.2	0.4	75.00	-48.2	22.2	135.6	145.5	-2.9	0	20.5	51.6

Maximum effort with normal resistance

Stroke Progress	V_{max} *[m/s]*	t_{pv} *[s]*	V_c *[m/s]*	V_r *[m/s]*	a_{max} *[m/s^2]*	t_{pa} *[s]*	T_{max} *[Nm]*	F_{t-max} *[N]*	F_{r-max} *[N]*	$F_{res-max}$ *[N]*	P_{max} *[w]*
1st trial	2.253	1.165	0	2.211	2.751	0.672	7.1	136.8	116.1	179.4	67.8
2nd trial	2.918	0.697	2.137	2.852	1.919	0.355	5.9	125.0	106.0	163.9	104.4
3rd trial	3.378	0.555	2.857	3.357	1.393	0.274	4.9	105.4	89.4	138.2	106.1

Stroke Progress	PP *[s]*	RP *[s]*	PP/CT *[%]*	θc *[°]*	θ_r *[°]*	θ_{E-min} *[°]*	θ_{E-max} *[°]*	θ_{T-min} *[°]*	θ_{T-max} *[°]*	θ_{s-min} *[°]*	θ_{s-max} *[°]*
1st trial	1.08	0.4	72.97	-25.8	28.6	91.6	121.1	-2.5	3.2	36.0	54.6
2nd trial	0.56	0.44	56.00	-34.7	23.3	99.9	130.7	-2.5	1.1	27.9	52.8
3rd trial	0.48	0.4	54.55	-34.7	27.8	97.3	121.5	-4.6	0.4	33.0	52.7

Maximum effort with twice-normal resistance

Stroke Progress	V_{max} *[m/s]*	t_{pv} *[s]*	V_c *[m/s]*	V_r *[m/s]*	a_{max} *[m/s^2]*	t_{pa} *[s]*	T_{max} *[Nm]*	F_{t-max} *[N]*	F_{r-max} *[N]*	$F_{res-max}$ *[N]*	P_{max} *[w]*
1st trial	0.8832	2.058	0	0.7912	0.587	0.755	6.4	127.6	108.3	167.4	31.5
2nd trial	1.477	1.296	0.8832	1.404	0.8411	0.619	6.1	122.1	103.6	160.1	53
3rd trial	1.727	0.942	1.451	1.772	0.5783	0.495	5.6	110.9	94.1	145.5	68.2

Stroke Progress	PP *[s]*	RP *[s]*	PP/CT *[%]*	θc *[°]*	θ_r *[°]*	θ_{E-min} *[°]*	θ_{E-max} *[°]*	θ_{T-min} *[°]*	θ_{T-max} *[°]*	θ_{s-min} *[°]*	θ_{s-max} *[°]*
1st trial	1.76	0.36	83.02	-26.6	12.5	98.8	126.3	-2.8	1.8	27.6	40.5
2nd trial	1	0.48	67.57	-25.2	30.2	102.9	126.5	-2.5	1.4	31.3	44.3
3rd trial	0.72	0.44	62.07	-26.6	22.8	111.0	129.2	-2.9	0	29.4	52.1

Maximum effort with normal resistance

Stroke Progress	V_{max} *[m/s]*	t_{pv} *[s]*	V_c *[m/s]*	V_r *[m/s]*	a_{max} *[m/s²]*	t_{pa} *[s]*	T_{max} *[Nm]*	$F_{t\text{-}max}$ *[N]*	$F_{r\text{-}max}$ *[N]*	$F_{res\text{-}max}$ *[N]*	P_{max} *[w]*
1st trial	3.617	1.15	0	3.48	5.248	0.53	14	373.3	316.7	489.5	226.5
2nd trial	4.245	0.69	3.577	4.171	1.726	0.4	7.6	201.9	171.3	264.8	233.9
3rd trial	4.681	0.51	4.208	4.587	1.393	0.26	6.2	165.6	140.5	217.1	210

Right

Stroke Progress	PP *[s]*	RP *[s]*	PP/CT *[%]*	θc *[°]*	θ_r *[°]*	$\theta_{E\text{-}min}$ *[°]*	$\theta_{E\text{-}max}$ *[°]*	$\theta_{T\text{-}min}$ *[°]*	$\theta_{T\text{-}max}$ *[°]*	$\theta_{s\text{-}min}$ *[°]*	$\theta_{s\text{-}max}$ *[°]*
1st trial	0.96	0.36	72.73	-47.3	42.4	105.1	134.6	1	7.1	24.7	80.6
2nd trial	0.56	0.32	63.64	-40.6	49.4	103.4	131.0	0	3.5	28.5	64.4
3rd trial	0.36	0.28	56.25	-22.6	45	91.2	124.5	-0.5	4.4	33.6	67.7

Left

Stroke Progress	PP *[s]*	RP *[s]*	PP/CT *[%]*	θc *[°]*	θ_r *[°]*	$\theta_{E\text{-}min}$ *[°]*	$\theta_{E\text{-}max}$ *[°]*	$\theta_{s\text{-}min}$ *[°]*	$\theta_{s\text{-}max}$ *[°]*
1st trial	0.96	0.36	72.73	-47.3	42.4	105.1	134.6	24.7	80.6
2nd trial	0.56	0.32	63.64	-40.6	49.4	103.4	131.0	28.5	64.4
3rd trial	0.36	0.28	56.25	-22.6	45	91.2	124.5	33.6	67.7

Maximum effort with twice-normal resistance

Stroke Progress	V_{max} *[m/s]*	t_{pv} *[s]*	V_c *[m/s]*	V_r *[m/s]*	a_{max} *[m/s²]*	t_{pa} *[s]*	T_{max} *[Nm]*	$F_{t\text{-}max}$ *[N]*	$F_{r\text{-}max}$ *[N]*	$F_{res\text{-}max}$ *[N]*	P_{max} *[w]*
1st trial	1.724	1.74	0	1.669	1.437	1.080	12.3	326.9	277.3	428.7	132.4
2nd trial	2.195	0.85	1.664	2.155	1.034	0.37	9.4	251.1	213.0	329.3	166.9
3rd trial	2.6	0.77	2.163	2.552	0.8762	0.32	8.4	224.1	190.1	293.9	194.1

Right

Stroke Progress	PP *[s]*	RP *[s]*	PP/CT *[%]*	θc *[°]*	θ_r *[°]*	$\theta_{E\text{-}min}$ *[°]*	$\theta_{E\text{-}max}$ *[°]*	$\theta_{T\text{-}min}$ *[°]*	$\theta_{T\text{-}max}$ *[°]*	$\theta_{s\text{-}min}$ *[°]*	$\theta_{s\text{-}max}$ *[°]*
1st trial	1.56	0.56	73.58	-50.3	36.7	102.7	135.8	1.1	7.6	22.5	81.3
2nd trial	0.68	0.48	58.62	-47.8	31.1	107.2	137.8	0	3.7	23.8	64.4
3rd trial	0.6	0.44	57.69	-45	36.3	106.0	134.3	-1.1	3.3	26.2	73.3

Left

Stroke Progress	PP *[s]*	RP *[s]*	PP/CT *[%]*	θc *[°]*	θ_r *[°]*	$\theta_{E\text{-}min}$ *[°]*	$\theta_{E\text{-}max}$ *[°]*	$\theta_{s\text{-}min}$ *[°]*	$\theta_{s\text{-}max}$ *[°]*
1st trial	1.76	0.4	81.48	-52.7	18.8	100.7	145.7	25.6	91.9
2nd trial	0.8	0.32	71.43	-38.8	25.3	97.5	136.6	21.5	68.0
3rd trial	0.72	0.36	66.67	-39.5	30.3	93.2	136.8	26.4	69.2

Maximum effort with normal resistance

Stroke Progress	V_{max} *[m/s]*	t_{pv} *[s]*	V_c *[m/s]*	V_r *[m/s]*	a_{max} *[m/s²]*	t_{pa} *[s]*	T_{max} *[Nm]*	$F_{t\text{-}max}$ *[N]*	$F_{r\text{-}max}$ *[N]*	$F_{res\text{-}max}$ *[N]*	P_{max} *[w]*
1st trial	2.931	0.959	0	2.902	4.74	0.640	40.9	846.0	717.6	1109.3	490.4
2nd trial	3.404	0.529	2.339	3.37	3.075	0.301	40.8	952.3	807.7	1248.8	657.3
3rd trial	3.903	0.557	3.209	3.698	2.147	0.343	42.1	654.3	555.0	858.0	1032

Stroke Progress	PP *[s]*	RP *[s]*	PP/CT *[%]*	θc *[°]*	θ_r *[°]*	$\theta_{E\text{-}min}$ *[°]*	$\theta_{E\text{-}max}$ *[°]*	$\theta_{T\text{-}min}$ *[°]*	$\theta_{T\text{-}max}$ *[°]*	$\theta_{s\text{-}min}$ *[°]*	$\theta_{s\text{-}max}$ *[°]*
1st trial	0.92	0.4	69.70	-29.5	41	105.3	128.6	3	10.1	29.1	70.8
2nd trial	0.48	0.36	57.14	-23.2	40.4	100.9	123.9	2.1	9.5	22.4	71.8
3rd trial	0.4	0.44	47.62	-23.6	45	98.6	127.2	5.6	9.2	26.7	82.6

Maximum effort with twice-normal resistance

Stroke Progress	V_{max} *[m/s]*	t_{pv} *[s]*	V_c *[m/s]*	V_r *[m/s]*	a_{max} *[m/s²]*	t_{pa} *[s]*	T_{max} *[Nm]*	$F_{t\text{-}max}$ *[N]*	$F_{r\text{-}max}$ *[N]*	$F_{res\text{-}max}$ *[N]*	P_{max} *[w]*
1st trial	3.238	1.297	0	2.947	5.748	0.999	87.3	1158.7	982.8	1519.3	1043
2nd trial	4.321	0.688	2.752	4.198	4.696	0.429	86.8	1840.7	1561.2	2413.6	1399
3rd trial	3.504	0.585	2.468	3.441	3.557	0.362	90	1661.3	1409.1	2178.4	2196

Stroke Progress	PP *[s]*	RP *[s]*	PP/CT *[%]*	θc *[°]*	θ_r *[°]*	$\theta_{E\text{-}min}$ *[°]*	$\theta_{E\text{-}max}$ *[°]*	$\theta_{T\text{-}min}$ *[°]*	$\theta_{T\text{-}max}$ *[°]*	$\theta_{s\text{-}min}$ *[°]*	$\theta_{s\text{-}max}$ *[°]*
1st trial	1.16	0.44	72.50	-31.6	50.5	113.3	138.9	2.6	9.5	20.5	62.2
2nd trial	0.6	0.44	57.69	-32.2	34	108.7	133.9	6	9.2	21.8	79.9
3rd trial	0.52	0.28	65.00	-17.6	21	108.3	122.4	7.3	10.2	27.2	79.2

Maximum effort with normal resistance

Stroke Progress	V_{max} *[m/s]*	t_{pv} *[s]*	V_c *[m/s]*	V_r *[m/s]*	a_{max} *[m/s²]*	t_{pa} *[s]*	T_{max} *[Nm]*	F_{t-max} *[N]*	F_{r-max} *[N]*	$F_{res-max}$ *[N]*	P_{max} *[w]*
1st trial	3.154	1.009	0	2.928	5.055	0.503	21.5	424.0	359.6	556.0	235.9
2nd trial	4.284	0.598	3.109	3.956	3.049	0.326	15.6	327.7	277.9	429.7	387.1
3rd trial	5.21	0.555	4.245	4.798	2.646	0.294	13.1	285.8	242.4	374.7	420

Stroke Progress	PP *[s]*	RP *[s]*	PP/CT *[%]*	θc *[°]*	θ_r *[°]*	θ_{E-min} *[°]*	θ_{E-max} *[°]*	θ_{T-min} *[°]*	θ_{T-max} *[°]*	θ_{s-min} *[°]*	θ_{s-max} *[°]*
1st trial	0.84	0.36	70.00	-29	41.5	115.9	144.0	-1.8	5.8	16.4	44.1
2nd trial	0.4	0.36	52.63	32.6	26.9	112.5	146.6	-0.9	0.9	18.3	56.4
3rd trial	0.32	0.36	47.06	-31	41.8	107.6	139.1	-0.9	0.9	18.1	58.3

Maximum effort with twice-normal resistance

Stroke Progress	V_{max} *[m/s]*	t_{pv} *[s]*	V_c *[m/s]*	V_r *[m/s]*	a_{max} *[m/s²]*	t_{pa} *[s]*	T_{max} *[Nm]*	F_{t-max} *[N]*	F_{r-max} *[N]*	$F_{res-max}$ *[N]*	P_{max} *[w]*
1st trial	1.385	0.946	0	1.362	2.558	0.495	52	1040.0	882.1	1363.7	305.8
2nd trial	2.35	0.751	1.359	2.255	2.085	0.387	44.9	927.0	786.3	1215.5	604.2
3rd trial	3.015	0.71	2.339	2.907	1.542	0.382	30.1	644.3	546.5	844.9	574.7

Stroke Progress	PP *[s]*	RP *[s]*	PP/CT *[%]*	θc *[°]*	θ_r *[°]*	θ_{E-min} *[°]*	θ_{E-max} *[°]*	θ_{T-min} *[°]*	θ_{T-max} *[°]*	θ_{s-min} *[°]*	θ_{s-max} *[°]*
1st trial	0.88	0.32	73.33	-25.6	24.4	107.2	128.4	-2.6	5.8	24.4	42.8
2nd trial	0.6	0.28	68.18	-26.6	36.4	100.0	122.6	-1.8	2.2	25.5	57.0
3rd trial	0.52	0.32	61.90	-31	42.4	109.4	140.3	-1.7	0.9	17.7	58.3

Maximum effort with normal resistance

Stroke Progress	V_{max} *[m/s]*	t_{pv} *[s]*	V_c *[m/s]*	V_r *[m/s]*	a_{max} *[m/s²]*	t_{pa} *[s]*	T_{max} *[Nm]*	F_{t-max} *[N]*	F_{r-max} *[N]*	$F_{res-max}$ *[N]*	P_{max} *[w]*
1st trial	3.007	1.107	0	2.857	4.267	0.667	11.5	218.7	185.5	286.7	146.7
2nd trial	3.744	0.598	2.975	3.598	2.164	0.342	6.9	149.1	126.5	195.5	149.9
3rd trial	4.445	0.58	3.738	4.258	1.98	0.324	6.2	131.0	111.1	171.7	158.3

Stroke Progress	PP *[s]*	RP *[s]*	PP/CT *[%]*	θc *[°]*	θ_r *[°]*	θ_{E-min} *[°]*	θ_{E-max} *[°]*	θ_{T-min} *[°]*	θ_{T-max} *[°]*	θ_{s-min} *[°]*	θ_{s-max} *[°]*
1st trial	0.96	0.44	68.57	-32.7	46.4	108.1	135.2	-2.2	15.4	23.8	73.5
2nd trial	0.44	0.4	52.38	-33	40.1	106.1	131.0	5.7	8.5	25.2	82.9
3rd trial	0.4	0.4	50.00	-36	43.6	108.4	134.7	5.4	8.3	23.6	76.1

Maximum effort with twice-normal resistance

Stroke Progress	V_{max} *[m/s]*	t_{pv} *[s]*	V_c *[m/s]*	V_r *[m/s]*	a_{max} *[m/s²]*	t_{pa} *[s]*	T_{max} *[Nm]*	F_{t-max} *[N]*	F_{r-max} *[N]*	$F_{res-max}$ *[N]*	P_{max} *[w]*
1st trial	1.635	1.625	0	1.53	1.717	0.909	12.8	251.4	213.2	329.6	90.6
2nd trial	2.147	0.917	1.632	2.061	1.069	0.531	9.5	185.6	157.4	243.4	120.3
3rd trial	2.607	0.92	2.145	2.508	0.9901	0.507	8.4	165.4	140.3	216.8	132.5

Stroke Progress	PP *[s]*	RP *[s]*	PP/CT *[%]*	θc *[°]*	θ_r *[°]*	θ_{E-min} *[°]*	θ_{E-max} *[°]*	θ_{T-min} *[°]*	θ_{T-max} *[°]*	θ_{s-min} *[°]*	θ_{s-max} *[°]*
1st trial	1.4	0.32	81.40	-28.2	32.8	111.8	135.8	-1.9	10.5	23.3	69.3
2nd trial	0.72	0.32	69.23	-29.3	34.3	108.6	134.8	3	9.2	22.9	69.8
3rd trial	0.68	0.4	62.96	-32.7	41.2	108.4	138.2	2.7	8.4	21.1	72.3

Maximum effort with normal resistance

Stroke Progress	V_{max} *[m/s]*	t_{pv} *[s]*	V_c *[m/s]*	V_r *[m/s]*	a_{max} *[m/s²]*	t_{pa} *[s]*	T_{max} *[Nm]*	$F_{t\text{-}max}$ *[N]*	$F_{r\text{-}max}$ *[N]*	$F_{res\text{-}max}$ *[N]*	P_{max} *[w]*
1st trial	2.584	1.09	0	2.321	3.408	0.47	25.5	424.7	360.2	556.8	329
2nd trial	3.677	0.55	2.576	3.293	2.865	0.27	35.2	587.3	498.2	770.1	804.6
3rd trial	4.658	0.51	3.667	4.153	2.751	0.23	27.9	465.7	395.0	610.6	854.6

Right

Stroke Progress	PP *[s]*	RP *[s]*	PP/CT *[%]*	θc *[°]*	θ_r *[°]*	$\theta_{E\text{-}min}$ *[°]*	$\theta_{E\text{-}max}$ *[°]*	$\theta_{T\text{-}min}$ *[°]*	$\theta_{T\text{-}max}$ *[°]*	$\theta_{s\text{-}min}$ *[°]*	$\theta_{s\text{-}max}$ *[°]*
1st trial	0.88	0.32	73.33	-9.3	49.9	125.1	156.0	8.5	10	14.3	62.4
2nd trial	0.32	0.24	57.14	0	50.4	116.3	162.5	15.6	18.7	9.1	67.1
3rd trial	0.36	0.24	60.00	-0.8	44.3	115.0	158.5	15.5	20.1	11.4	91.2

Left

Stroke Progress	PP *[s]*	RP *[s]*	PP/CT *[%]*	θc *[°]*	θ_r *[°]*	$\theta_{E\text{-}min}$ *[°]*	$\theta_{E\text{-}max}$ *[°]*	$\theta_{s\text{-}min}$ *[°]*	$\theta_{s\text{-}max}$ *[°]*
1st trial	0.72	0.24	75.00	6.2	53.7	128.7	150.3	21.9	46.5
2nd trial	0.24	0.2	54.55	4.7	56.7	109.5	150.2	23.3	49.5
3rd trial	0.24	0.2	54.55	5.6	61.3	107.0	146.6	24.3	53.0

Maximum effort with twice-normal resistance

Stroke Progress	V_{max} *[m/s]*	t_{pv} *[s]*	V_c *[m/s]*	V_r *[m/s]*	a_{max} *[m/s²]*	t_{pa} *[s]*	T_{max} *[Nm]*	$F_{t\text{-}max}$ *[N]*	$F_{r\text{-}max}$ *[N]*	$F_{res\text{-}max}$ *[N]*	P_{max} *[w]*
1st trial	1.814	1.7	0	1.709	1.63	0.64	33.5	559.0	474.1	733.0	261.4
2nd trial	2.444	0.74	1.811	2.329	1.332	0.36	25.3	421.0	357.1	552.0	409.8
3rd trial	2.923	0.66	2.437	2.805	1.13	0.33	26.2	437.3	370.9	573.5	541.6

Right

Stroke Progress	PP *[s]*	RP *[s]*	PP/CT *[%]*	θc *[°]*	θ_r *[°]*	$\theta_{E\text{-}min}$ *[°]*	$\theta_{E\text{-}max}$ *[°]*	$\theta_{T\text{-}min}$ *[°]*	$\theta_{T\text{-}max}$ *[°]*	$\theta_{s\text{-}min}$ *[°]*	$\theta_{s\text{-}max}$ *[°]*
1st trial	1.48	0.32	82.22	-21.1	49.6	119.0	145.2	3.7	10	20.4	52.3
2nd trial	0.52	0.36	59.09	-6.1	46.4	125.3	154.3	-2.7	11.9	20.2	62.5
3rd trial	0.44	0.36	55.00	-8.7	45.7	127.9	158.9	8.9	11.7	17.3	61.3

Left

Stroke Progress	PP *[s]*	RP *[s]*	PP/CT *[%]*	θc *[°]*	θ_r *[°]*	$\theta_{E\text{-}min}$ *[°]*	$\theta_{E\text{-}max}$ *[°]*	$\theta_{s\text{-}min}$ *[°]*	$\theta_{s\text{-}max}$ *[°]*
1st trial	1.44	0.32	81.82	-10.8	46.9	132.9	147.4	16.8	43.4
2nd trial	0.52	0.36	59.09	-3.7	46.8	132.4	165.2	8.1	44.3
3rd trial	0.44	0.36	55.00	-3.7	51.5	134.1	158.9	11.1	40.9

Maximum effort with normal resistance

Stroke Progress	V_{max} *[m/s]*	t_{pv} *[s]*	V_c *[m/s]*	V_r *[m/s]*	a_{max} *[m/s^2]*	t_{pa} *[s]*	T_{max} *[Nm]*	$F_{t\text{-}max}$ *[N]*	$F_{r\text{-}max}$ *[N]*	$F_{res\text{-}max}$ *[N]*	P_{max} *[w]*
1st trial	4.093	1.212	0	3.88	5.196	0.59	43.4	706.3	599.1	926.2	745
2nd trial	5.123	0.586	4.056	4.902	2.742	0.289	26	433.3	367.5	568.2	908
3rd trial	5.801	0.495	5.089	5.607	2.006	0.254	21.6	360.3	305.6	472.5	911.4

Right

Stroke Progress	PP *[s]*	RP *[s]*	PP/CT *[%]*	θc *[°]*	θ_r *[°]*	$\theta_{E\text{-}min}$ *[°]*	$\theta_{E\text{-}max}$ *[°]*	$\theta_{T\text{-}min}$ *[°]*	$\theta_{T\text{-}max}$ *[°]*	$\theta_{s\text{-}min}$ *[°]*	$\theta_{s\text{-}max}$ *[°]*
1st trial	1.04	0.32	76.47	-50.1	48.6	95.7	136.7	-2.2	9.7	32.0	79.5
2nd trial	0.4	0.32	55.56	-37.3	45	99.7	134.3	4.2	8.1	30.5	77.1
3rd trial	0.32	0.32	50.00	-34.1	42.5	99.2	132.0	2.1	5.9	31.2	73.6

Left

Stroke Progress	PP *[s]*	RP *[s]*	PP/CT *[%]*	θc *[°]*	θ_r *[°]*	$\theta_{E\text{-}min}$ *[°]*	$\theta_{E\text{-}max}$ *[°]*	$\theta_{s\text{-}min}$ *[°]*	$\theta_{s\text{-}max}$ *[°]*
1st trial	1.04	0.32	76.47	-43.5	51.3	109.3	142.3	26.7	64.4
2nd trial	0.4	0.28	58.82	-28	48.3	101.2	138.5	27.1	77.9
3rd trial	0.36	0.28	56.25	-29.7	45	99.6	134.6	29.9	77.7

Maximum effort with twice-normal resistance

Stroke Progress	V_{max} *[m/s]*	t_{pv} *[s]*	V_c *[m/s]*	V_r *[m/s]*	a_{max} *[m/s^2]*	t_{pa} *[s]*	T_{max} *[Nm]*	$F_{t\text{-}max}$ *[N]*	$F_{r\text{-}max}$ *[N]*	$F_{res\text{-}max}$ *[N]*	P_{max} *[w]*
1st trial	2.755	1.41	0	2.671	2.76	0.63	47.4	789.3	669.5	1035.0	574.8
2nd trial	3.598	0.72	2.739	3.543	1.796	0.36	32.2	536.0	454.6	702.8	782.6
3rd trial	4.19	0.62	3.588	4.124	1.463	0.30	28.1	467.7	396.7	613.2	875.8

Right

Stroke Progress	PP *[s]*	RP *[s]*	PP/CT *[%]*	θc *[°]*	θ_r *[°]*	$\theta_{E\text{-}min}$ *[°]*	$\theta_{E\text{-}max}$ *[°]*	$\theta_{T\text{-}min}$ *[°]*	$\theta_{T\text{-}max}$ *[°]*	$\theta_{s\text{-}min}$ *[°]*	$\theta_{s\text{-}max}$ *[°]*
1st trial	1.24	0.32	79.49	-46.7	38.5	99.9	135.3	1.1	6.5	31.9	64.9
2nd trial	0.6	0.24	71.43	-45.6	37.9	103.6	130.2	1.4	5	27.1	64.6
3rd trial	0.48	0.24	66.67	-42.3	38.1	104.8	133.8	1.7	4.3	29.1	65.2

Left

Stroke Progress	PP *[s]*	RP *[s]*	PP/CT *[%]*	θc *[°]*	θ_r *[°]*	$\theta_{E\text{-}min}$ *[°]*	$\theta_{E\text{-}max}$ *[°]*	$\theta_{s\text{-}min}$ *[°]*	$\theta_{s\text{-}max}$ *[°]*
1st trial	1.2	0.28	81.08	-33.4	44.2	103.8	137.1	27.9	70.7
2nd trial	0.64	0.24	72.73	-38.3	45	104.6	133.0	27.8	64.7
3rd trial	0.48	0.24	66.67	-32.3	45	99.1	135.3	32.3	71.8

Maximum effort with normal resistance

Stroke Progress	V_{max} *[m/s]*	t_{pv} *[s]*	V_c *[m/s]*	V_r *[m/s]*	a_{max} *[m/s²]*	t_{pa} *[s]*	T_{max} *[Nm]*	F_{t-max} *[N]*	F_{r-max} *[N]*	$F_{res-max}$ *[N]*	P_{max} *[w]*
1st trial	4.093	0.672	0	3.859	5.196	0.34	19	316.7	268.6	415.3	334.2
2nd trial	5.123	0.566	4.053	5.036	2.742	0.28	11.7	194.4	164.9	254.9	407.2
3rd trial	5.801	0.664	5.089	5.664	2.006	0.26	9.7	161.6	137.1	211.9	408.8

Right

Stroke Progress	PP *[s]*	RP *[s]*	PP/CT *[%]*	θc *[°]*	θ_r *[°]*	θ_{E-min} *[°]*	θ_{E-max} *[°]*	θ_{T-min} *[°]*	θ_{T-max} *[°]*	θ_{s-min} *[°]*	θ_{s-max} *[°]*
1st trial	0.56	0.6	48.28	-26.2	46.4	112.2	133.2	3.1	6.8	27.7	50.4
2nd trial	0.48	0.64	42.86	-42.7	46.4	114.5	132.8	0.3	3.1	21.8	54.1
3rd trial	0.4	0.68	37.04	-42.7	47.1	111.9	137.9	0.7	3.1	20.6	55.3

Left

Stroke Progress	PP *[s]*	RP *[s]*	PP/CT *[%]*	θc *[°]*	θ_r *[°]*	θ_{E-min} *[°]*	θ_{E-max} *[°]*	θ_{s-min} *[°]*	θ_{s-max} *[°]*
1st trial	0.68	0.56	54.84	-50.2	41.6	101.6	144.6	30.6	55.3
2nd trial	0.52	0.6	46.43	-43.8	45	109.4	131.6	22.9	57.4
3rd trial	0.44	0.68	39.29	-46.7	43.7	105.1	135.6	29.6	60.0

Maximum effort with twice-normal resistance

Stroke Progress	V_{max} *[m/s]*	t_{pv} *[s]*	V_c *[m/s]*	V_r *[m/s]*	a_{max} *[m/s²]*	t_{pa} *[s]*	T_{max} *[Nm]*	F_{t-max} *[N]*	F_{r-max} *[N]*	$F_{res-max}$ *[N]*	P_{max} *[w]*
1st trial	2.755	1.61	0	2.565	2.76	0.670	31.1	518.7	439.9	680.1	377.6
2nd trial	3.598	0.98	2.739	3.477	1.796	0.532	21.1	352.0	298.6	461.6	514.2
3rd trial	4.19	0.85	3.588	4.106	1.463	0.448	18.4	307.3	260.6	402.9	575.4

Right

Stroke Progress	PP *[s]*	RP *[s]*	PP/CT *[%]*	θc *[°]*	θ_r *[°]*	θ_{E-min} *[°]*	θ_{E-max} *[°]*	θ_{T-min} *[°]*	θ_{T-max} *[°]*	θ_{s-min} *[°]*	θ_{s-max} *[°]*
1st trial	1.28	0.64	66.67	-43.2	36.7	107.7	134.7	1.4	7.4	30.4	55.3
2nd trial	0.76	0.64	54.29	-40.1	40.1	112.8	134.3	0	3.9	26.6	51.3
3rd trial	0.64	0.6	51.61	-43.2	38.8	115.4	130.6	-0.3	3.5	24.7	48.4

Left

Stroke Progress	PP *[s]*	RP *[s]*	PP/CT *[%]*	θc *[°]*	θ_r *[°]*	θ_{E-min} *[°]*	θ_{E-max} *[°]*	θ_{s-min} *[°]*	θ_{s-max} *[°]*
1st trial	1.36	0.52	72.34	-45	42.9	100.5	129.4	31.1	60.6
2nd trial	0.92	0.52	63.89	-49.8	31.3	106.9	139.5	27.6	56.6
3rd trial	0.72	0.56	56.25	-47.4	39.6	107.5	141.4	25.9	53.2

B3: T1-T8 Paraplegia

Maximum effort with normal resistance

Stroke Progress	V_{max} *[m/s]*	t_{pv} *[s]*	V_c *[m/s]*	V_r *[m/s]*	a_{max} *[m/s²]*	t_{pa} *[s]*	T_{max} *[Nm]*	F_{t-max} *[N]*	F_{r-max} *[N]*	$F_{res-max}$ *[N]*	P_{max} *[w]*
1st trial	4.295	1.118	0	4.014	5.897	0.680	30.4	592.3	502.4	776.7	565.2
2nd trial	5.651	0.597	4.213	5.438	3.461	0.298	21.1	447.7	379.7	587.0	693.6
3rd trial	6.595	0.497	5.58	6.39	2.742	0.212	19.9	437.7	371.2	573.9	836.3

Stroke Progress	PP *[s]*	RP *[s]*	PP/CT *[%]*	θc *[°]*	θ_r *[°]*	θ_{E-min} *[°]*	θ_{E-max} *[°]*	θ_{T-min} *[°]*	θ_{T-max} *[°]*	θ_{s-min} *[°]*	θ_{s-max} *[°]*
1st trial	0.96	0.68	58.54	-36.9	54.3	81.0	133.0	-1.1	3.8	40.6	79.9
2nd trial	0.44	0.6	42.31	-41.5	58.8	88.2	133.4	-2.1	6	33.7	83.3
3rd trial	0.32	0.56	36.36	-37.7	51.9	87.6	137.7	-2.1	4.9	34.6	81.1

Maximum effort with twice-normal resistance

Stroke Progress	V_{max} *[m/s]*	t_{pv} *[s]*	V_c *[m/s]*	V_r *[m/s]*	a_{max} *[m/s²]*	t_{pa} *[s]*	T_{max} *[Nm]*	F_{t-max} *[N]*	F_{r-max} *[N]*	$F_{res-max}$ *[N]*	P_{max} *[w]*
1st trial	2.605	1.437	0	2.492	2.602	0.506	31	602.7	511.2	790.3	345.2
2nd trial	3.648	0.804	2.581	3.522	2.199	0.437	29.1	571.7	484.9	749.6	613.5
3rd trial	4.295	0.651	3.625	4.127	1.603	0.326	24.8	502.7	426.4	659.1	674.9

Stroke Progress	PP *[s]*	RP *[s]*	PP/CT *[%]*	θc *[°]*	θ_r *[°]*	θ_{E-min} *[°]*	θ_{E-max} *[°]*	θ_{T-min} *[°]*	θ_{T-max} *[°]*	θ_{s-min} *[°]*	θ_{s-max} *[°]*
1st trial	1.24	0.52	70.45	-24.6	59.5	86.8	134.4	-2.1	4.3	34.9	63.3
2nd trial	0.64	0.48	57.14	-32.9	51.9	83.4	125.4	-1.6	2.7	33.5	82.2
3rd trial	0.44	0.44	50.00	-32.8	58.6	83.2	130.0	-2.7	3.2	34.0	72.4

Maximum effort with normal resistance

Stroke Progress	V_{max} *[m/s]*	t_{pv} *[s]*	V_c *[m/s]*	V_r *[m/s]*	a_{max} *[m/s²]*	t_{pa} *[s]*	T_{max} *[Nm]*	F_{t-max} *[N]*	F_{r-max} *[N]*	$F_{res-max}$ *[N]*	P_{max} *[w]*
1st trial	4.305	0.999	0	3.935	6.703	0.633	24.2	469.7	398.4	615.9	387.7
2nd trial	6.329	0.578	4.211	5.848	5.406	0.302	23.1	517.0	438.5	677.9	728.6
3rd trial	7.617	0.5	6.237	7.239	3.889	0.250	19.5	460.0	390.2	603.2	805.2

Stroke Progress	PP *[s]*	RP *[s]*	PP/CT *[%]*	θc *[°]*	θ_r *[°]*	θ_{E-min} *[°]*	θ_{E-max} *[°]*	θ_{T-min} *[°]*	θ_{T-max} *[°]*	θ_{s-min} *[°]*	θ_{s-max} *[°]*
1st trial	0.84	0.48	63.64	-31.9	41	102.0	130.6	-1.5	4.3	36.9	42.3
2nd trial	0.4	0.52	43.48	-41	37.8	109.2	126.6	1.1	3.2	33.9	62.9
3rd trial	0.32	0.52	38.10	-35.3	40.3	109.4	129.4	-2.7	1.1	35.9	67.7

Maximum effort with twice-normal resistance

Stroke Progress	V_{max} *[m/s]*	t_{pv} *[s]*	V_c *[m/s]*	V_r *[m/s]*	a_{max} *[m/s²]*	t_{pa} *[s]*	T_{max} *[Nm]*	F_{t-max} *[N]*	F_{r-max} *[N]*	$F_{res-max}$ *[N]*	P_{max} *[w]*
1st trial	3.817	1.298	0	3.359	4.977	0.958	29.4	610.3	517.7	800.3	339.7
2nd trial	5.457	0.718	3.288	5.01	6.203	0.450	30.2	650.7	551.9	853.2	631.6
3rd trial	6.784	0.55	4.889	6.101	5.765	0.320	30.5	658.3	558.4	863.2	858.3

Stroke Progress	PP *[s]*	RP *[s]*	PP/CT *[%]*	θc *[°]*	θ_r *[°]*	θ_{E-min} *[°]*	θ_{E-max} *[°]*	θ_{T-min} *[°]*	θ_{T-max} *[°]*	θ_{s-min} *[°]*	θ_{s-max} *[°]*
1st trial	1.12	0.56	66.67	-30.7	34.5	106.7	126.0	1.1	5.6	30.1	44.7
2nd trial	0.56	0.52	51.85	-46.7	29.9	108.7	125.4	3	5.5	33.8	61.2
3rd trial	0.36	0.48	42.86	-37.2	36.3	112.3	123.7	2.2	4.4	35.9	62.8

Maximum effort with normal resistance

Stroke Progress	V_{max} *[m/s]*	t_{pv} *[s]*	V_c *[m/s]*	V_r *[m/s]*	a_{max} *[m/s²]*	t_{pa} *[s]*	T_{max} *[Nm]*	F_{t-max} *[N]*	F_{r-max} *[N]*	$F_{res-max}$ *[N]*	P_{max} *[w]*
1st trial	2.87	1.258	0	2.647	4.749	0.805	5	360.0	305.3	472.1	221.9
2nd trial	4.468	0.543	2.81	4.032	4.574	0.282	18.2	443.7	376.3	581.8	491.4
3rd trial	5.714	0.454	4.416	5.336	3.776	0.213	20.3	441.0	374.0	578.3	589.2

Stroke Progress	PP *[s]*	RP *[s]*	PP/CT *[%]*	θc *[°]*	θ_r *[°]*	θ_{E-min} *[°]*	θ_{E-max} *[°]*	θ_{T-min} *[°]*	θ_{T-max} *[°]*	θ_{s-min} *[°]*	θ_{s-max} *[°]*
1st trial	1.08	0.36	75.00	-24.4	33.7	96.1	129.6	4.8	9.6	29.6	70.8
2nd trial	0.36	0.32	52.94	-24.9	34	99.9	133.0	4.9	9.2	30.6	73.3
3rd trial	0.28	0.28	50.00	-20.2	38.5	100.8	135.0	6.7	11	29.3	69.6

Maximum effort with twice-normal resistance

Stroke Progress	V_{max} *[m/s]*	t_{pv} *[s]*	V_c *[m/s]*	V_r *[m/s]*	a_{max} *[m/s²]*	t_{pa} *[s]*	T_{max} *[Nm]*	F_{t-max} *[N]*	F_{r-max} *[N]*	$F_{res-max}$ *[N]*	P_{max} *[w]*
1st trial	1.609	1.154	0	1.58	2.059	0.581	19.7	390.7	331.4	512.3	135.1
2nd trial	2.423	0.622	1.617	2.387	1.901	0.286	19.7	432.7	367.0	567.3	263
3rd trial	3.041	0.582	2.416	3.002	1.56	0.275	18.4	427.7	362.7	560.8	348.6

Stroke Progress	PP *[s]*	RP *[s]*	PP/CT *[%]*	θc *[°]*	θ_r *[°]*	θ_{E-min} *[°]*	θ_{E-max} *[°]*	θ_{T-min} *[°]*	θ_{T-max} *[°]*	θ_{s-min} *[°]*	θ_{s-max} *[°]*
1st trial	1.04	0.28	78.79	-7.3	30.8	102.5	125.5	1.3	5.9	29.7	39.6
2nd trial	0.52	0.28	65.00	-11.3	36.6	103.4	127.2	3.1	7.4	28.2	42.6
3rd trial	0.48	0.28	63.16	-18.1	35.7	102.5	132.7	3.6	7.8	27.2	56.1

Maximum effort with normal resistance

Stroke Progress	V_{max} *[m/s]*	t_{pv} *[s]*	V_c *[m/s]*	V_r *[m/s]*	a_{max} *[m/s²]*	t_{pa} *[s]*	T_{max} *[Nm]*	F_{t-max} *[N]*	F_{r-max} *[N]*	$F_{res-max}$ *[N]*	P_{max} *[w]*
1st trial	4.124	1.077	0	4.098	6.688	0.599	34.4	676.0	573.4	886.4	488.4
2nd trial	5.218	0.591	3.506	5.007	5.362	0.354	27.2	566.0	480.1	742.2	666.5
3rd trial	5.675	0.495	4.839	5.528	2.953	0.304	23.5	546.0	463.1	715.9	717.8

Stroke Progress	PP *[s]*	RP *[s]*	PP/CT *[%]*	θc *[°]*	θ_r *[°]*	θ_{E-min} *[°]*	θ_{E-max} *[°]*	θ_{T-min} *[°]*	θ_{T-max} *[°]*	θ_{s-min} *[°]*	θ_{s-max} *[°]*
1st trial	1.04	0.4	72.22	-42.6	30.1	91.8	118.2	-3	1.4	33.4	60.9
2nd trial	0.48	0.36	57.14	-32.6	39.4	98.0	130.0	-3	1	30.6	62.8
3rd trial	0.4	0.36	52.63	-32.5	35.7	107.5	126.4	-4	4.8	36.8	80.1

Maximum effort with twice-normal resistance

Stroke Progress	V_{max} *[m/s]*	t_{pv} *[s]*	V_c *[m/s]*	V_r *[m/s]*	a_{max} *[m/s²]*	t_{pa} *[s]*	T_{max} *[Nm]*	F_{t-max} *[N]*	F_{r-max} *[N]*	$F_{res-max}$ *[N]*	P_{max} *[w]*
1st trial	3.507	1.286	0	3.301	5.73	0.538	61.9	1396.0	1184.1	1830.5	330
2nd trial	4.702	0.785	1.772	4.684	8.148	0.481	29.1	606.3	514.3	795.1	584.4
3rd trial	4.868	0.599	3.622	4.66	4.048	0.36	31.6	632.3	536.3	829.2	737.6

Stroke Progress	PP *[s]*	RP *[s]*	PP/CT *[%]*	θc *[°]*	θ_r *[°]*	θ_{E-min} *[°]*	θ_{E-max} *[°]*	θ_{T-min} *[°]*	θ_{T-max} *[°]*	θ_{s-min} *[°]*	θ_{s-max} *[°]*
1st trial	1.24	0.36	77.50	-43	19.2	91.0	121.7	-1	0	30.9	60.6
2nd trial	0.76	0.6	55.88	-45	36.6	96.7	121.2	-1	0.3	33.2	72.7
3rd trial	0.38	0.56	40.43	-37.3	35.5	98.1	119.5	-0.7	0.7	35.0	61.2

B4: T9-T12 Paraplegia

Maximum effort with normal resistance

Stroke Progress	V_{max} *[m/s]*	t_{pv} *[s]*	V_c *[m/s]*	V_r *[m/s]*	a_{max} *[m/s²]*	t_{pa} *[s]*	T_{max} *[Nm]*	F_{t-max} *[N]*	F_{r-max} *[N]*	$F_{res-max}$ *[N]*	P_{max} *[w]*
1st trial	4.865	0.715	0	3.79	7.149	0.318	25.34	526.0	446.1	689.7	592.9
2nd trial	5.985	0.469	4.863	5.391	3.601	0.319	17.2	419.7	356.0	550.3	901.4
3rd trial	7.354	0.358	5.828	7.276	3.583	0.122	17.1	370.3	314.1	485.6	980.6

Stroke Progress	PP *[s]*	RP *[s]*	PP/CT *[%]*	θc *[°]*	θ_r *[°]*	θ_{E-min} *[°]*	θ_{E-max} *[°]*	θ_{T-min} *[°]*	θ_{T-max} *[°]*	θ_{s-min} *[°]*	θ_{s-max} *[°]*
1st trial	0.42	0.32	56.76	-33.3	50.8	103.1	129.4	7.5	12.1	35.7	89.2
2nd trial	0.32	0.36	47.06	-26.9	52	100.9	133.9	3.5	9.2	35.8	101.3
3rd trial	0.28	0.26	51.85	-27.6	50.6	98.7	132.2	5.7	8.9	34.5	87.3

Maximum effort with twice-normal resistance

Stroke Progress	V_{max} *[m/s]*	t_{pv} *[s]*	V_c *[m/s]*	V_r *[m/s]*	a_{max} *[m/s²]*	t_{pa} *[s]*	T_{max} *[Nm]*	F_{t-max} *[N]*	F_{r-max} *[N]*	$F_{res-max}$ *[N]*	P_{max} *[w]*
1st trial	2.802	0.959	0	2.271	2.707	0.409	26.5	523.3	443.9	686.2	454.9
2nd trial	3.709	0.76	2.791	3.472	2.375	0.421	27.5	556.7	472.2	729.9	867.7
3rd trial	4.382	0.628	3.698	4.208	1.77	0.361	24.1	594.3	504.1	779.3	878.8

Stroke Progress	PP *[s]*	RP *[s]*	PP/CT *[%]*	θc *[°]*	θ_r *[°]*	θ_{E-min} *[°]*	θ_{E-max} *[°]*	θ_{T-min} *[°]*	θ_{T-max} *[°]*	θ_{s-min} *[°]*	θ_{s-max} *[°]*
1st trial	0.6	0.32	65.22	-32.3	36.5	94.7	126.7	3.4	9.1	26.5	81.6
2nd trial	0.52	0.36	59.09	-28	47.8	96.2	136.8	4.5	8	21.6	92.4
3rd trial	0.44	0.28	61.11	-19.2	52.4	99.2	145.5	8.6	11.9	23.7	94.6

Maximum effort with normal resistance

Stroke Progress	V_{max} *[m/s]*	t_{pv} *[s]*	V_c *[m/s]*	V_r *[m/s]*	a_{max} *[m/s²]*	t_{pa} *[s]*	T_{max} *[Nm]*	$F_{t\text{-}max}$ *[N]*	$F_{r\text{-}max}$ *[N]*	$F_{res\text{-}max}$ *[N]*	P_{max} *[w]*
1st trial	4.108	0.963	0	3.819	6.089	0.548	46.5	775.0	657.3	1016.2	1111
2nd trial	5.688	0.614	4.103	5.42	3.995	0.326	44.5	742.0	629.3	973.0	1770
3rd trial	6.913	0.498	5.672	6.569	3.356	0.247	32.1	535.0	453.8	701.5	1645.2

Stroke Progress	PP *[s]*	RP *[s]*	PP/CT *[%]*	θc *[°]*	θ_r *[°]*	$\theta_{E\text{-}min}$ *[°]*	$\theta_{E\text{-}max}$ *[°]*	$\theta_{T\text{-}min}$ *[°]*	$\theta_{T\text{-}max}$ *[°]*	$\theta_{s\text{-}min}$ *[°]*	$\theta_{s\text{-}max}$ *[°]*
1st trial	0.66	0.32	67.35	-16.1	52.1	101.2	137.5	8.3	14.9	33.0	79.2
2nd trial	0.44	0.4	52.38	-34.3	64.3	97.1	142.3	8.1	14	29.1	87.8
3rd trial	0.32	0.4	44.44	-29.6	65.1	94.6	135.4	11.1	13.2	38.9	98.7

Maximum effort with twice-normal resistance

Stroke Progress	V_{max} *[m/s]*	t_{pv} *[s]*	V_c *[m/s]*	V_r *[m/s]*	a_{max} *[m/s²]*	t_{pa} *[s]*	T_{max} *[Nm]*	$F_{t\text{-}max}$ *[N]*	$F_{r\text{-}max}$ *[N]*	$F_{res\text{-}max}$ *[N]*	P_{max} *[w]*
1st trial	2.916	1.255	0	2.614	4.581	0.707	56.8	946.3	802.7	1240.9	512
2nd trial	4.275	0.739	2.906	3.957	3.417	0.437	49	816.3	692.4	1070.4	1570
3rd trial	5.095	0.626	4.262	4.875	2.296	0.386	34.7	577.7	490.0	757.5	1278

Stroke Progress	PP *[s]*	RP *[s]*	PP/CT *[%]*	θc *[°]*	θ_r *[°]*	$\theta_{E\text{-}min}$ *[°]*	$\theta_{E\text{-}max}$ *[°]*	$\theta_{T\text{-}min}$ *[°]*	$\theta_{T\text{-}max}$ *[°]*	$\theta_{s\text{-}min}$ *[°]*	$\theta_{s\text{-}max}$ *[°]*
1st trial	1.2	0.28	81.08	-25	45.7	100.6	137.4	2.6	16.6	34.4	90.2
2nd trial	0.52	0.36	59.09	-25.8	56.9	101.5	142.9	9.9	15.5	31.1	80.0
3rd trial	0.44	0.36	55.00	-29.9	53.9	100.4	132.2	7.3	10.2	37.9	88.6

Maximum effort with normal resistance

Stroke Progress	V_{max} *[m/s]*	t_{pv} *[s]*	V_c *[m/s]*	V_r *[m/s]*	a_{max} *[m/s²]*	t_{pa} *[s]*	T_{max} *[Nm]*	F_{t-max} *[N]*	F_{r-max} *[N]*	$F_{res-max}$ *[N]*	P_{max} *[w]*
1st trial	4.387	1.222	0	3.627	8.236	0.841	23.5	471.3	399.8	618.0	335.1
2nd trial	6.144	0.511	4.319	5.43	4.933	0.242	19.5	430.7	365.3	564.7	611.3
3rd trial	7.746	0.484	6.077	6.939	4.652	0.225	15.6	361.3	306.5	473.8	685.7

Stroke Progress	PP *[s]*	RP *[s]*	PP/CT *[%]*	θc *[°]*	θ_r *[°]*	θ_{E-min} *[°]*	θ_{E-max} *[°]*	θ_{T-min} *[°]*	θ_{T-max} *[°]*	θ_{s-min} *[°]*	θ_{s-max} *[°]*
1st trial	1	0.64	60.98	-31.8	66.8	95.8	139.7	-0.4	13	32.3	82.7
2nd trial	0.28	0.48	36.84	-15.2	57.2	104.6	128.3	6.8	13.5	34.3	85.1
3rd trial	0.24	0.32	42.86	-19.3	62.4	93.1	131.2	6.8	11.6	29.4	78.9

Maximum effort with twice-normal resistance

Stroke Progress	V_{max} *[m/s]*	t_{pv} *[s]*	V_c *[m/s]*	V_r *[m/s]*	a_{max} *[m/s²]*	t_{pa} *[s]*	T_{max} *[Nm]*	F_{t-max} *[N]*	F_{r-max} *[N]*	$F_{res-max}$ *[N]*	P_{max} *[w]*
1st trial	3.937	1.06	0	3.372	8.166	0.717	26	578.7	490.8	758.8	125.8
2nd trial	6.017	0.541	3.575	6.425	6.449	0.277	18	372.0	315.5	487.8	217.7
3rd trial	7.41	0.442	5.727	6.918	4.959	0.222	18.5	520.3	441.3	682.3	309.6

Stroke Progress	PP *[s]*	RP *[s]*	PP/CT *[%]*	θc *[°]*	θ_r *[°]*	θ_{E-min} *[°]*	θ_{E-max} *[°]*	θ_{T-min} *[°]*	θ_{T-max} *[°]*	θ_{s-min} *[°]*	θ_{s-max} *[°]*
1st trial	0.88	0.48	64.71	-31	54	93.8	127.5	1.8	12.1	37.8	80.0
2nd trial	0.36	0.44	45.00	-27.8	58.9	103.8	127.9	5.9	11.3	36.9	91.2
3rd trial	0.28	0.44	38.89	-25.7	57.8	92.9	124.7	5.4	11.4	33.1	89.7

Maximum effort with normal resistance

Stroke Progress	V_{max} *[m/s]*	t_{pv} *[s]*	V_c *[m/s]*	V_r *[m/s]*	a_{max} *[m/s²]*	t_{pa} *[s]*	T_{max} *[Nm]*	F_{t-max} *[N]*	F_{r-max} *[N]*	$F_{res-max}$ *[N]*	P_{max} *[w]*
1st trial	4.755	0.819	0	4.542	9.69	0.485	42.7	858.0	727.7	1125.1	430.7
2nd trial	6.048	0.425	4.618	5.664	4.284	0.219	24.3	563.7	478.1	739.1	586.8
3rd trial	6.942	0.352	5.975	6.55	3.075	0.167	19.6	534.0	452.9	700.2	600.3

Stroke Progress	PP *[s]*	RP *[s]*	PP/CT *[%]*	θc *[°]*	θ_r *[°]*	θ_{E-min} *[°]*	θ_{E-max} *[°]*	θ_{T-min} *[°]*	θ_{T-max} *[°]*	θ_{s-min} *[°]*	θ_{s-max} *[°]*
1st trial	0.72	0.28	72.00	-24.7	21.3	129.9	139.7	2.9	6.2	21.7	56.2
2nd trial	0.28	0.28	50.00	-25.8	28	126.3	140.6	2.1	6.3	23.7	66.0
3rd trial	0.2	0.28	41.67	-24.5	23.3	126.1	143.3	3.6	6.3	18.9	72.9

Maximum effort with twice-normal resistance

Stroke Progress	V_{max} *[m/s]*	t_{pv} *[s]*	V_c *[m/s]*	V_r *[m/s]*	a_{max} *[m/s²]*	t_{pa} *[s]*	T_{max} *[Nm]*	F_{t-max} *[N]*	F_{r-max} *[N]*	$F_{res-max}$ *[N]*	P_{max} *[w]*
1st trial	3.974	0.881	0	3.935	7.184	0.563	63.7	1489.7	1263.5	1953.3	306.8
2nd trial	4.702	0.515	3.572	4.618	3.627	0.302	30.6	644.3	546.5	844.9	433.4
3rd trial	5.359	0.481	4.392	5.16	3.18	0.276	27.2	595.7	505.2	781.1	540.6

Stroke Progress	PP *[s]*	RP *[s]*	PP/CT *[%]*	θc *[°]*	θ_r *[°]*	θ_{E-min} *[°]*	θ_{E-max} *[°]*	θ_{T-min} *[°]*	θ_{T-max} *[°]*	θ_{s-min} *[°]*	θ_{s-max} *[°]*
1st trial	0.84	0.28	75.00	-22.9	14.4	128.9	138.3	3.6	9.8	25.8	63.4
2nd trial	0.44	0.28	61.11	-24.9	16.4	128.1	138.9	1.8	6.9	21.2	69.8
3rd trial	0.36	0.28	56.25	-25.5	24.8	128.7	134.5	1.4	5.1	24.7	62.0

B5: L&S Paraplegia

Maximum effort with normal resistance

Stroke Progress	V_{max} *[m/s]*	t_{pv} *[s]*	V_c *[m/s]*	V_r *[m/s]*	a_{max} *[m/s^2]*	t_{pa} *[s]*	T_{max} *[Nm]*	$F_{t\text{-}max}$ *[N]*	$F_{r\text{-}max}$ *[N]*	$F_{res\text{-}max}$ *[N]*	P_{max} *[w]*
1st trial	6.6	1.329	0	6.082	7.999	0.864	23.5	697.0	591.2	913.9	561.5
2nd trial	8.414	0.453	6.545	7.862	5.432	0.218	22.4	567.0	480.9	743.5	1147
3rd trial	9.917	0.445	8.324	9.447	4.652	0.216	21	515.0	436.8	675.3	1318

Stroke Progress	PP *[s]*	RP *[s]*	PP/CT *[%]*	θc *[°]*	θ_r *[°]*	$\theta_{E\text{-}min}$ *[°]*	$\theta_{E\text{-}max}$ *[°]*	$\theta_{T\text{-}min}$ *[°]*	$\theta_{T\text{-}max}$ *[°]*	$\theta_{s\text{-}min}$ *[°]*	$\theta_{s\text{-}max}$ *[°]*
1st trial	1.04	0.6	63.41	-49	88.2	74.9	165.7	1.2	36	19.1	121.7
2nd trial	0.28	0.52	35.00	-16.3	73.1	77.4	162.6	20.1	24.7	9.8	124.9
3rd trial	0.28	0.4	41.18	-19.7	75.5	81.3	158.3	21	25.8	10.9	138.0

Maximum effort with twice-normal resistance

Stroke Progress	V_{max} *[m/s]*	t_{pv} *[s]*	V_c *[m/s]*	V_r *[m/s]*	a_{max} *[m/s^2]*	t_{pa} *[s]*	T_{max} *[Nm]*	$F_{t\text{-}max}$ *[N]*	$F_{r\text{-}max}$ *[N]*	$F_{res\text{-}max}$ *[N]*	P_{max} *[w]*
1st trial	3.919	1.02	0	3.522	4.065	0.477	44.9	997.0	845.6	1307.3	866.9
2nd trial	5.023	0.454	3.916	4.986	5.793	0.206	25.5	543.3	460.8	712.5	1022
3rd trial	5.872	0.417	5.005	5.751	2.348	0.144	23.9	572.0	485.2	750.0	1014

Stroke Progress	PP *[s]*	RP *[s]*	PP/CT *[%]*	θc *[°]*	θ_r *[°]*	$\theta_{E\text{-}min}$ *[°]*	$\theta_{E\text{-}max}$ *[°]*	$\theta_{T\text{-}min}$ *[°]*	$\theta_{T\text{-}max}$ *[°]*	$\theta_{s\text{-}min}$ *[°]*	$\theta_{s\text{-}max}$ *[°]*
1st trial	0.74	0.48	60.66	-27.3	89	75.0	164.6	18.4	35.1	21.8	122.7
2nd trial	0.36	0.4	47.37	-17.5	77.3	75.3	161.5	22.6	26	9.2	136.6
3rd trial	0.28	0.4	41.18	-16	80.4	75.4	167.6	23	28.9	6.3	129.9

Maximum effort with normal resistance

Stroke Progress	V_{max} *[m/s]*	t_{pv} *[s]*	V_c *[m/s]*	V_r *[m/s]*	a_{max} *[m/s²]*	t_{pa} *[s]*	T_{max} *[Nm]*	F_{t-max} *[N]*	F_{r-max} *[N]*	$F_{res-max}$ *[N]*	P_{max} *[w]*
1st trial	4.524	1.058	0	4.353	6.79	0.693	29.3	586.3	497.3	768.8	382.3
2nd trial	6.269	0.481	4.258	5.98	5.634	0.235	23.6	517.3	438.8	678.4	597.9
3rd trial	7.071	0.399	5.94	6.823	3.496	0.200	18	457.0	387.6	599.2	601.8

Stroke Progress	PP *[s]*	RP *[s]*	PP/CT *[%]*	θc *[°]*	θ_r *[°]*	θ_{E-min} *[°]*	θ_{E-max} *[°]*	θ_{T-min} *[°]*	θ_{T-max} *[°]*	θ_{s-min} *[°]*	θ_{s-max} *[°]*
1st trial	0.96	0.4	70.59	-27.2	30.8	118.8	137.9	4.8	9.8	28.7	64.2
2nd trial	0.36	0.44	45.00	-27.9	36.3	116.3	130.3	4.5	7.6	28.3	70.3
3rd trial	0.28	0.44	38.89	-22.6	38.4	118.9	137.6	3.4	7.7	22.7	67.4

Maximum effort with twice-normal resistance

Stroke Progress	V_{max} *[m/s]*	t_{pv} *[s]*	V_c *[m/s]*	V_r *[m/s]*	a_{max} *[m/s²]*	t_{pa} *[s]*	T_{max} *[Nm]*	F_{t-max} *[N]*	F_{r-max} *[N]*	$F_{res-max}$ *[N]*	P_{max} *[w]*
1st trial	3.584	1.154	0	3.103	7.78	0.817	67.1	888.0	753.2	1164.4	959.2
2nd trial	4.883	0.509	3.077	4.861	5.266	0.276	78.3	1246.7	1057.4	1634.7	1208
3rd trial	5.754	0.454	5.202	5.717	2.041	0.271	80.1	1208.7	1025.2	1584.9	1782

Stroke Progress	PP *[s]*	RP *[s]*	PP/CT *[%]*	θc *[°]*	θ_r *[°]*	θ_{E-min} *[°]*	θ_{E-max} *[°]*	θ_{T-min} *[°]*	θ_{T-max} *[°]*	θ_{s-min} *[°]*	θ_{s-max} *[°]*
1st trial	1	0.4	71.43	-30.2	40.1	121.1	133.9	-1.4	6.5	25.3	52.1
2nd trial	0.48	0.4	54.55	-32.2	29.7	120.4	135.3	1.4	4.5	24.3	71.7
3rd trial	0.4	0.44	47.62	-31	42.4	118.8	134.8	2.4	5.2	24.9	71.8